AD-A062 204 NAVAL POSTGRADUATE SCHOOL MONTEREY CALIF F/G 13/11
AN EXPERIMENTAL COMPARISON OF ENHANCED HEAT TRANSFER CONDENSER --ETC(U)
SEP 78 J H FENNER
UNCLASSIFIED NPS69-78-015 NL

1 OF 2
AD A062204

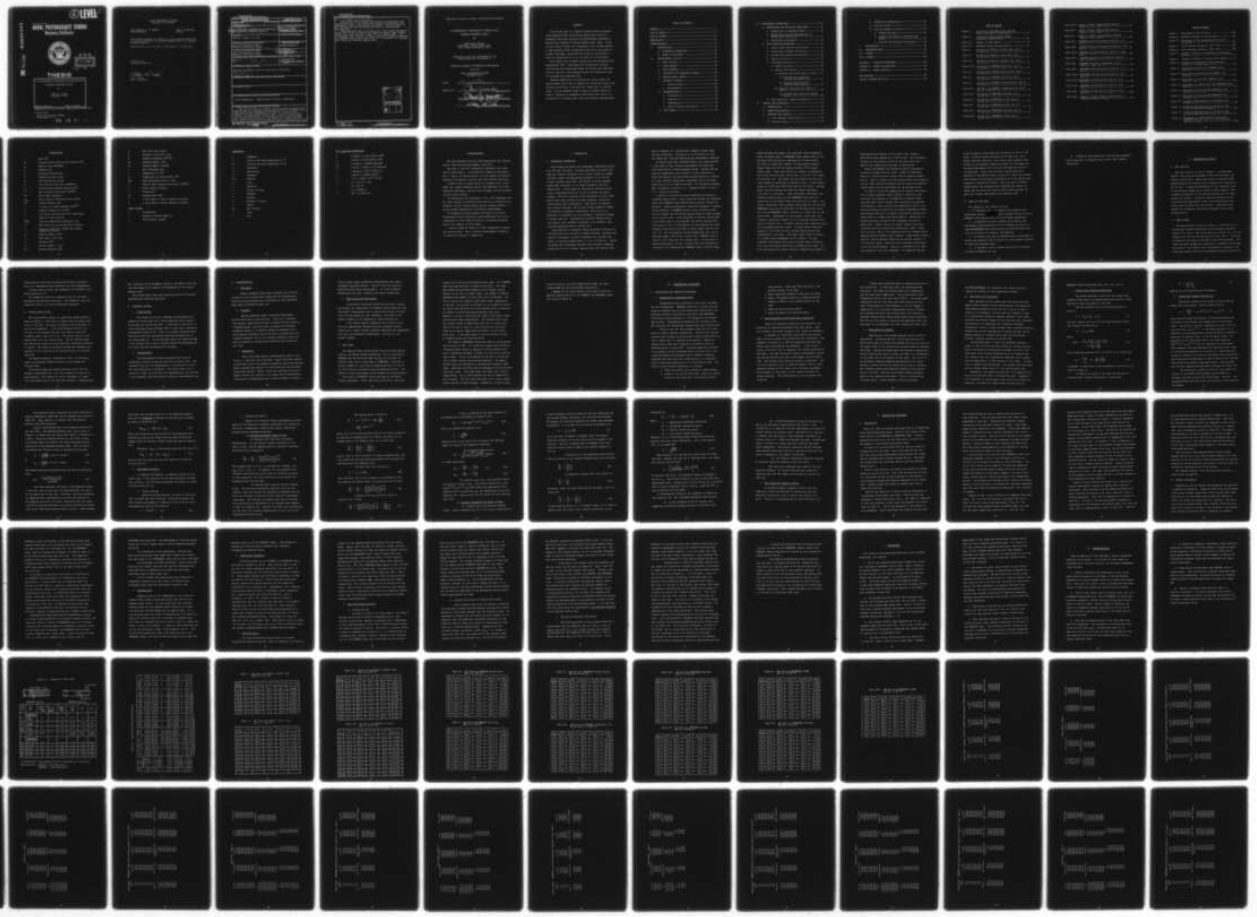

NPS 69-78-015

# NAVAL POSTGRADUATE SCHOOL

## Monterey, California




# THESIS

AN EXPERIMENTAL COMPARISON OF ENHANCED HEAT TRANSFER CONDENSER TUBING

by

James H. Fenner
September 1978

Thesis Advisor: Paul J. Marto

Approved for public release; distribution unlimited.

Prepared for:

Naval Sea Systems Command
Washington, D. C.

NAVAL POSTGRADUATE SCHOOL
Monterey, California

Rear Admiral T. F. Dedman
Superintendent

Jack R. Borsting
Provost

This thesis prepared in conjunction with research supported in part by the Naval Sea Systems Command under work request N0002477-WR74134.



Released as a
Technical Report by:

William M. Tolles

W. M. Tolles
Dean of Research

UNCLASSIFIED

SECURITY CLASSIFICATION OF THIS PAGE (When Data Entered)

| REPORT DOCUMENTATION PAGE | READ INSTRUCTIONS BEFORE COMPLETING FORM |
|---|---|
| 1. REPORT NUMBER (14) NPS 69-78-015 / 2. GOVT ACCESSION NO. | 3. RECIPIENT'S CATALOG NUMBER |
| 4. TITLE (and Subtitle) (6) AN EXPERIMENTAL COMPARISON OF ENHANCED HEAT TRANSFER CONDENSER TUBING | 5. TYPE OF REPORT & PERIOD COVERED (9) Master's Thesis, September 1978 |
| | 6. PERFORMING ORG. REPORT NUMBER |
| 7. AUTHOR(s) James H. Fenner, LT, USN | 8. CONTRACT OR GRANT NUMBER(s) |
| 9. PERFORMING ORGANIZATION NAME AND ADDRESS Naval Postgraduate School Monterey, California 93940 | 10. PROGRAM ELEMENT, PROJECT, TASK AREA & WORK UNIT NUMBERS N0002477-WR74134 |
| 11. CONTROLLING OFFICE NAME AND ADDRESS (11) Naval Postgraduate School Monterey, California 93940 | 12. REPORT DATE September 1978 |
| | 13. NUMBER OF PAGES 177 |
| 14. MONITORING AGENCY NAME & ADDRESS(if different from Controlling Office) (10) James Henry / Fenner | 15. SECURITY CLASS. (of this report) UNCLASSIFIED |
| | 15a. DECLASSIFICATION/DOWNGRADING SCHEDULE |

16. DISTRIBUTION STATEMENT (of this Report)

Approved for public release; distribution unlimited.

(12) 178 p.

17. DISTRIBUTION STATEMENT (of the abstract entered in Block 20, if different from Report)

18. SUPPLEMENTARY NOTES

19. KEY WORDS (Continue on reverse side if necessary and identify by block number)

Film Condensation, Enhanced Heat Transfer, Condensers

20. ABSTRACT (Continue on reverse side if necessary and identify by block number)

Ten 15.9 mm (5/8 in.) nominal outside diameter geometrically enhanced tubes of different metals were tested to determine their heat transfer and hydrodynamic performance. Results were compared to smooth copper-nickel tubes. Steam at about 21kPa (3 psia) was condensed on the outside surface of each enhanced tube, horizontally mounted in the center of a dummy tube bank. Each tube was cooled on the inside by water at velocities of

DD FORM 1 JAN 73 1473 EDITION OF 1 NOV 68 IS OBSOLETE S/N 0102-014-6601

78 12 1

UNCLASSIFIED

SECURITY CLASSIFICATION OF THIS PAGE (When Data Entered)

2.7 to 7.6 m/sec (3 to 25 ft/sec).

The overall heat transfer coefficient was determined from experimental data. The inside heat transfer coefficients were determined using the Wilson plot technique. Friction factor in the enhanced section was determined from the cooling water pressure drop.

Enhanced geometries (utilizing pitch, helix angle and groove depth) were found to improve the corrected overall heat transfer coefficient by as much as 2 times that for smooth tubes. Use of enhanced tubes in place of smooth tubes will permit a decrease in condenser tube surface area from 17 to 53 percent for constant heat loads and constant pumping power.

Approved for public release; distribution unlimited

# AN EXPERIMENTAL COMPARISON OF ENHANCED HEAT TRANSFER CONDENSER TUBING

by

James Henry Fenner
Lieutenant, United States Navy
B.S., Miami University, 1973

Submitted in partial fulfillment of the
requirements for the degree of

MASTER OF SCIENCE IN MECHANICAL ENGINEERING

from the

NAVAL POSTGRADUATE SCHOOL
September 1978

Author James H. Fenner

Approved by: Paul J. Marto
Thesis Advisor

Paul J. Marto
Chairman, Department of Mechanical Engineering

William M. Tolles
Dean of Science and Engineering

## ABSTRACT

Ten 15.9 mm (5/8 in.) nominal outside diameter geometrically enhanced tubes of different metals were tested to determine their heat transfer and hydrodynamic performance. Results were compared to smooth copper-nickel tubes. Steam at about 21kPa (3 psia) was condensed on the outside surface of each enhanced tube, horizontally mounted in the center of a dummy tube bank. Each tube was cooled on the inside by water at velocities of 2.7 to 7.6 m/sec (3 to 25 ft/sec).

The overall heat transfer coefficient was determined from experimental data. The inside and outside heat transfer coefficients were determined using the Wilson plot technique. Friction factor in the enhanced section was determined from the cooling water pressure drop.

Enhanced geometries (utilizing pitch, helix angle and groove depth) were found to improve the corrected overall heat transfer coefficient by as much as 2 times that for smooth tubes. Use of enhanced tubes in place of smooth tubes will permit a decrease in condenser tube surface area from 17 to 53 percent for constant heat loads and constant pumping power.

TABLE OF CONTENTS

## LIST OF TABLES

## LIST OF FIGURES

## NOMENCLATURE

| | |
|---|---|
| A | Area ($m^2$) |
| Ac | Cross sectional area of test section ($m^2$) |
| $c_p$ | Specific heat ($kJ/kg^oC$) |
| D | Diameter (m) |
| e | Tube groove depth (mm) |
| f | Fanning friction factor |
| Fc | Flow calibration factor |
| G | Flow rate per unit area ($kg/m^2sec$) |
| $g_c$ | Gravitational constant ($kg\ m/N\ sec^2$) |
| h | Heat transfer coefficient ($W/m^{2o}C$) |
| HA | Helix Angle (degrees) |
| $h_{fg}$ | Latent heat of vaporization (W sec/kg) |
| ID | Inside diameter (mm) |
| j | j factor in Colburn Analogy ($StPr^{2/3}$) |
| k | Thermal conductivity ($W/m^oC$) |
| K | Flow abrupt entrance and exit coefficient |
| L | Length of test tube (m) |
| LMTD | Log mean temperature difference ($^oC$) |
| $\dot{m}$ | Mass flow rate of cooling water (kg/sec) |
| M | Slope of Wilson Plot output from linear regression program |
| Nu | Nusselt number = hD/k |
| p | Tube spiral pitch (mm) |
| P | Pressure (kPa) |
| Pr | Prandtl number = $\mu c_p/k$ |
| Pw | Wetted perimeter (mm) |

| | |
|---|---|
| Q | Heat flow rate (W/sec) |
| $\dot{Q}$ | Volumetric flow rate ($\ell$/m) |
| R | Thermal resistance ($m^{2o}C/W$) |
| Re | Reynolds number = DG/$\mu$ |
| St | Stanton number = Nu/RePr |
| t | Wall thickness (mm) |
| T | Temperature ($^oC, ^oK$) |
| Tc | Temperature of cooling water ($^oC$) |
| TPF | Tube performance factor = 2j/f |
| U | Overall heat transfer coefficient ($W/m^{2o}C$) |
| v | Water velocity (m/sec) |
| V | Volume ($m^3$) |
| Wp | Pumping power (kW) |
| X | x axis input to linear regression program |
| Y | y axis input to linear regression program |

GREEK SYMBOLS

| | |
|---|---|
| $\Delta$ | Differential |
| $\mu$ | Dynamic viscosity (kg/m hr) |
| $\rho$ | Fluid density ($kg/m^3$) |

Subscripts

| | |
|---|---|
| a | Augmented |
| b | Fluid at the bulk temperature in $^{o}C$ |
| br | Fluid at the bulk temperature in $^{o}K$ |
| c | Corrected |
| cn | Contraction |
| e | Expansion |
| ext | External |
| f | Film |
| h | Hydraulic |
| i | Inside, or inlet |
| m | Measured |
| n | Nominal |
| o | Outside, or outlet |
| s | Smooth |
| TS | Test section |
| v | vapor |
| w | wall |

## SI to English Conversions

| | |
|---|---|
| h | 1 $W/m^{2o}C$ = 0.1761 $BTU/hr\ ft^{2o}F$ |
| k | 1 $W/m^{o}C$ = 0.5778 $BTU/hr\ ft^{o}F$ |
| $c_p$ | 1 $kJ/kg^{o}C$ = 0.23884 $BTU/lbm^{o}F$ |
| Q | 1 W/sec = 9.4781 x $10^{-4}$ $BTU/sec^2$ |
| $\mu$ | 1 kg/m hr = 2419.2 lbm/ft hr |
| $\rho$ | 1 $kg/m^3$ = 0.06243 $lbm/ft^3$ |
| P | Pa = 1.45038 x $10^{-4}$ $lbf/in^2$ |
| T | $^{o}C = 5/9\ (^{o}F - 32)$ |
| | $^{o}K = 5/9\ ^{o}R$ |
| L | 1 m = 3.2808 ft |
| A | 1 $m^2$ = 10.7639 $ft^2$ |

ACKNOWLEDGEMENT

The work presented here has been supported by Mr. Charles Miller, Naval Sea Systems Command, Code 0331.

Any work of this sort necessarily represents the influence of many people. I am especially indebted to Professor Paul J. Marto, my thesis advisor, for his support and patient guidance in helping me overcome even the smallest obstacles.

A special note of appreciation is extended to Mr. James Selby, Mr. Thomas Christian and Mr. Ken Mothersell for their technical assistance, and Mrs. Marty Delgado for her deciphering and typing talents.

The assistance and cooperation of Mr. Bruce Henderson and Mr. James Withers of Wolverine Tube Division of Universal Oil Products, and Mr. Robert Perkins and Mr. Richard Siebers of Spiral Tubing Corporation is gratefully acknowledged.

The Graphics and Photographic Divisions of the Naval Postgraduate School Educational Media Department are to be recognized for their special efforts in helping me produce many of the figures in this thesis.

I wish to thank my family for their enthusiastic support and understanding. Their constant encouragement allowed me to bring this project to completion.

# I. INTRODUCTION

## A. BACKGROUND INFORMATION

Ship design has become an increasingly integrated process over the past few years. Systems approaches are being utilized that require attention to the entire complex of communications, combat and engineering equipment to be carried within a desired hull form. The desire to obtain maximum operational efficiency is no longer dependent upon hull design alone. Every system is reviewed for possible reductions in manufacturing costs as well as weight and space savings. Efforts to achieve these reductions in naval steam power plants must include the steam condenser, which has traditionally been overdesigned. Application of enhanced heat transfer methods, such as tube surface geometry changes or promotion of dropwise condensation, would allow for reduction in condenser size with perhaps a resulting savings in weight and cost. Enhanced heat transfer methods would also permit lower condenser pressures to be achieved, thus reducing operating costs by saving fuel.

Investigation of condenser design processes by Search [1], indicated that with the use of computer methods, enhanced heat transfer techniques in marine condensers can increase heat loads, at constant pumping power, by up to 50 percent. Search concluded that enhancement methods could decrease condenser weight and cost for constant pumping power and constant heat

load as compared to a conventional condenser design under the same conditions. Savings of up to 40 percent in size and weight were reported depending upon enhancement technique.

In recent years many research efforts have been directed to the study of heat transfer enhancement techniques and their application to heat exchanger design. Bergles [2] has recently summarized a wide variety of tests conducted to study the behavior and performance characteristics of convective heat transfer enhancement techniques both with single phase as well as two phase processes. He categorized enhancement techniques as passive (i.e., enhanced tubes) or active (i.e., surface vibration).

A variety of studies have been conducted pertaining to condenser applications. Palen, Cham and Taborek [3] conducted tests with TURBOTEC tubes manufactured by Spiral Tubing Corporation. Bundle configuration tests were designed to compare the performance of TURBOTEC tubes to that of smooth tubes. The test bundle had 196 25.4 mm outside diameter tubes arranged in 16 vertical rows. Steam pressures of 379 kPa and 724 kPa on the shell side of the condenser and bundle cooling water flow rates of 47.9 to 100.8 kg/sec on the tubeside were used. Average cooling water bulk temperatures ranged from 118.3 to 171.1 $^{o}$C. The experimental results showed that for a given Reynolds number, the friction factor for a TURBOTEC tube is from 10 to 15 times that of a smooth tube. On the basis of bundle performance, the heat transfer rate was increased by a factor of 2.5 comparing the TURBOTEC tubes to smooth tubes.

Young, Withers and Lampert [4] conducted bundle comparison tests of smooth tubes to KORODENSE tubes manufactured by the Wolverine Tube Division of Universal Oil Products (UOP). Two sizes of tubes were tested: 15.9 mm outside diameter copper tubes and 25.4 mm outside diameter 90-10 copper-nickel tubes. Tubes were tested in a bundle configuration with three vertical rows, with either 1 to 9 or 1 to 7 tubes per vertical row. The middle row was offset such that the tubes formed an equilateral triangular pitch. Steam temperatures of 37.8°C and 100°C were used for the tests. Cooling water velocity through each tube was varied from about 0.91 m/sec to 1.98 m/sec. Under isothermal conditions, the tubeside pressure drop for the KORODENSE tubes was five times that of the smooth tubes for both sizes of tubes. The inside, water-side, heat transfer coefficient for the 25.4 mm KORODENSE tube was 2.2 times that of the smooth tube, while the 15.9 mm KORODENSE tube's value was 2.7 times that of the smooth tube. Enhancement of the outside, steam-side, heat transfer coefficient showed a 30 to 40 percent increase over that of a smooth tube. Catchpole and Drew [5] conducted tests on five radially grooved tubes. In these tests, steam was supplied at 13.79 kPa and the cooling water velocity was maintained at 3.05 m/sec. The tubes could either be tested in a single tube arrangement or as a bundle. All heat transfer coefficients and friction factors were calculated as if the tube being tested were a standard plain tube. All five tube geometries tested yielded a combined improvement of

approximately 40 percent in the overall heat transfer coefficient when compared to a smooth tube. The percentage increase in the friction factor of the test tubes over a smooth tube ranged from 33 percent to 264 percent.

Newson and Hodgson [6] condensed steam at atmospheric pressure on single vertical tubes. Combs [7] conducted tests on a single vertical fluted tube for ammonia condensation. Tests on single vertical fluted tubes were conducted also by Combs, Mailen and Murphy [8] utilizing six different fluorocarbons and one hydrocarbon as the working fluids.

In order to allow for comparison of enhanced tube types with a single apparatus under identical conditions, and alleviate the confusion of attempting to compare results obtained under widely varying test procedures and physical environments, a test facility was designed and initial construction begun by Beck [9] at the Naval Postgraduate School that permits testing of a single, horizontally mounted condenser tube in a dummy tube bundle matrix. Completion of construction and testing of this condenser was done by Pence [10]. Pence's tests on a smooth copper-nickel tube indicated that the facility was technically sound. Using this facility, Reilly [11] conducted tests on enhanced tubes manufactured by General Atomic Company. Three General Atomic spirally fluted aluminum tubes with an outside diameter of 15.9 mm were tested. Each tube had a different helix angle of 30, 45 and 60 degrees. Steam at a pressure of 20.7 kPa was supplied to the test condenser. The enhanced tube was

cooled by water on the inside at velocities of 0.91 to 7.62 m/sec. Friction factor increases of 10 times that for a smooth tube were observed. The overall heat transfer coefficient of the enhanced tubes was as much as 1.75 times the corresponding smooth tube value for the same mass flow of cooling water. Inside heat transfer coefficients were observed to increase by about a factor of 3 while the outside heat transfer coefficients decreased by 10 to 29 percent when compared to smooth tube values. Reilly's tests of smooth copper-nickel and aluminum tubes confirmed the results of Pence, and his work with General Atomic tubes provided the basis for further experiments with enhanced tubes.

## B. GOALS OF THIS WORK

The purpose of this thesis was then:

1. to determine the heat transfer and pressure drop performance characteristics of four different spirally fluted TURBOTEC tubes manufactured by Spiral Tubing Corporation,

2. to determine the heat transfer and pressure drop performance characteristics of five different spirally corrugated KORODENSE tubes manufactured by Wolverine Tube Division of Universal Oil Products, Incorporated,

3. to compare each type of enhanced tube's performance to smooth tube operation and to results of other research efforts on similarly enhanced tubes,

4. to estimate if any of these tubes would be suitable for naval condenser use, and

5. to identify what geometrical tube design parameters may be important in enhancing the overall heat transfer coefficient.

# II. EXPERIMENTAL FACILITY

## A. TEST FACILITY

The test facility is seen in Figure 1. As mentioned earlier, the layout was designed by Beck [9] and built and tested by Pence [10]. Operational tests of enhanced tubes manufactured by the General Atomic Company were conducted by Reilly [11]. A detailed description of the components used in the various systems may be found in these reports. Only a general description of the various systems will be found within this report. Particular attention however will be focused on the experimental tubes, their construction and their location within the test section. Calibration procedures for components requiring calibration are outlined by Reilly [11].

## B. STEAM SYSTEM

The steam system is shown in Figure 2. The boiler is an electrically heated Fulton Boiler which produces saturated steam at 45.4 kg/hr. The steam leaves the boiler via a 19.1 mm diameter line and the boiler-isolation valve (MS-1). The water contained in the steam is removed by the steam separator. The steam continues through the system past a flowmeter and through the throttle valve (MS-3) where the pressure is reduced. The steam next passes through the desuperheater wherein water from

the feed system is injected in order to remove some of the sensible heat from the steam. The steam continues into the test condenser where part of it is condensed on the test tube. The steam not condensed is collected in the vapor outlet and sent to the secondary condenser wherein the latent heat of vaporization is removed. If the boiler fails, steam may be provided via the house-steam-cross-connect valve (MS-2). Steam could be routed around the test condenser to the secondary condenser via the bypass valve (MS-4). All steam lines (except the section downstream of MS-3, see [10]) were insulated with 25.4 mm thick fiberglass insulation.

## C. TEST CONDENSER

The test condenser is shown in Figures 3, 4, and 5. Steam enters via the top. It then passes through the expansion section over the baffle separators, and through three layers of 150 mesh screen and a flow straightener into the tube bundle. The condensate collects at the bottom of the test condenser where it flows through two 12.7 mm diameter lines to the hotwell.

The viewing windows, shown in Figure 3 and Figure 4, allow viewing of the condensation process. Two types of pyrex glass windows were used. One type was a standard pyrex glass plate 12.7 mm thick. The second type of window was an Owens-Corning pyrex glass with a transparent electrically conducting coating applied over one surface. A Lambda power supply set at 20 VDC

and 2.2 Amp was used with this window to supply power to the electrically conducting surface to minimize fogging effects.

The tube sheet arrangement is as seen in Figure 5. There are eight 15.9 mm OD, 18 gauge, 90-10 copper-nickel tubes arranged in a typical condenser configuration, with a spacing to diameter ratio (S/D) of 1.5, around a single test tube. The test tube is the only tube with water passing through it. This arrangement was selected to best simulate the steam flow conditions in an actual condenser.

The test condenser is insulated with a 51 mm thick sheet of Johns-Manville Aerotube insulation.

## D. CONDENSATE AND FEEDWATER SYSTEMS

The condensate and feedwater systems are shown in Figure 6. The test condenser hotwell collects the condensate from the test tube, while the secondary condenser hotwell collects the condensate from the secondary condenser. Valve C-1 allows isolation of the test condenser hotwell so the condensate mass from the test condenser may be measured. Valve C-4 is a vent valve between the test condenser hotwell and the test condenser. The condensate is pumped from the hotwells to the feedwater tank by the condensate pump. The feed pump routes the water from the feed tank to the boiler via the solenoid-controlled valve FW-3, a hot-water filter, and the boiler-isolation valve, FW-4.

The feedwater temperature is maintained between 54.4$^{o}$C and 60.0$^{o}$C by thermostat controlled heaters. This reduces

fluctuations in the boiler output and provides a source of water at a temperature near saturation for the desuperheater.

If house steam is used, the condensate is returned to the house system via C-3.

The condensate lines are insulated with 19.1 mm thick Johns-Manville Aerotube insulation. The feedwater lines are insulated with 12.7 mm thick fiberglass insulation.

## E. COOLING WATER SYSTEM

The cooling water system is a partially-closed system as shown in Figure 7. The water is pumped from the supply tank via a 5.6 kw pump. The water is routed to the test tube via one of two rotameters. A low flow rotameter allows up to 5.6 $\ell$/m to flow through the test tube, while a high flow rotameter permits up to 71.2 $\ell$/m. The water returns to the supply tank via a dry cooling tower. The dry cooling tower was constructed using four large plate/fin radiators connected in series. The water was directed through the radiators and outside air was forced over the cooling surface by a centrifugal fan.

The bypass-rotameter, downstream of CW-C, is provided to permit an increased volume of water to flow through the cooling tower.

The system piping was reduced from 25.4 mm to 15.9 mm diameter (approximate OD of all test tubes) at a distance of approximately 0.76 m ahead of the test condenser to insure fully developed flow at the test-tube entrance. Pressure taps

were installed in the permanent piping at the ends of the test tube (see Figure 8) to permit the measurement of the overall pressure drop.

The cooling water lines were insulated with 25.4 mm thick Johns-Manville Aerotube insulation.

## F. SECONDARY SYSTEMS

### 1. Vacuum System

The vacuum in the test condenser is maintained by a mechanical vacuum pump and a vacuum regulator which induces an air leak into the vacuum line. A cold trap at the inlet of the vacuum pump forces incoming vapor to pass over a system of refrigerated copper coils. This is to remove entrained water from the vacuum line and prevent moisture contamination of the vacuum pump oil. The vacuum pump outlet is vented through a roof exhaust fan to avoid a health hazard from breathing any oil vapor that may be exhausted by the pump.

### 2. Desuperheater

The desuperheater removes sensible heat from the superheated steam by injecting feed water at about 60°C. The feedwater flow into the desuperheater is controlled by valve DS-1 and measured by a rotameter. The excess water is collected in a tank, located below the desuperheater, and returned to the feedwater tank periodically during the experimental runs.

## G. INSTRUMENTATION

### 1. Flow Rates

Fulton rotameters were used to measure the flow rate of water in the cooling water system and the desuperheater, while an Ellison Annubar and a differential water manometer were used to determine steam flow.

### 2. Pressure

Several different types of pressure measurement devices were used in this facility. They were: a Bourdon tube pressure gauge which was used to measure boiler pressure, a compound gauge which was used to measure the secondary condenser pressure, an absolute pressure transducer and a 760 mm mercury manometer which were used to measure the test condenser pressure, and a 3.6 m mercury manometer which was used to measure the cooling water pressure drop across the test tube.

### 3. Temperature

There were three types of thermocouples used in this facility. Stainless steel sheathed, copper-constantan thermocouples were used as the primary temperature monitoring devices. Eleven temperatures required for data reduction were measured using these devices. Table I lists the locations monitored. Figure 2 shows the location of six vapor space thermocouples. Cooling water thermocouples were located as shown in Figure 7.

Teflon coated copper-constantan thermocouples were used as secondary measuring devices. Table II lists the locations monitored using these thermocouples. An iron-constantan thermocouple was used to measure the boiler temperature.

4. Data Collection and Display

An autodata collection system was utilized to record and display the temperatures in degrees Celsius obtained from the primary thermocouples and to record and display the pressure in cm Hg inside the test condenser. See Table I for channel numbers of the temperature monitoring devices.

A 28 channel digital pyrometer uas utilized to display the temperatures obtained from the secondary thermocouples and a single channel pyrometer displayed the temperature from the iron-constantan thermocouple. See Table II for channel numbers.

## H. TEST TUBES

The enhanced tubes tested during this study were manufactured by the Spiral Tubing Corporation, with a trade name of TURBOTEC, and the Wolverine Tube Division of Universal Oil Products (UOP), with a trade name of KORODENSE. Each had an overall length of 1.22 m and an enhanced section of 0.914 m. All were helically spiraled along the enhanced section. The method of spiral development varied however with manufacturer.

Four types of TURBOTEC tubing were made by the Spiral Tubing Corporation. These tubes were three-start, helically

fluted, with flute pitch determining tube type. All TURBOTEC tubes were manufactured of copper (Alloy 122). The tubes were formed by externally making a set of equally spaced dimples at one end of a smooth tube. The number of dimples determines the number of flutes that will be produced. The tube is placed in a mandrel lathe under slight compression at one end. As the tube is twisted, it is allowed to draw-in on itself (self-shorten) until the desired pitch is obtained. The amount of self-shortening determines tube pitch. Figures 9, 10 and 11 show close-up views of the High, Medium and Low pitch tubes respectively. The Variable pitch tube (not shown) varies in appearance from that of a High pitch tube at one end to that of a Low pitch tube at the other. There is no special significance attached to the Variable pitch tube. It was made simply to see if tube pitch could be changed during the forming process.

Two types of KORODENSE tubing were made by the Wolverine Tube Division of UOP. All tubes were single-start helically corrugated tubes formed by passing a rotating smooth tube under a mechanism designed to indent the tube to the desired groove depth. Pitch is determined by the rate at which the tube is drawn through the grooving mechanism. The deeper grooved tubes are designated as Maximum Heat Transfer (MHT) tubes. Shallower grooved tubes are designated as Low Pressure Drop (LPD) tubes. Three MHT tubes were made: one of 90/10 Copper-Nickel, one of 3003-Aluminum and one of commercially pure Titanium. Two LPD tubes were made: one of 90/10 Copper-Nickel and one of 3003-Aluminum. Figures 12, 13 and 14 show

close-up views of the 90/10 Copper-Nickel-MHT, the 3003-Aluminum-MHT and the Titanium-MHT respectively.

A summary of all tubes tested is provided in Table III. Special characteristics of the TURBOTEC and KORODENSE tubes are listed in Table IV.

# III. EXPERIMENTAL PROCEDURES

## A. INSTALLATION AND OPERATING PROCEDURES

### 1. Preparation of Condenser Tubes

Thermocouples were installed on each tube to measure the wall temperature. TURBOTEC tubes have a larger diameter along the enhanced section than along their smooth ends, and required different installation procedures than KORODENSE tubes whose outside diameter is not changed by the enhancement process. Standardized procedures given by Reilly [11] were followed for thermocouple mounting and tube installation.

Prior to any run, the condenser tubes had to be prepared to insure filmwise condensation. Exterior and interior surfaces were cleaned to insure proper wetting characteristics and to insure that all deposits were removed. Copper and copper-nickel tubes were prepared in accordance with the procedure given in Pence [10]. Aluminum tubes were prepared in accordance with the procedure given in Reilly [11]. To clean and prepare the titanium tube, a chemical cleaning procedure was used which was a modification of a procedure used in descaling titanium prior to acid pickling [12]. The steps in this cleaning process are as follows:

a. Swab tube surface with acetone to remove grease.

b. Using a 1.91 cm test tube brush, brush the inside surface of the tube with a 50 percent sulfuric

acid solution. Also apply this solution to the outside surface of the tube.

c. Rinse inside and outside of tube with tap water.

d. Apply a 50 percent solution of sodium hydroxide (heated to 95°C) to the outside surface of the tube.

e. Rinse the tube with tap water.

f. Rinse thoroughly with distilled water.

2. System Operation and Steady State Conditions

Pence [10] developed and Reilly [11] modified a detailed set of operating procedures for this system. They are included, with minor changes, in this report as Appendix A.

In general it takes about three hours from initial light off until steady state conditions are established. The feedwater is heated up to 60°C by energizing the feed tank heaters and recirculating the feedwater. After installation of the test tube is complete, the vacuum system can be activated. The data collection system is programmed, including setting the date and time in accordance with reference [13]. The cooling water system is placed in operation. The 71.2 ℓ/m rotameter is set at about 50 percent flow to allow adequate venting of both legs of the 3.66 meter manometer. The rotameter is then reset to the lowest flow point for system operation. The steam system can now be placed into operation.

Steady state conditions must be established prior to data collection. To determine this, two parameters were monitored. They were the cooling water inlet temperature and the steam vapor temperature. The cooling water inlet temperature did not rise more than 0.6°C/hr. The steam vapor temperature did not vary more than 3.3°C between the six vapor thermocouples in the condenser or did the change in temperature at an individual thermocouple exceed 0.3°C/min. The steaming conditions and cooling water flow conditions remained constant while establishing steady state conditions. The time for the system to stabilize was generally about one hour which is in agreement with that reported by Reilly [11].

3. Maintenance Procedures

Periodically, the systems required various forms of maintenance. Following each run, the boiler received two bottom blow downs to remove any sediment that may have settled. The supply tank in the cooling water system required occasional refilling. Treated tap water which ran through a commercially rented resin bed was used to reduce the amount of contaminants in the water that could deposit on the tubes. The filter in the feedwater required changing approximately every three months to prevent low boiler levels due to lack of feedwater. The condenser glass window required cleaning after approximately five runs. This was true whether using the heated glass or the standard pyrex glass. Prior to reinstalling the pyrex glass, a light coating of Glycerol Reagent

ACS $HOCH_2CHOHOH_2OH$, was applied to the inside surface to enhance the viewing of the condensation process.

## B. DATA REDUCTION PROCEDURES

Data obtained in this thesis were evaluated using the smooth inside diameter as the characteristic flow dimension. This method presents the data in such a way as to make it useful to the designer. The data was not reduced in terms of a conventional hydraulic diameter because of the widely different geometrical shapes of the tubes and the corresponding difficulty in measuring such a hydraulic diameter. Furthermore, there is recent evidence that a modified hydraulic diameter may be more appropriate in describing heat and momentum transfer in turbulent flow than the conventional hydraulic diameter defined as 4 Ac/Pw [14].

As mentioned above, to meet the condenser designer's needs, it was felt that the data should be reduced using the smooth end diameter following the procedure of Reilly [11]. This would allow a direct substitution of an enhanced tube for a smooth tube and is especially important when considering the comparison of a wide variety of tube types. In addition, a nominal area was defined. The nominal area was based on the outside surface area of a 15.9 mm OD smooth tube.

Appendix B, the sample calculations, is a complete listing of the equations used to evaluate the data. Appendix C is a derivation of the probable error in the data reduction equations, followed by a sample error analysis for the

KORODENSE Copper-Nickel-MHT tube, (No. K-2), Run 12.

1. Overall Heat Transfer Coefficient

The method employed to arrive at the overall heat transfer coefficient is straightforward and similar to that employed by many researchers in the past.

The heat transfer rate to the cooling water is given by

$$Q = \dot{m}\, c_p\, (Tc_o - Tc_i) \quad . \tag{1}$$

The heat transfer rate can also be found from the overall heat transfer coefficient by

$$Q = U_n\, A_n\, LMTD \quad , \tag{2}$$

where

$$LMTD = \frac{(T_v - Tc_i) - (T_v - Tc_o)}{\ln\left(\frac{T_v - Tc_i}{T_v - Tc_o}\right)} \quad . \tag{3}$$

After combining equations (1), (2) and (3) it is found that

$$U_n = \frac{\dot{m}\, c_p}{A_n} \ln\left(\frac{T_v - Tc_i}{T_v - Tc_o}\right) \quad . \tag{4}$$

A schematic illustration of the procedures to arrive at $U_n$ is shown in Figure 15.

To remove the effect of the tube wall material, a corrected heat transfer coefficient is found from

$$U_c = \frac{1}{\frac{1}{U_n} - \frac{1}{R_w}} \quad , \tag{5}$$

where $R_w$ is the calculated wall resistance.

2. Inside Heat Transfer Coefficient

The Nusselt number on the inside is found from the Sieder Tate relationship, found in Holman [15] as:

$$Nu = \frac{h_i D_i}{k_b} = C_i \, Re^{0.8} \, Pr^{1/3} \, (\mu/\mu_w)^{0.14}. \tag{6}$$

With this well-known correlation, all fluid properties are evaluated at the average bulk temperature of the cooling water. The effect of the wall temperature is only felt by a viscosity ratio $(\mu/\mu_w)^{0.14}$. In the above equation, $C_i$ is referred to as the Sieder Tate coefficient which is normally expressed as between 0.023 - 0.027 for smooth tubes. The remainder of the right hand side of the above equation $(Re^{0.8} \, Pr^{1/3} (\mu/\mu_w)^{0.14})$ will be referred to as the Sieder Tate parameter, and the procedure for arriving at this value is illustrated schematically in Figure 16. The Wilson plot is used to arrive at the value of the Sieder Tate coefficient. The Wilson plot was developed in 1915 by Wilson [16], and has been modified by several researchers since. The procedure used in this research was developed by Briggs and Young [17].

The Wilson plot is merely a plot of $1/U_n$ versus the inverse of the Sieder Tate parameter which should be a straight line when varying the cooling water velocity. The reasoning behind the Wilson plot can be seen in the following development.

The overall heat transfer coefficient can be written as:

$$U_n = \frac{1}{\frac{D_o}{D_i h_i} + R_w + \frac{1}{h_o}} \quad . \tag{7}$$

The inverse of equation (7) is:

$$\frac{1}{U_n} = \frac{D_o}{D_i h_i} + R_w + \frac{1}{h_o} \quad . \tag{8}$$

If $(R_w + \frac{1}{h_o})$ is assumed to be constant, and equation (6) is solved for $h_i$ in terms of the Sieder Tate parameter, equation (8) can be rewritten as:

$$\frac{1}{U_n} = \frac{D_o}{C_i k_b} \, Re^{-0.8} \, Pr^{-1/3} \, (\mu/\mu_w)^{-0.14} + B \quad , \tag{9}$$

where $B = R_w + \frac{1}{h_o}$ = constant.

The form of equation (9) is then exactly that of a straight line,

$$Y = MX + B \quad , \tag{10}$$

where:

$$Y = \frac{1}{U_n} \quad , \tag{10a}$$

$$X = \frac{1}{\text{Sieder Tate parameter}} \quad , \text{ and} \tag{10b}$$

$$M = \frac{D_o}{C_i k_b} \quad . \tag{10c}$$

The values of $1/U_n$ and the Sieder Tate parameter are obtained by varying the water velocity and holding the other parameters, such as water temperatures, steam vapor

temperatures and condenser tube wall temperature, nearly constant. When $1/U_n$ is plotted versus $Re^{-0.8}\ Pr^{-1/3}\ (\mu/\mu_w)^{-0.14}$, a linear regression subroutine [18] fits these points to a straight line and then solves for the slope, M, and the intercept, B. Knowing the slope, M, the Sieder Tate coefficient $C_i$ can be found from equation (10c). The inside heat transfer coefficient, $h_i$, is then found from equation (6).

Once the inside heat transfer coefficient, $h_i$, is known, then the Nusselt number can be solved for in equation (6), to find the Stanton number,

$$St = \frac{Nu}{RePr} = \frac{h}{c_p G} \quad . \tag{11}$$

The cooling water properties ($\rho$, $\mu$, k, $c_p$, and Pr) are solved for as shown in Appendix B. Appendix B also demonstrates the procedure for arriving at the water viscosity evaluated at the condenser tube wall, $\mu_w$.

3. Outside Heat Transfer Coefficient

The outside heat transfer coefficient, $h_o$, can now be found from equation (7) knowing $U_n$, $h_i$ and $R_w$. Figure 17 schematically illustrates the various steps outlined above.

4. Friction Factor

The friction factor for the test tube is found from:

$$f_a = \frac{(\rho_b)(\Delta P_{TS})(2g_c)}{4(L_{TS}/D_i)\ G^2} \quad . \tag{12}$$

The variables used in equation (12) are solved for as shown in Appendix B, while the inside diameters are listed in Table III. $\Delta P_{TS}$, however, is reduced from the measured pressure drop outlined below.

$\Delta P_{TS}$ is the pressure drop in the enhanced section of the test tube. The measured pressure drop, $\Delta P_m$ as seen in Figure 8, is taken over the entire tube length, a distance of 1.299 m. Since the enhanced section is only 0.914 m long, the pressure drop over each of the smooth ends must be subtracted off of the measured pressure drop. This is done by calculating the friction factor in the smooth ends using:

$$f_s = \frac{0.079}{Re^{0.25}} \quad \text{for } Re < 30{,}000 \quad , \tag{13}$$

or

$$f_s = \frac{0.046}{Re^{0.2}} \quad \text{for } Re > 30{,}000 \quad . \tag{14}$$

The smooth-end-section pressure drops can then be calculated from,

$$\Delta P_s = \frac{(f_s)(4)(L_S/D_i)(G^2)}{(\rho_b)(2g_c)} \tag{15}$$

The cross sectional flow area of the enhanced section of the test tube is less than the cross sectional flow area of the smooth end of the tube. Therefore, the water undergoes an expansion and a contraction at the exit and entrance to the enhanced section of the tube. Associated with the expansion and contraction processes are certain irreversible losses which cause additional pressure drops to occur. These pressure

drops must also be subtracted off of the measured pressure drop and are estimated following the calculational procedure as shown in reference [19]:

$$\Delta P_{e/cn} = \rho v_{TS}^2 (K_e + K_{cn}) \quad . \tag{16}$$

Since the variations in the contraction and expansion coefficients $K_{cn}$ and $K_e$ are slight over the range of Reynolds numbers used, an average of these values was used in equation (16).

Therefore, $\Delta P_{TS}$ is found using equations (15) and (16):

$$\Delta P_{TS} = \Delta P_m - \Delta P_s - \Delta P_{e/cn} \quad , \tag{17}$$

and the friction factor for the test section is solved for in equation (12).

5. Performance Criteria

To compare the enhanced, or augmented tubes with the smooth tube, it was necessary to use some meaningful performance criteria. The following procedures are similar to those outlined by Reilly [11].

a. Colburn Analogy

Using the Colburn Analogy, as found in reference [20], provided one such criterion. Using this analogy, the heat transfer performance is compared to the friction factor performance as seen by the relation:

$$j = StPr^{2/3} = f/2 \quad . \tag{18}$$

b. Surface Area Ratios

Bergles [21] outlines several performance criteria based on the inside heat transfer coefficients by solving for the ratio of augmented to smooth tube surface areas while holding various parameters constant.

(1) External Resistance Equal to Zero.

(a) Constant Heat Load with Increasing Pumping Power. If the external thermal resistance is set equal to zero, and the pumping power is allowed to increase, one such ratio is defined by

$$\frac{A_a}{A_s} = \frac{h_s}{h_a} = \frac{Nu_s/Pr^{1/3}(\mu/\mu_w)^{0.14}}{Nu_a/Pr^{1/3}(\mu/\mu_w)^{0.14}} \quad . \qquad (19)$$

This assumes that Q, $\dot{m}$, $D_i$, $T_b$ and LMTD are constant, and $R_{ext} = R_w + 1/h_o = 0$. In equation (19) the augmented heat transfer coefficient $h_a$ is the value $h_i$ referred to earlier. In this situation, the flow velocities for the smooth and augmented tubes are the same.

(b) Constant Heat Load and Constant Pumping Power. The area ratio defined by equation (19) does not, however, take into account the increase in pressure drop and hence the increase in friction factor caused by enhancement techniques. The increase in pressure drop can be included when evaluating the performance of an enhanced tube compared to that of a smooth tube. Bergles [21] shows this by defining an area ratio for constant pumping power as well as for the conditions defined earlier.

The pumping power is given by:

$$Wp = (\rho\ v\ \frac{\pi}{4} D^2)\ 4\ f\ (\frac{L}{D})\ (\frac{v^2}{2g_c}) \qquad (20)$$

$$= (\frac{\rho}{2g_c})\ (\pi DL)\ fv^3 \quad ,$$

where $\pi DL$ is the inside surface area for the tube in question. By setting the pumping power of a smooth tube equal to the pumping power of an enhanced tube, it is found that:

$$\frac{A_a}{A_s} = \frac{v_s^3\ f_s}{v_a^3\ f_a} = \frac{Re_s^3\ f_s}{Re_a^3\ f_a} \quad . \qquad (21)$$

Notice, that in this situation of constant pumping power, the flow velocities and hence Reynolds numbers are different for the smooth and the augmented tube.

The heat flow rate is given by:

$$Q = h_i\ A_i\ LMTD_i \quad . \qquad (22)$$

Since the heat flow is also assumed to be constant in both the enhanced and smooth tubes, the area ratio can be found

$$\frac{A_a}{A_s} = \frac{h_s}{h_a} = \frac{Nu_s/Pr^{1/3}(\mu/\mu_w)^{0.14}}{Nu_a/Pr^{1/3}(\mu/\mu_w)^{0.14}} \quad . \qquad (23)$$

Equation (21) can now be set equal to equation (23) to show:

$$\frac{A_a}{A_s} = \frac{Nu_s/Pr^{1/3}(\mu/\mu_w)^{0.14}}{Nu_a/Pr^{1/3}(\mu/\mu_w)^{0.14}} = \frac{Re_s^3\ f_s}{Re_a^3\ f_a} \quad . \qquad (24)$$

If $Nu_s$ is replaced in the above equation by the Sieder-Tate relationship as found in [15]:

$$Nu_s = 0.027\ Re_s^{0.8}\ Pr^{1/3}(\mu/\mu_w)^{0.14} \quad , \qquad (25)$$

and $f_s$ is replaced by equation (14)

$$f_s = \frac{.046}{Re_s^{0.2}} \quad , \qquad (14)$$

equation (24) can be solved for the smooth tube Reynolds number in terms of the augmented conditions:

$$Re_s = \sqrt{\frac{0.027\ f_a\ Re_a^3}{0.046\ Nu_a/Pr^{1/3}(\mu/\mu_w)^{0.14}}} \quad . \qquad (26)$$

In these expressions,

$$Re_s = \frac{G_s D_i}{\mu} = \frac{\rho D_i v_s}{\mu} \quad , \text{ and} \qquad (27a)$$

$$Re_a = \frac{G_a D_i}{\mu} = \frac{\rho D_i v_a}{\mu} \quad . \qquad (27b)$$

To find the area ratio, the procedure begins by choosing a value of $Re_a$. The related quantities $f_a$ and $Nu_a/Pr^{1/3}(\mu/\mu_w)^{0.14}$ are then found from experimental data. Equation (26) is solved for $Re_s$, and knowing $Re_s$ and $f_s$ from equation (14), equation (24) can be solved for the resulting area ratio.

(2) External Resistance Not Equal to Zero.

(a) Constant Heat Load Constant Pumping Power. Since a sizeable portion of the overall resistance in

a naval condenser could be caused by the wall resistance and the outside thermal resistance, the area ratios as defined by Bergles [21] should be expanded to include these external resistances. If the heat flow is written by equation (2):

$$Q = U_n A_n \text{ LMTD} \quad , \tag{2}$$

and a thin wall thickness is assumed, then the external resistance effects on the area ratio can be included in the analysis. The wall thickness must be assumed to be small since the nominal area is based on an outside diameter of 15.9 mm.

Invoking all of the assumptions made earlier, then the results of the constant pumping power case are again:

$$\frac{A_a}{A_s} = \frac{v_s^3 f_s}{v_a^3 f_a} \quad . \tag{21}$$

In addition, constant heat flow results in:

$$\frac{A_a}{A_s} = \frac{U_s}{U_a} \quad . \tag{28}$$

As before, these two area ratios can be set equal, and it is found that:

$$\frac{A_a}{A_s} = \frac{U_s}{U_a} = \frac{v_s^3 f_s}{v_a^3 f_a} \quad . \tag{29}$$

As mentioned by Search [1] , for smooth tubes, it is found in general that the overall heat transfer coefficient can be

correlated by:

$$U_s = C\sqrt{v_s} = F_1F_2F_3C'\sqrt{v_s} \qquad (30)$$

where

$C'$ = empirically determined coefficient

$F_1$ = cleanliness correction factor

$F_2$ = material correction factor

$F_3$ = inlet water correction factor.

Therefore, C is a coefficient which varies with tube size, material and water inlet temperature. Also, from equation (14), it is known that

$$f_s = \frac{.046}{Re_s^{0.2}} \quad . \qquad (14)$$

When equations (14) and (30) are substituted into equation (29), together with the use of equation (27a), the smooth tube velocity can be found:

$$v_s = \left[\frac{f_a v_a^3 C}{(U_a)(.046)} \left(\frac{\rho D_i}{\mu}\right)^{1/5}\right]^{\frac{1}{2.3}} \quad . \qquad (31)$$

To find the area ratio, the procedure begins by choosing a value of $v_a$. The related values of $U_a$ and $f_a$ are found from experimental data. Equation (31) is then solved for $v_s$ and this value is used in equation (30) to find $U_s$. Equation (29) is then solved for the area ratio.

In selecting the values of the constants to substitute into equation (31), the following procedures were utilized:

(1) $U_a$ was corrected to 21.1°C coolant inlet temperature using the procedure defined in reference [22],

(2) C' was determined by using the values of $U_n$ and $v_s$ for the smooth copper-nickel tube in Run 7, and solving for C' in equation (30) with application of correction factors defined in reference [22]. The value for C' was not a constant over the range of flows observed; therefore, an average volue of C' = 2883 was computed and used. As mentioned above, C varies for a given tube size, material and water inlet temperature. The related correction factors obtained from reference [23] were applied to the above value of C' as shown in Appendix B, the sample calculations.

(3) The dynamic viscosities used were obtained in the data reduction program at each flow point.

The area ratio equations were added to the data reduction program. The values obtained above using both equations (24) and (29) appear in the table of results for each tube.

6. Data Reduction Computer Program

An existing computer program of Reilly [11] for reduction of data was modified to include the area ratio equations (24) and (29), and to convert the results to SI units. Details of the program may be found in Reilly [11].

# IV. RESULTS AND DISCUSSION

## A. INTRODUCTION

Table III lists the various runs made and the corresponding tubes used during these tests. Table IV lists special characteristics of the TURBOTEC and KORODENSE tubes. Tables V through XVII contain all the raw data used to evaluate the performance of the enhanced and smooth tubes.

In Table III it can be seen that all runs for tubes K-1 through K-5 were data runs. Run 10 for tube K-3 was not a full data run as the thermocouple measuring tube wall temperature detached about halfway through the run. Therefore, the thermocouple was reattached and the tube was retested during run 13.

Tube T-1 was initially run solely for practice of system operation and not for data. Run 4 was the data run for tube T-1, while runs 18 and 19 were performed to take movies of the alternate flooding and draining phenomena of the condensate. Similar movies were taken to compare this tube to tubes T-3a and T-3b.

Tube T-2 was observed to vibrate visually and audibly at its maximum cooling water flow rates. Tube T-3a was also observed to vibrate during data run 6. The onset of vibration of tube T-3a occurred at much lower cooling water flow rates than for tube T-2. Run 16 was conducted to take movies of this phenomena. Movies were made with varying cooling water

flow rates through the tube to observe the initiation of tube vibration. This was done both with and without steam condensing on the tube. Vibration was observed to begin visually at a cooling water velocity of about 1 m/sec when steam was not supplied to the condenser. With steam supplied however, vibration was not visually detectable until velocities of about 3 m/sec. This was felt to be due to the damping effect of the added mass of the condensate flooding the tube grooves. Audible evidence of the vibration was heard both with and without steam supplied to the condenser at cooling water velocities of about 1.8 m/sec and above.

It was decided to run the Low Pitch TURBOTEC (T-3b) with additional supports to see if the vibration could be controlled, and to observe the effect on tube performance. For run 17 the 1 meter active length of the tube was supported by two circular braces equally spaced such that the active length was reduced to three equal lengths of 1/3 meter each. Again, during this run, movies were made of the condensation process. No vibration was observed either visually or audibly. Copies of the 16 mm movie film showing the vibration phenomena, both with and without condensation taking place, are available on request.

Figures 18 and 19 also illustrate the phenomena mentioned above. As a note of clarification, the reader may wish to refer to Figure 5 while studying Figures 18 and 19. The pictures are views upward between the smooth dummy half-tube and the smooth dummy whole tube below it, such that the

bottom of the enhanced tube can be seen just below the smooth dummy half-tube. Figure 18 shows condensation on tube T-3a. The cooling water velocity is 3 m/sec. A drop of condensate can be seen falling off the tube on the left side of the photograph. On the right side, the condensate can be seen to be building up to form a drop. Notice that all grooves are flooded with condensate. It was also observed that the condensate on the tightly pitched tube T-3 dropped off of the tube between the flute tips. In contrast to this, condensate on the longer pitched tube T-1 was observed to begin drop growth in the groove space between flute tips, but as the drop grew in size it would slide over and drop off of the flute tip. This phenomena is easily observed in the 16 mm movie film, mentioned earlier, and the reader is urged to request a copy of this film if further study is desired. Figure 19 shows a view of condensate on tube T-3a with a higher cooling water velocity of 4 m/sec. The light reflections off the surface of the condensate in the figure are due to surface ripples on the condensate from the vibration.

Tubes S-1 and S-2 were smooth tubes run to ensure that earlier experimental results for smooth tubes could be duplicated. Run 2 for tube S-1a was conducted without properly cleaning the outside of the tube, leaving it with a stained appearance. This tube is designated as "fouled" in Table III. For run 7, the tube was properly prepared in accordance with the procedure outlined by Pence [10], and this tube, S-1b, is designated as "clean" in Table III. Tube S-2

was an additional smooth tube picked at random from a lot of tubes manufactured by Alaskan Copper Works. This tube was observed to have a surface that appeared to have roller marks from the manufacturing process, giving it a "rippled" look, and is designated as such in Table III. The ripples were measured to be about a maximum of 0.03 mm in depth. It should be noted that this tube is not an enhanced tube, and was tested to see if the roller marks would have an effect on the tube's performance when compared to the other smooth tubes mentioned above.

Tube GA-2 was a tube manufactured by General Atomic Company and was one of the tubes tested by Reilly [11]. This tube was re-run here as run 3 which was performed for further practice in system operation and to gain a few data points to confirm the reproducibility of his results.

The computer results of all data runs are provided in Tables XVIII through XXX.

## B. SMOOTH TUBE RESULTS

Comparative plots of smooth tube parameters are provided in Figures 20 through 25. Figure 20 shows that the corrected overall heat transfer coefficient versus cooling water mass flow rate of all the smooth tubes matches the results of Reilly [11] within an uncertainty of ±7 percent. The variation of the corrected overall heat transfer coefficient for tube S-1a "fouled" is related to the variance of the outside heat transfer coefficient seen by comparing the results

shown in Tables XVIII and XIX. The reason for this variance in the "fouled" tube is not clear. It could be that improper preparation of tube S-1a renders this set of data unreliable as evidenced by the variations in the outside heat transfer coefficient.

Comparison of the corrected pressure drop versus cooling water mass flow rate, shown by Figure 21, reveals that the effect of the "ripples" on tube S-2 is carried through to the tube's inside surface. The slight increase of the corrected pressure drop compared to that for tube S-1b "clean" is evident at flow rates above about 0.4 kg/sec and reaches a value of about 6.6 percent at a flow rate of 1.06 kg/sec. This is still seen to be within the uncertainly band, and indicates that this tube does not suffer a severe degradation in performance due to the "rippling."

As seen in Tables XVIII, XIX and XX, the Sieder-Tate coefficient for all of the smooth tubes was about 0.025, which is the same as that reported by Reilly [11], and is within ±8 percent of the values of .023 or .027, which are most often found in the literature. Figure 22 shows that the linear regression subroutine used to obtain the slope for the Wilson plot fit the S-1b tube (run 7, "clean") data very well. Variations reflect minor changes in the bulk properties of the cooling water. The constancy of the Sieder-Tate coefficient used in the Nusselt relation over the range of flows is further shown in Figure 23.

The effect of the increased corrected pressure drop for tube S-2 "rippled" is also seen in Figure 24, which shows the fanning friction factor versus Reynolds number. At higher Reynolds numbers, tube S-2 is seen to have slightly higher values of friction factor than either tubes S-1a or S-1b.

Figure 25 reflects the use of the Colburn Analogy by the use of a tube performance factor, 2j/f, versus Reynolds number. In 1883, Reynolds [24] mathematically expressed, for smooth tubes, the analogy between heat transfer and momentum transfer as:

$$St = f/2 \quad . \tag{32}$$

In 1933, Colburn [25] extended this analogy to include Prandtl number effects:

$$StPr^{2/3} = j = f/2 \quad . \tag{33}$$

It can be seen that all of the smooth tubes average about 10 percent higher than the Colburn Analogy, reflecting the uncertainty in the measured Sieder-Tate coefficients.

## C. ENHANCED TUBE RESULTS

### 1. Heat Transfer Coefficients

The corrected overall heat transfer coefficient versus cooling water mass flow rate comparisons are shown in Figures 26 and 27. Figure 26, for the TURBOTEC tubes, shows an

increase of about 100 percent in the corrected overall heat transfer coefficient over the smooth tube value at 0.6 kg/sec for tube T-3a (Run 17), and Figure 27, for the KORODENSE tubes, shows an increase of 46 percent for tube K-5 (Run 14) at the same cooling water mass flow rate. For comparison purposes, Reilly [11] reported an increase of 53 percent in corrected overall heat transfer coefficient for his 45 degree helix angle General Atomic tube at the same cooling water mass flow rate.

Of interest in Figure 26 is the effect of vibration on the TURBOTEC tube performance, as indicated by the solid data points. It can be seen that by comparing tubes T-3a (Run 6) and T-3b (Run 17), there is a significant improvement in the corrected overall heat transfer coefficient when the vibrations do not occur. As indicated earlier in the photographs, these tube vibrations cause the condensate to have surface waves which may hold up the condensate drainage off the exterior of the tube. By additng the additional tube supports, and preventing vibration, the drainage was not affected, leading to higher outside heat transfer coefficients.

Cunningham and Milne [26] reported experimental results of "roped" tubes manufactured by Yorkshire Imperial Metals, Ltd. These are similar in shape to KORODENSE tubes, but are manufactured with differing numbers of indentation (groove) starts. It was found that in geometry, the KORODENSE tube K-5 most closely resembled the "roped" tubes. Figure 28 shows how tube K-5, a 1-start tube, compares to the "roped" tubes of

Cunningham and Milne [26]. The performance of tube K-5 agrees fairly well to the "roped" tubes if the following differences are noted:

(1) differences in wall resistance - tube K-5 was made from Titanium and most likely has a higher wall resistance than that of the "YORCALBRO" alloy used in their tube [26];

(2) differences in steam conditions - steam velocities used with the "roped" tubes are not given by Cunningham and Milne [26] and no comparison can be made with the steam conditions used in these tests; and

(3) the "roped" tube experiments were conducted at atmospheric pressure (101 kPa), while the pressure used throughout these tests was maintained at about 21 kPa.

2. Pressure Drop

Figures 29 and 30 are comparisons of the corrected pressure drop versus cooling water mass flow rate for the enhanced tubes tested. It can be seen that the corrected pressure drops for the enhanced tubes increase at a faster rate than the corrected drops for the smooth tubes. For a cooling water mass flow rate of 0.6 kg/sec, tube T-3a (Run 17), Figure 29, shows a factor of 11 increase in pressure drop over that for a smooth tube while tube K-5 (Run 14), Figure 30, shows a factor of 4 increase. A cause for these increases can be seen by referring to Table IV and Figures 11 and 14. Tube K-5 has the largest helix angle and tightest pitch of the KORODENSE tubes, and tube T-3 has the largest helix angle and

tightest pitch of all the TURBOTEC tubes. These geometries increase the restrictions to internal flow, therefore increasing the pressure drops.

3. Sieder-Tate Parameters

The Wilson plots for the TURBOTEC and KORODENSE tubes are shown by Figures 31 and 32. These are provided to show how well the linear regression subroutine fits the data. Of particular interest are the solid data points shown in Figure 31. These points reflect data affected by vibration of tubes T-2 (Run 5) and T-3a (Run 6). Use of this data would have greatly affected the values obtained for the Sieder-Tate coefficient in an erroneous way. Consequently, the vibration affected data were not used in obtaining a linear regression fit. Figure 33 shows that tube T-3b (Run 17), with an average $C_i$ of .128 ± .01, reflects a factor of about 5 increase over that for a smooth tube, and that it is slightly improved over that for tube T-3a (Run 6). This indicates that the effect of tube vibration may cause deterioration of inside heat transfer as well as the deterioration of outside heat transfer mentioned earlier. From Figure 34, tube K-5 (Run 14), with a $C_i$ of about .065 ± .008, shows a factor of about 2.6 increase over the smooth tube value. These increases presumably are due to increased surface area, turbulence and swirl effects.

4. Friction Factor

The corrected pressure drop results are further reflected by Figures 35 and 36. Here, as expected, the friction

factors for the enhanced tubes are greater than for smooth tubes. Again, tube T-3b (Run 17) shows the largest friction factor overall and tube K-5 (Run 14) shows the largest friction factor for the KORODENSE tubes. Both of these tubes have large helix angles, verifying the effect of helix angle on pressure drop shown with the General Atomic tubes tested by Reilly [11]. The other KORODENSE tubes appear to have friction factors nearer to the smooth tube. For Runs 9 and 13 this is because the low pressure drop (LPD) tubes were used. Tubes for Runs 11 and 12 on the other hand, which are manufactured for maximum heat transfer (MHT), and therefore have deeper indentations, have slightly higher friction factors than LPD tubes. Tube K-5 (Run 14) however, not only has deep indentations but has a significantly smaller pitch (therefore tighter twist) than the other MHT tubes, perhaps causing its higher pressure drop performance.

5. Tube Performance Criteria

a. Colburn Analogy

As shown in section B of this chapter, the Colburn Analogy can be used to define a performance factor that directly relates heat transfer to pressure drop. Comparisons of this tube performance factor (2j/f) versus Reynolds number are shown in Figures 37 and 38. The effect of friction factor is seen to dominate heat transfer (i.e., it requires more of a pressure drop increase to get an increase in heat transfer) for all the TURBOTEC tubes which have high friction factors.

This is also true of the KORODENSE tube, K-5 (Run 14). On the other hand, tubes K-1 (Run 9) through K-4 (Run 11) have friction factors near the smooth tube results (Figure 36), and these lower friction factors give higher results in Figure 38 than tube K-5 (Run 14) agreeing closely with the Colburn Analogy. The analogy therefore appears to break down for the deeply grooved TURBOTEC tubes and for the tightly pitched, yet shallower grooved, KORODENSE K-5 tube. The reader should be cautioned that all of the above-mentioned results in Figures 37 and 38 have been obtained using a smooth inside diameter, $D_i$. If an appropriately defined hydraulic diameter, $D_h$ were used to reduce the data, it is expected that all the tube performance factors would increase, but the relative magnitudes of the performance factors would remain approximately the same.

b. Surface Area Ratios at Constant Heat Loads

Use of surface area ratios as defined by equation (24) provides an additional performance parameter more useful perhaps for the design engineer than the Colburn Analogy. As explained in Chapter III, with this area ratio method, it is essential that the additional frictional resistance of the enhanced tubes be taken into account by evaluating the area ratio for a constant pumping power. Assuming that the external thermal resistance is zero ($R_{ext} = 0$), Figure 39 shows that this area ratio makes all of the enhanced tubes appear very good for condenser use, with tube T-3b showing

the greatest reduction in required surface area. It is also seen that tube GA-2, the 45 degree helix angle General Atomic tube [11], appears to perform very much like tube T-3b. The results of this figure however, are for an external resistance equal to zero and therefore neglect the effect of wall resistance and outside resistance.

Area ratios for a nonzero external resistance can also be found, and are shown in Figure 40. Again, tube T-3b is seen to have the best overall performance. However, tube GA-2 is now seen to fall between the TURBOTEC and KORODENSE tubes, reflecting the effect of external resistance on this tube. It should be noted that the Reynolds numbers used in the surface area ratio figures are Reynolds numbers for existing smooth tube condensers ($Re_s$). For example, using a cooling water velocity of 2.74 m/sec (the maximum scoop injection velocity as specified in Reference [22]), the related smooth tube Reynolds number is calculated to be about 40,000. Entering Figure 40 with this Reynolds number, it is seen that tube T-3b would allow for approximately a 53 percent reduction in the required surface area.

c. Internal and External Performance

Table XXXI gives ratios of the average Sieder-Tate coefficients for the augmented tube data ($\overline{C}i_a$) to that of smooth tube data ($\overline{C}i_s$), and average outside heat transfer coefficients for the augmented tube data ($\overline{h}o_a$) to that of smooth tube data ($\overline{h}o_s$) for each of the tube types. Since

increases in corrected overall heat transfer coefficient are related to enhancement of both the inside and outside heat transfer coefficients together, it is clear again that tube T-3b gives the best overall performance. This condfirms the low area ratios observed for this tube in Figures 39 and 40.

Further study of Tables IV and XXXI indicate that the inside and outside heat transfer coefficients are related to change in pitch (for approximately constant groove depth). This is reflected in Figure 41. In this figure, values of the ratios of $\overline{C}i_a/\overline{C}i_s$ and $\overline{h}o_a/\overline{h}o_s$ (from Table XXXI) are plotted versus varying pitch (for constant groove depth). The trends of the data in the $\overline{C}i_a/\overline{C}i_s$ curve reveal that there is perhaps an optimum pitch (at a constant groove depth) to increase the inside heat transfer coefficient. This could be due to the fact that as pitch changes from being very large to very small, the nature of the internal flow changes from predominately swirling motion to turbulent mixing. The optimum pitch could therefore be the one that produces a combination of both these mechanisms. That outside heat transfer improves with decreased pitch is seen in the $\overline{h}o_a/\overline{h}o_s$ curve. With reduced pitch, condensate drainage improves and more channels are provided presenting more tube surface area to the steam flow. The variations in $\overline{h}o_a/\overline{h}o_s$, as noted in Table XXXI, may be caused partially by the uncertainly in the wall resistance used in the Wilson plot technique. Calculation of the actual wall resistance for an enhanced tube with severe corrugations requires a complicated analysis.

It should also be noted that the relative positions of the data for the KORODENSE, General Atomic and TURBOTEC tubes in Figure 41 are related to their respective average groove depths.

The results discussed above show correlation with the work of Catchpole and Drew [5]. Comparison with their data for a groove depth of 0.6 mm with data shown in Figure 41 shows that there is good general agreement. In their results for the 0.6 mm groove depth, decreasing pitch from about 12.8 mm to 6.4 mm increased the $\overline{Ci}_a/\overline{Ci}_s$ ratio from 2.1 to 2.6, and this same decrease in pitch followed the same trend of Figure 41 for increasing the outside heat transfer coefficient, with a maximum $\overline{ho}_a/\overline{ho}_s$ ratio of about 1.7 for their 0.6 mm groove depth tube.

## V. CONCLUSIONS

As a result of the above-mentioned tests, the following conclusions are reached.

1. All of the enhanced tubes herein tested would allow for a savings of condenser surface area. Again, related to an earlier example, for a naval condenser with a scoop injection velocity of 2.74 m/sec (9ft/sec) the corresponding smooth tube Reynolds number , is calculated to be about 40,000. Entering Figure 40 with this Reynolds number, it is seen that enhanced tubes would allow for condenser surface areas varying from 83 percent to 47 percent of the smooth tube condenser surface area.

2. The maximum corrected overall heat transfer coefficient was obtained with tube T-3b, and was about 2 times that of the corresponding smooth tube. This is a result of this tube's highest combined improvement in the inside heat transfer coefficient ($\overline{Ci}_a/\overline{Ci}_s$) = 5.0) and the outside heat transfer coefficient ($\overline{ho}_a/\overline{ho}_s$ = 1.3).

3. The largest pressure drops measured for all the enhanced tubes were for tube T-3b. This is due to this tube's severe geometric deformation, presenting the highest degree of restriction to cooling water flow.

4. The best surface area ratios were for tubes T-3b, T-4 and T-2. Again, this is due to these tubes' combined

improvement in the inside and outside heat transfer coefficents for their respective pressure drops. As a result of its lower outside heat transfer coefficient, tube GA-2 was seen to have a higher surface area ratio when external resistance was taken into account. An improvement on this tube could be made however, if its outside heat transfer coefficient was increased.

5. The effect of pitch, which relates to helix angle, (with constant groove depth) on improved heat transfer performance was displayed. The data shows that $\overline{C}i_a/\overline{C}i_s$ could possibly achieve an optimum value for a properly chosen pitch. This could be due to the fact that the choice of pitch could provide the best combination of internal flow swirl and turbulence. The fact that decreasing pitch improves the outside heat transfer coefficient by improving condensate drainage and presenting more tube surface to the steam flow was also determined.

6. Based upon $D_i$ (and not $D_h$) the Colburn Analogy was found to be valid for tubes K-1, K-2, K-3, and K-4; and invalid for deep grooved, and/or tightly pitched tubes.

7. Tube vibration was seen to cause a decrease in the corrected overall heat transfer coefficient for several of the TURBOTEC tubes. This decrease could be caused by the hold up of condensate in the grooves, affecting condensate drainage, as well as by a deterioriation in the inside heat transfer coefficient.

## VI. RECOMMENDATIONS

From the results of this experiment, several unanswered questions can be posed. In an effort to offer ideas for continued use of the test facility, the following recommendations are made.

1. Further investigate the parameters (pitch, groove depth and helix angle) in an attempt to find the desired combination of these parameters that will produce the optimum tube. Along with this effort, newly conceived enhanced tubes should be tested and ranked with those previously tested.

2. Tests of the General Atomic 45 degree helix tube, the KORODENSE Titanium-MHT tube, and the TURBOTEC Low Pitch tube should be expanded to include tests of horizontally mounted tubes in vertical banks. This is needed to determine the effect of condensate drainage from tubes at the top of the bank on the heat transfer coefficient of the tubes near the bottom of the bank.

3. The fouling characteristics of any tube under test should be determined. This includes the cooling water side as well as the steam side. Fouling could prove to be especially critical in the use of tubes with geometries that have possible cooling water flow stagnation areas such as tightly spiralled tubes.

4. In addition to geometric enhancement, tests should be conducted to determine the effectiveness of dropwise condensation promoters. These could be applied to tubes such as those manufactured by General Atomic Company to improve the outside heat transfer coefficient and therefore the tubes' overall performance.

5. Tests should be performed using TURBOTEC tubes of copper-nickel. This would provide stronger tubes than those tested in this experiment, and should decrease the tendency toward vibration with decreased pitch as found with copper 122.

6. Testing of enhanced tubes should be done in a vertical orientation. This would determine the effect of condensate drainage vertically rather than horizontally off the tube's surface which has been shown to be very effective using refrigerants [7,8].

# VII. TABLES

Table I. Location of Stainless Steel Sheathed Copper Constantan Thermocouples.

| Channel Number | Location | Channel Number | Location |
|---|---|---|---|
| 40 | $Tc_i$ | 47 | $T_v$ |
| 41 | $Tc_o$ | 48 | $T_v$ |
| 42 | $Tc_o$ | 49 | $T_v$ |
| 43 | $Tc_o$ | 50 | $T_v$ |
| 44 | $Tc_o$ | 51 | $T_w$ |
| 45 | $T_v$ | 52 | Hotwell |
| 46 | $T_v$ | | |

Table II. Location of Teflon Coated Copper Constantan Thermocouples

| Channel Number | Location | Channel Number | Location |
|---|---|---|---|
| 1 | Hot Well | 6 | Condensate Header |
| 2 | Feedwater Tank | 7 | $T_c$ into Cooling Tower |
| 3 | Condenser Window | 8 | $T_c$ out of Cooling Tower |
| 4 | $Tc_i$ | 9 | Cooling Tower Ambient |
| 5 | $Tc_o$ | | |

Table III. Summary of Test Tubes

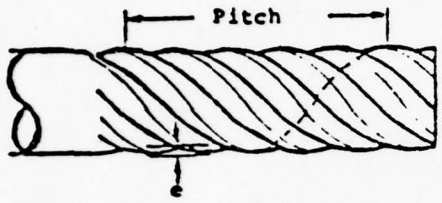


TURBOTEC Schematic

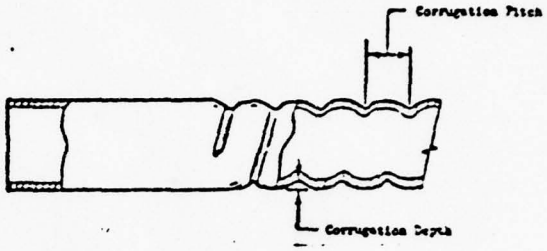


KORODENSE Schematic

| Tube No. | Tube Type | Helix (a) Angle (Deg) | No. of Groove Starts n | Groove Depth (mm) e | Pitch (mm) p | $p/D_o$ | $e/D_o$ |
|---|---|---|---|---|---|---|---|
| | TURBOTEC | | | | | | |
| T-1 | High Pitch | 30 | 3 | 2.67 | 50.48 | 3.18 | 0.168 |
| T-2 | Medium Pitch | 45 | 3 | 3.25 | 36.78 | 2.32 | 0.205 |
| T-3 a&b | Low Pitch | 60 | 3 | 3.35 | 22.58 | 1.42 | 0.211 |
| T-4 | Variable Pitch | 40/60 | 3 | 3.23 | 37.31/ 23.97 | 2.35/ 1.51 | 0.203/ 0.214 |
| | KORODENSE | | | | | | |
| K-1 | CuNi-LPD | 65 | 1 | 0.36 | 9.81 | 0.62 | 0.022 |
| K-2 | CuNi-MHT | 70 | 1 | 0.51 | 9.64 | 0.61 | 0.032 |
| K-3 | Aℓ-LPD | 64 | 1 | 0.41 | 9.67 | 0.61 | 0.026 |
| K-4 | Aℓ-MHT | 74 | 1 | 0.58 | 9.58 | 0.60 | 0.037 |
| K-5 | Ti-MHT | 75 | 1 | 0.61 | 5.97 | 0.38 | 0.038 |

(a) Helix Angle = angle measured from tube horizontal axis to flute axis

Twist Direction: TURBOTEC - left-handed spiral
KORODENSE - right-handed spiral

# Table IV. Enhanced Tubing Characteristics

| Tube No. | Tube Type | Material | Run No. | Date | Type Run | $A_h$ ($\times 10^4$ $m^2$) | $A_c$* ($\times 10^4$ $m^2$) | $D_i$ (mm) | $D_o$ (mm) | $T_w$ (mm) | $K_w$ (W/m°C) | $R_w$ ($\times 10^6$) ($m^2$ °C/W) | $\varepsilon_c + \varepsilon_e$ |
|---|---|---|---|---|---|---|---|---|---|---|---|---|---|
| | KORODENSE | | | | | | | | | | | | |
| K-1 | CuNi-LPD | 90-10 CuNi | 9 | 13 JUL 78 | Data | 456.04 | 1.354 | 13.39 | 15.88 | 1.24 | 44.65 | 33.315 | 0.015 |
| K-2 | CuNi-MHT | 90-10 CuNi | 12 | 17 JUL 78 | Data | 456.04 | 1.316 | 13.39 | 15.88 | 1.24 | 44.65 | 30.315 | 0.030 |
| K-3 | Al-LPD | Al (3003) | 10 | 15 JUL 78 | Data | 456.04 | 1.343 | 13.39 | 15.88 | 1.24 | 172.75 | 7.836 | 0.015 |
| | | | 13 | 18 JUL 78 | Data | | | | | | | | |
| K-4 | Al-MHT | Al (3003) | 11 | 16 JUL 78 | Data | 456.04 | 1.305 | 13.39 | 15.88 | 1.24 | 172.75 | 7.836 | 0.030 |
| K-5 | Ti-MHT | Titanium | 14 | 19 JUL 78 | Data | 456.04 | 1.409 | 14.48 | 15.88 | 0.70 | 17.00 | 43.007 | 0.075 |
| | TURBOTEC | | | | | | | | | | | | |
| T-1 | High Pitch | Cu (122) | 1 | 27 APR 78 | Practice | 456.04 | 1.296 | 14.45 | 15.88 | 0.71 | 339.22 | 2.196 | 0.145 |
| | | | 4 | 12 JUN 78 | Data | | | | | | | | |
| | | | 18 | 21 AUG 78 | Movie | | | | | | | | |
| | | | 19 | 24 AUG 78 | Movie | | | | | | | | |
| T-2 | Medium Pitch | Cu (122) | 5 | 13 JUN 78 | Data | 456.04 | 1.110 | 14.45 | 15.88 | 0.71 | 339.22 | 2.196 | 0.255 |
| T-3a | Low Pitch (u) | Cu (122) | 6 | 14 JUN 78 | Data | 456.04 | 0.842 | 14.45 | 15.88 | 0.71 | 339.22 | 2.196 | 0.475 |
| | | | 16 | 3 AUG 78 | Movie | | | | | | | | |
| T-3b | Low Pitch (s) | Cu (122) | 17 | 6 AUG 78 | Movie/Data | 456.04 | 0.842 | 14.45 | 15.88 | 0.71 | 339.22 | 2.196 | 0.475 |
| T-4 | Variable Pitch | Cu (122) | 15 | 28 JUL | Data | 456.04 | 0.963 | 14.45 | 15.88 | 0.71 | | 2.196 | 0.360 |
| | SMOOTH | | | | | | | | | | | | |
| S-1a | "fouled" | 90-10 CuNi | 2 | 11 MAY 78 | Data | 456.04 | 1.375 | 13.23 | 15.88 | 1.32 | 44.65 | 32.351 | 0.0 |
| S-1b | "clean" | | 7 | 11 MAY 78 | Data | | | | | | | | |
| S-2 | "rippled" | 90-10 CuNi | 8 | 12 JUL 78 | Data | 456.04 | 1.398 | 13.34 | 15.88 | 1.27 | 44.65 | 30.991 | 0.0 |
| GA-2 | 45° General Atomic | Al (6061) | 3 | 22 MAY 78 | Practice | 456.04 | 0.984 | 13.31 | 16.00 | 3.66 | 237.11 | 7.706 | 0.330 |

*$A_c$ was determined by measuring the liquid volume contained within the enhanced section of each tube end dividing by the enhanced section length.

Table V. Raw Data for Smooth "fouled" CuNi, Run 2, 11 MAY 78.

| % Flow | $T_v$(°C) | $T_w$(°K) | $Tc_i$(°C) | $Tc_o$(°C) | ΔP ( Pa) |
|---|---|---|---|---|---|
| 10 | 61.7 | 316.0 | 19.0 | 28.1 | 1.098 |
| 20 | 63.9 | 309.5 | 18.0 | 25.3 | 3.609 |
| 30 | 63.3 | 304.5 | 18.0 | 23.3 | 7.373 |
| 40 | 63.3 | 301.9 | 17.0 | 22.2 | 12.708 |
| 50 | 64.2 | 300.5 | 17.0 | 21.6 | 18.827 |
| 60 | 64.7 | 298.8 | 17.0 | 20.9 | 26.200 |
| 67 | 65.0 | 299.9 | 17.0 | 20.6 | 32.005 |

Table VI. Raw Data for Smooth "clean" CuNi, Run 7, 11 JUN 78.

| % Flow | $T_v$(°C) | $T_w$(°K) | $Tc_i$(°C) | $Tc_o$(°C) | ΔP ( Pa) |
|---|---|---|---|---|---|
| 10 | 67.2 | 325.7 | 19.2 | 29.3 | 1.004 |
| 15 | 66.9 | 322.7 | 19.0 | 27.6 | 2.040 |
| 20 | 66.8 | 320.3 | 19.0 | 26.6 | 3.514 |
| 30 | 67.0 | 317.0 | 19.0 | 25.0 | 7.531 |
| 40 | 67.1 | 317.1 | 19.3 | 24.3 | 12.551 |
| 50 | 67.2 | 317.0 | 19.5 | 23.8 | 18.764 |
| 60 | 67.0 | 317.3 | 19.4 | 23.2 | 25 793 |
| 70 | 66.8 | 317.8 | 19.2 | 22.6 | 34.171 |
| 80 | 66.6 | 317.4 | 19.0 | 22.2 | 43.427 |
| 90 | 66.7 | 318.6 | 18.9 | 21.8 | 53.625 |
| | | | | | |

Table VII. Raw Data for Smooth "rippled" CuNi, Run 8, 12 JUL 78.

| % Flow | $T_v$(°C) | $T_w$(°K) | $Tc_i$(°C) | $Tc_o$(°C) | ΔP (kPa) |
|---|---|---|---|---|---|
| 10 | 67.5 | 316.9 | 17.4 | 27.8 | 0.941 |
| 15 | 67.3 | 310.8 | 17.1 | 25.9 | 2.165 |
| 20 | 67.5 | 307.9 | 17.0 | 24.8 | 3.577 |
| 30 | 67.4 | 304.3 | 17.0 | 23.3 | 7.562 |
| 40 | 67.4 | 303.0 | 17.3 | 22.5 | 13.085 |
| 50 | 67.4 | 300.4 | 17.7 | 22.1 | 19.423 |
| 60 | 67.6 | 298.9 | 17.8 | 21.7 | 26.860 |
| 70 | 67.5 | 298.2 | 17.9 | 21.5 | 35.457 |
| 80 | 67.7 | 297.8 | 18.0 | 21.2 | 44.776 |
| 90 | 67.7 | 297.4 | 18.1 | 21.0 | 55.790 |

Table VIII. Raw Data for TURBOTEC Hi Pitch, Run 4, 12 JUN 78

| % Flow | $T_v$(°C) | $T_w$(°K) | $Tc_i$(°C) | $Tc_o$(°C) | ΔP (kPa) |
|---|---|---|---|---|---|
| 10 | 67.5 | 323.8 | 21.9 | 37.0 | 1.977 |
| 15 | 67.4 | 320.7 | 21.2 | 33.8 | 4.079 |
| 20 | 67.7 | 318.2 | 20.9 | 31.6 | 6.997 |
| 25 | 67.9 | 316.4 | 20.8 | 30.3 | 10.512 |
| 30 | 66.5 | 314.6 | 20.7 | 29.2 | 14.779 |
| 40 | 64.6 | 311.9 | 20.6 | 27.7 | 25.950 |
| 50 | 63.4 | 309.1 | 20.5 | 26.6 | 41.544 |
| 60 | 63.7 | 307.3 | 20.5 | 25.9 | 59.556 |
| 70 | 63.8 | 306.1 | 20.4 | 25.2 | 81.488 |
| 80 | 63.8 | 304.9 | 20.3 | 24.7 | 106.999 |
| 83.5 | 63.5 | 304.5 | 20.1 | 24.4 | 116.412 |

Table IX. Raw Data for TURBOTEC Medium Pitch, Run 5, 12 JUN 78.

| % Flow | $T_v$(°C) | $T_w$(°K) | $Tc_i$(°C) | $Tc_o$(°C) | ΔP (kPa) |
|---|---|---|---|---|---|
| 10 | 66.4 | 325.4 | 19.2 | 38.5 | 2.573 |
| 15 | 66.1 | 321.8 | 18.8 | 35.0 | 6.589 |
| 20 | 65.8 | 319.8 | 18.5 | 32.4 | 11.673 |
| 25 | 66.0 | 318.6 | 18.5 | 30.6 | 18.199 |
| 30 | 66.6 | 317.1 | 18.4 | 29.2 | 26.514 |
| 40 | 67.1 | 313.6 | 18.4 | 27.3 | 44.996 |
| 50 | 66.6 | 311.7 | 18.6 | 26.1 | 69.596 |
| 60 | 66.2 | 309.7 | 18.6 | 25.2 | 100.159 |
| 70 | 64.7 | 306.4 | 18.6 | 23.9 | 136.871 |
| 75 | 64.0 | 306.0 | 18.5 | 23.6 | 157.831 |

Table X. Raw Data for TURBOTEC Low Pitch, Run 6, 14 JUN 78.

| % Flow | $T_v$(°C) | $T_w$(°K) | $Tc_i$(°C) | $Tc_o$(°C) | ΔP (kPa) |
|---|---|---|---|---|---|
| 10 | 66.2 | 324.0 | 19.6 | 44.3 | 8.880 |
| 15 | 67.0 | 320.0 | 19.5 | 40.5 | 18.513 |
| 20 | 67.1 | 317.4 | 19.5 | 37.5 | 31.472 |
| 25 | 67.1 | 314.8 | 19.6 | 35.0 | 48.825 |
| 30 | 67.2 | 312.6 | 19.6 | 33.1 | 66.867 |
| 35 | 67.0 | 310.8 | 19.6 | 31.2 | 91.154 |
| 40 | 67.1 | 309.7 | 19.7 | 30.2 | 115.189 |
| 45 | 67.4 | 308.9 | 19.6 | 29.2 | 146.567 |
| 50 | 67.4 | 309.1 | 19.6 | 28.1 | 182.338 |
| 60 | 67.5 | 307.9 | 19.4 | 26.6 | 258.869 |

Table XI. Raw Data for TURBOTEC Variable Pitch, Run 15, 28 JUL 78.

| % Flow | $T_v$(°C) | $T_w$(°K) | $Tc_i$(°C) | $Tc_o$(°C) | ΔP (kPa) |
|---|---|---|---|---|---|
| 10 | 66.6 | 321.6 | 19.0 | 41.3 | 5.648 |
| 15 | 66.5 | 318.3 | 19.0 | 37.4 | 11.986 |
| 20 | 66.8 | 316.0 | 19.3 | 35.0 | 20.427 |
| 25 | 66.9 | 314.4 | 19.7 | 33.4 | 29.025 |
| 30 | 66.6 | 312.9 | 20.0 | 31.9 | 43.239 |
| 35 | 66.8 | 311.7 | 20.1 | 31.0 | 57.547 |
| 40 | 66.8 | 310.2 | 20.5 | 30.1 | 74.523 |
| 50 | 66.9 | 308.2 | 20.8 | 28.7 | 113.745 |
| 60 | 66.9 | 306.7 | 21.2 | 28.0 | 164.578 |
| 68&5 | 66.9 | 306.0 | 21.6 | 27.6 | 214.155 |

Table XII. Raw Data for TURBOTEC "supported" Low Pitch, Run 17, 6 AUG 78.

| % Flow | $T_v$(°C) | $T_w$(°K) | $Tc_i$(°C) | $Tc_o$(°C) | ΔP (kPa) |
|---|---|---|---|---|---|
| 10 | 66.5 | 321.9 | 20.9 | 45.2 | 7.939 |
| 15 | 66.6 | 318.0 | 20.9 | 41.4 | 14.748 |
| 20 | 66.8 | 316.1 | 21.5 | 38.9 | 30.499 |
| 25 | 66.7 | 314.7 | 22.3 | 37.3 | 46.188 |
| 30 | 67.0 | 313.6 | 23.1 | 36.2 | 65.329 |
| 35 | 66.9 | 312.5 | 23.6 | 35.1 | 88.580 |
| 40 | 66.9 | 311.7 | 24.1 | 34.4 | 112.428 |
| 45 | 66.9 | 311.4 | 24.6 | 33.9 | 141.093 |
| 50 | 67.1 | 311.1 | 25.0 | 33.5 | 173.050 |
| 57 | 67.2 | 310.8 | 25.7 | 33.1 | 220.274 |

Table XIII. Raw Data for KORODENSE CuNi-LPD, Run 9, 13 JUL 78

| % Flow | $T_v$(°C) | $T_w$(°K) | $Tc_i$(°C) | $Tc_o$(°C) | ΔP (kPa) |
|---|---|---|---|---|---|
| 10 | 66.8 | 313.7 | 19.1 | 32.1 | 1.600 |
| 15 | 66.9 | 310.5 | 19.2 | 29.9 | 3.263 |
| 20 | 66.8 | 308.5 | 19.8 | 28.8 | 5.585 |
| 25 | 67.1 | 306.5 | 19.9 | 27.8 | 8.252 |
| 30 | 66.6 | 305.6 | 19.9 | 26.9 | 11.455 |
| 40 | 66.3 | 303.8 | 19.9 | 25.5 | 18.952 |
| 50 | 66.6 | 302.7 | 19.8 | 24.7 | 27.456 |
| 60 | 66.7 | 302.2 | 20.2 | 24.5 | 37.685 |
| 70 | 66.9 | 302.4 | 20.7 | 24.5 | 48.510 |
| 80 | 67.0 | 302.6 | 21.3 | 24.7 | 60.528 |
| 88.9 | 67.0 | 302.4 | 21.9 | 24.9 | 71.573 |

Table XIV. Raw Data for KORODENSE Aℓ-LPD, Run 13, 18 JUL 78

| % Flow | $T_v$(°C) | $T_w$(°K) | $Tc_i$(°C) | $Tc_o$(°C) | ΔP (kPa) |
|---|---|---|---|---|---|
| 10 | 65.5 | 321.1 | 23.5 | 36.6 | 1.506 |
| 15 | 65.8 | 317.1 | 23.6 | 34.7 | 3.232 |
| 20 | 66.3 | 314.6 | 23.8 | 33.3 | 5.460 |
| 25 | 66.3 | 312.5 | 24.0 | 32.2 | 8.284 |
| 30 | 66.7 | 311.4 | 24.1 | 31.5 | 11.735 |
| 40 | 66.7 | 309.7 | 24.3 | 30.4 | 19.423 |
| 50 | 66.6 | 307.6 | 24.5 | 29.6 | 28.993 |
| 60 | 66.6 | 307.1 | 24.6 | 29.1 | 30.630 |
| 70 | 65.1 | 305.7 | 23.7 | 27.3 | 52.088 |
| 80 | 65.8 | 305.1 | 23.0 | 26.3 | 66.208 |

Table XV. Raw Data for KORODENSE Aℓ-MHT, Run 11, 16 JUL 78

| % Flow | $T_v$(°C) | $T_w$(°K) | $Tc_i$(°C) | $Tc_o$(°C) | ΔP (kPa) |
|---|---|---|---|---|---|
| 10 | 66.8 | 315.1 | 16.7 | 34.3 | 2.385 |
| 15 | 66.9 | 311.6 | 16.5 | 30.8 | 5.052 |
| 20 | 67.3 | 309.6 | 16.6 | 28.6 | 8.692 |
| 25 | 67.3 | 308.3 | 16.7 | 27.3 | 12.771 |
| 30 | 67.1 | 307.4 | 16.9 | 26.0 | 17.885 |
| 40 | 67.1 | 306.1 | 17.2 | 24.5 | 29.244 |
| 50 | 67.3 | 305.4 | 17.5 | 23.8 | 42.235 |
| 60 | 67.1 | 304.6 | 17.9 | 23.3 | 57.202 |
| 70 | 67.1 | 303.9 | 18.2 | 22.9 | 72.766 |
| 80 | 67.2 | 303.7 | 18.5 | 22.6 | 91.467 |

Table XVI. Raw Data for KORODENSE CuNi-MHT, Run 12, 17 JUL 78

| % Flow | $T_v$(°C) | $T_w$(°K) | $Tc_i$(°C) | $Tc_o$(°C) | ΔP (kPa) |
|---|---|---|---|---|---|
| 10 | 67.5 | 323.8 | 24.0 | 37.6 | 1.914 |
| 15 | 67.6 | 321.6 | 23.6 | 34.8 | 4.393 |
| 20 | 67.6 | 318.8 | 23.3 | 32.8 | 7.374 |
| 25 | 67.5 | 316.7 | 23.1 | 31.2 | 11.139 |
| 30 | 67.4 | 315.6 | 23.0 | 30.2 | 15.312 |
| 40 | 67.6 | 314.6 | 22.9 | 28.8 | 24.883 |
| 50 | 67.6 | 314.0 | 22.9 | 27.8 | 36.148 |
| 60 | 67.6 | 313.4 | 22.9 | 27.3 | 48.856 |
| 70 | 67.6 | 313.5 | 23.0 | 26.8 | 62.944 |
| 80 | 67.6 | 312.7 | 23.1 | 26.5 | 77.472 |

Table XVII. Raw Data for KORODENSE Ti-MHT, Run 14, 19 JUL 78

| % Flow | $T_v$(°C) | $T_w$(°K) | $Tc_i$(°C) | $Tc_o$(°C) | ΔP (kPa) |
|---|---|---|---|---|---|
| 10 | 68.3 | 328.2 | 20.7 | 35.8 | 2.353 |
| 15 | 67.9 | 327.5 | 20.9 | 33.0 | 5.554 |
| 20 | 69.0 | 326.8 | 20.5 | 30.8 | 9.947 |
| 25 | 67.0 | 326.7 | 21.4 | 30.2 | 15.595 |
| 30 | 67.2 | 326.6 | 22.3 | 29.7 | 22.341 |
| 40 | 67.2 | 326.4 | 22.8 | 28.8 | 38.438 |
| 50 | 67.2 | 326.1 | 23.0 | 28.1 | 58.834 |
| 60 | 67.0 | 326.0 | 23.4 | 27.7 | 82.713 |
| 70 | 67.1 | 326.0 | 23.6 | 27.4 | 110.043 |
| 80 | 67.4 | 325.8 | 23.8 | 27.3 | 139.067 |

## Table XVIII. Smooth "fouled" Copper-Nickel Results (Tube No. S-1a), Run 2

| VELOCITY M/SEC | UA W/(C*M**2) | UC W/(C*M**2) | HI W/(C*M**2) | HO W/(C*M**2) |
|---|---|---|---|---|
| 0.86 | 2578.181 | 2812.784 | 4276.855 | 13328.125 |
| 1.72 | 3760.523 | 4281.375 | 7238.723 | 14738.506 |
| 2.55 | 4035.515 | 4642.000 | 9814.387 | 10730.309 |
| 3.45 | 5207.305 | 6262.242 | 12185.671 | 16328.133 |
| 4.31 | 5504.438 | 6696.988 | 14477.785 | 15046.238 |
| 5.17 | 5601.059 | 6840.559 | 16635.094 | 13500.141 |
| 5.78 | 5635.047 | 6891.320 | 18209.602 | 12621.191 |

| REYNOLDS NO | PLAIN END REYN NO | FLOW RATE PER AREA KG/(SEC*M**2) | FRICTION FACTOR | SIEDER TATE CONSTANT |
|---|---|---|---|---|
| 12641.18 | 12641.17 | 858.15 | 0.00761073 | 0.02443808 |
| 24278.25 | 24278.24 | 1717.43 | 0.00615840 | 0.02455489 |
| 35620.24 | 35620.21 | 2576.95 | 0.00562853 | 0.02461505 |
| 46432.61 | 46432.56 | 3437.03 | 0.00550472 | 0.02466484 |
| 57604.84 | 57604.82 | 4296.73 | 0.00519661 | 0.02470686 |
| 68647.38 | 68647.38 | 5156.56 | 0.00502331 | 0.02472716 |
| 76351.88 | 76351.81 | 5758.47 | 0.00492223 | 0.02473880 |

# Table XVIII. Page 2

| NUSSELT NO | NU/PR1/3(U/LW)0.14 | STANTON NO | J FACTOR | PERFORM FACTOR |
|---|---|---|---|---|
| 89.26293 | 46.71525 | 0.00115060 | 0.0038995 | 1.0247335 |
| 151.76073 | 79.12450 | 0.00100660 | 0.0034001 | 1.1042223 |
| 206.21593 | 107.80220 | 0.00090957 | 0.0031239 | 1.1100168 |
| 256.72876 | 133.62505 | 0.00084658 | 0.0029579 | 1.0746927 |
| 305.28638 | 158.92203 | 0.00080451 | 0.0028271 | 1.0880566 |
| 351.06445 | 183.00517 | 0.00077020 | 0.0027209 | 1.0833006 |
| 384.47363 | 199.35751 | 0.00075495 | 0.0026751 | 1.0869360 |

| XIA | PRESSURE DROP (KPA) | PRANDTL NO | L/UW | DOTMS(KG/SEC) |
|---|---|---|---|---|
| 0.21556930-03 | 0.77832 | 5.92566 | 1.05511 | 0.1180370 |
| 0.16285160-03 | 2.52072 | 6.20621 | 1.04328 | 0.2362167 |
| 0.12012340-03 | 5.18527 | 6.36467 | 1.03220 | 0.3544374 |
| 0.96754550-04 | 9.01836 | 6.53106 | 1.02784 | 0.4727324 |
| 0.81440080-04 | 13.30386 | 6.58747 | 1.02475 | 0.5909770 |
| 0.70880560-04 | 18.52040 | 6.63986 | 1.02061 | 0.7092397 |
| 0.64752760-04 | 22.63042 | 6.67006 | 1.02453 | 0.7920263 |

## Table XIX. Smooth "clean" Copper-Nickel Results (Tube No. S-1b), Run 7

| VELOCITY M/SEC | UA W/(C*M**2) | UC W/(C*M**2) | HI W/(C*M**2) | HO W/(C*M**2) |
|---|---|---|---|---|
| 0.86 | 2551.070 | 2780.545 | 4480.840 | 10876.596 |
| 1.29 | 3216.989 | 3590.677 | 6119.797 | 12124.633 |
| 1.72 | 3751.287 | 4269.406 | 7635.596 | 12966.082 |
| 2.59 | 4381.453 | 5105.063 | 10426.012 | 12372.559 |
| 3.45 | 4814.906 | 5703.281 | 13111.527 | 11526.855 |
| 4.31 | 5057.223 | 6046.449 | 15652.320 | 11268.266 |
| 5.17 | 5376.238 | 6508.176 | 18086.816 | 11451.156 |
| 6.04 | 5563.680 | 6814.652 | 20436.492 | 11358.102 |
| 6.90 | 5948.414 | 7365.871 | 22674.238 | 12069.320 |
| 7.76 | 6061.363 | 7539.852 | 24953.184 | 11826.770 |

| REYNOLDS NO | PLAIN END REYN NO | FLOW RATE PER AREA KG/(SEC*M**2) | FRICTION FACTOR | SIEDER TATE CONSTANT |
|---|---|---|---|---|
| 12783.24 | 12783.23 | 858.00 | 0.00670025 | 0.02490020 |
| 18794.32 | 18794.32 | 1287.35 | 0.00602937 | 0.02495878 |
| 24790.90 | 24790.88 | 1716.75 | 0.00594483 | 0.02499033 |
| 36557.66 | 36557.66 | 2575.64 | 0.00581531 | 0.02504044 |
| 48531.84 | 48531.81 | 3434.67 | 0.00543385 | 0.02505326 |
| 60417.05 | 60417.00 | 4293.60 | 0.00519792 | 0.02506532 |
| 71967.81 | 71967.81 | 5152.86 | 0.00493744 | 0.02506707 |
| 83229.00 | 83229.00 | 6012.43 | 0.00469504 | 0.02511301 |
| 94466.19 | 94466.19 | 6872.02 | 0.00467473 | 0.02513338 |
| 105719.50 | 105719.50 | 7731.59 | 0.00455644 | 0.02514869 |

## Table XIX. Page 2

| [illegible] NO | NU/PR1/3(U/UW)C.14 | STANTON NO | J FACTOR | PERFORM FACTOR |
|---|---|---|---|---|
| [illegible] | 48.03020 | 0.00124804 | 0.0040508 | 1.2091541 |
| [illegible] | 65.53058 | 0.00113583 | 0.0037432 | 1.2416630 |
| [illegible] | 81.88513 | 0.00106266 | 0.0035309 | 1.1878777 |
| [illegible] | 111.95006 | 0.00096691 | 0.0032546 | 1.1193342 |
| [illegible] | 140.50266 | 0.00091188 | 0.0030796 | 1.1334839 |
| [illegible] | 167.45440 | 0.00087079 | 0.0029500 | 1.1350613 |
| [illegible] | 192.82350 | 0.00083839 | 0.0028562 | 1.1569414 |
| [illegible] | 216.82935 | 0.00081181 | 0.0027841 | 1.1578789 |
| [illegible] | 240.14354 | 0.00078759 | 0.0027166 | 1.1622629 |
| [illegible] | 262.93091 | 0.00077075 | 0.0026678 | 1.1709919 |

| XIA | PRESSURE DROP (KPA) | PRANDTL NO | L/LA | DOTMS(KG/SEC) |
|---|---|---|---|---|
| 0.26648240-03 | 0.68505 | 5.84756 | 1.07813 | 0.1180096 |
| 0.19659470-03 | 1.38747 | 5.98276 | 1.07357 | 0.1770688 |
| 0.15756530-03 | 2.43241 | 6.05663 | 1.06958 | 0.2361299 |
| 0.11540620-03 | 5.35503 | 6.17554 | 1.06282 | 0.3542839 |
| 0.91771560-04 | 8.89615 | 6.20627 | 1.06274 | 0.4724084 |
| 0.76675510-04 | 13.25750 | 6.23521 | 1.06405 | 0.5905461 |
| 0.66530270-04 | 18.19075 | 6.28796 | 1.06601 | 0.7087305 |
| 0.58882930-04 | 24.11877 | 6.35115 | 1.06868 | 0.8269585 |
| 0.53073100-04 | 30.62531 | 6.40126 | 1.06865 | 0.9451854 |
| 0.46226500-04 | 37.78212 | 6.43960 | 1.07266 | 1.0634117 |

Table XX. Smooth "rippled" Copper-Nickel Results (Tube No. S-2), Run 8

| VELOCITY M/SEC | LA W/(C*M**2) | UC W/(C*M**2) | HI W/(C*M**2) | HO W/(C*M**2) |
|---|---|---|---|---|
| 0.85 | 2507.875 | 2719.217 | 4312.445 | 10905.477 |
| 1.27 | 3145.711 | 3485.510 | 5833.457 | 12073.676 |
| 1.70 | 3652.149 | 4118.270 | 7259.043 | 12686.930 |
| 2.55 | 4329.695 | 5000.695 | 9852.945 | 12557.121 |
| 3.40 | 4706.750 | 5510.563 | 12366.640 | 11714.883 |
| 4.25 | 5029.652 | 5956.422 | 14658.504 | 11515.875 |
| 5.10 | 5341.840 | 6401.625 | 16916.852 | 11649.852 |
| 5.94 | 5641.773 | 6837.227 | 19066.727 | 11920.914 |
| 6.79 | 5737.844 | 6976.836 | 21201.586 | 11475.785 |
| 7.64 | 5935.281 | 7273.105 | 23264.711 | 11584.539 |

| REYNOLDS NO | PLAIN END REYN NO | FLOW RATE PER AREA KG/(SEC*M**2) | FRICTION FACTOR | SIEDER TATE CONSTANT |
|---|---|---|---|---|
| 12241.36 | 12241.36 | 845.43 | 0.00640622 | 0.02517331 |
| 17942.57 | 17942.58 | 1268.57 | C.CC695294 | 0.02524173 |
| 23611.58 | 23611.57 | 1691.75 | 0.00640115 | 0.02528082 |
| 34817.05 | 34817.05 | 2538.23 | 0.00614132 | 0.02533179 |
| 46153.02 | 46152.99 | 3384.58 | C.00604364 | 0.02534920 |
| 57723.41 | 57723.39 | 4230.70 | C.00572763 | C.C2534753 |
| 69057.31 | 69057.25 | 5077.05 | C.C0549C50 | C.C2535665 |
| 80405.81 | 80405.75 | 5923.38 | C.00532453 | 0.02536249 |
| 91718.75 | 91718.69 | 6769.76 | C.00513339 | 0.02536630 |
| 103126.00 | 103125.94 | 7616.04 | C.00506665 | C.02536996 |

## Table XX. Page 2

| NUSSELT NO | NU/PR1/3(U/UW)0.14 | STANTON NO | J FACTOR | PERFORM FACTOR |
|---|---|---|---|---|
| 50.85431 | 46.90327 | 0.00121665 | C.CC4C642 | 1.2688131 |
| 333.23285 | 63.86072 | 0.00109840 | 0.0037280 | 1.CEC1144 |
| 153.58606 | 79.66914 | 0.00102481 | C.CC35132 | 1.C976677 |
| 2C5.73592 | 1C8.91785 | 0.00C93C75 | C.0C32324 | 1.0526867 |
| 242.78ECS | 136.55585 | 0.00087392 | 0.0030486 | 1.008.444 |
| 311.81C06 | 163.31151 | 0.00082562 | 0.0C28928 | 1.0101194 |
| 356.55654 | 188.56353 | 0.00079564 | 0.0027807 | 1.0125251 |
| 4C5.1354C | 213.02852 | 0.00076941 | 0.0026931 | 1.0115747 |
| 45C.13306 | 236.73218 | 0.0007478C | C.0C26213 | 1.0212736 |
| 493.56602 | 260.02366 | 0.00072935 | 0.0025578 | 1.C092764 |

| XIA | PRESSURE DROP (KPA) | PRANCTL NC | L/LA | DCTPS(KG/SEC) |
|---|---|---|---|---|
| C.27674622C-C3 | 0.63076 | 6.05025 | 1.06071 | C.1160734 |
| C.20CC847C-03 | 1.52976 | 6.25276 | 1.04745 | C.17717C2 |
| C.16562C3C-C3 | 2.52236 | 6.34720 | 1.C412C | C.2362716 |
| C.1215335C-C3 | 5.44626 | 6.47216 | 1.03325 | 0.3544927 |
| C.97CC6795-C4 | 5.52901 | 6.51530 | 1.03032 | C.4726552 |
| C.81ECC7EC-C4 | 14.11046 | 6.51117 | 1.C2246 | C.55C8645 |
| C.71C7483C-C4 | 19.47865 | 6.53384 | 1.01838 | 0.7C50670 |
| C.62955200-C4 | 25.71184 | 6.5484C | 1.01653 | 0.8272675 |
| C.5671181C-04 | 32.37816 | 6.56251 | 1.01555 | 0.9454739 |
| C.51682C3C-04 | 4C.46204 | 6.567C5 | 1.01444 | 1.0636654 |

Table XXI. TURBOTEC High Pitch Results (Tube No. T-1), Run 4

| VELOCITY M/SEC | UN W/(C*M**2) | UC W/(C*M**2) | HI W/(C*M**2) | HO W/(C*M**2) |
|---|---|---|---|---|
| 0.72 | 4345.867 | 4387.746 | 6961.398 | 14261.211 |
| 1.08 | 5173.234 | 5232.688 | 9453.379 | 13348.801 |
| 1.45 | 5605.344 | 5675.211 | 11740.141 | 12100.102 |
| 1.81 | 6083.211 | 6165.590 | 13914.676 | 12011.875 |
| 2.17 | 6661.199 | 6760.105 | 15970.797 | 12634.234 |
| 2.89 | 7628.879 | 7758.883 | 19869.020 | 13586.664 |
| 3.61 | 8229.887 | 8381.391 | 23488.238 | 13784.102 |
| 4.34 | 8597.719 | 8763.203 | 26987.008 | 13621.789 |
| 5.06 | 8839.641 | 9014.664 | 30357.059 | 13378.457 |
| 5.78 | 9253.152 | 9445.113 | 33607.902 | 13662.793 |
| 6.04 | 9327.500 | 9522.582 | 34683.043 | 13634.508 |

| REYNOLDS NO | PLAIN END REYN NO | FLOW RATE PER AREA KG/(SEC*M**2) | FRICTION FACTOR | SIEDER TATE CONSTANT |
|---|---|---|---|---|
| 13091.02 | 13091.01 | 718.06 | 0.02607292 | 0.04356441 |
| 18877.66 | 18877.66 | 1077.82 | 0.02383088 | 0.04376480 |
| 24513.09 | 24513.07 | 1437.72 | 0.02303237 | 0.04390023 |
| 30196.27 | 30196.25 | 1797.58 | 0.02219686 | 0.04367545 |
| 35789.34 | 35789.31 | 2157.52 | 0.02166928 | 0.04403932 |
| 46917.60 | 46917.60 | 2877.45 | 0.02148015 | 0.04412690 |
| 57873.93 | 57873.90 | 3597.55 | 0.02217391 | 0.04419569 |
| 68930.00 | 68930.00 | 4317.55 | 0.02213186 | 0.04423466 |
| 79748.63 | 79748.63 | 5037.77 | 0.02232075 | 0.04427816 |
| 90575.19 | 90575.25 | 5757.55 | 0.02250340 | 0.04431063 |
| 93982.63 | 93982.63 | 6010.43 | 0.02248217 | 0.04434135 |

## Table XXI. Page 2

| NUSSELT NO | NU/PR1/3(U/UW)0.14 | STANTON NO | J FACTOR | PERFORM FACTOR |
|---|---|---|---|---|
| 156.30679 | 85.64661 | 0.00231856 | 0.0069142 | 0.5303742 |
| 213.23642 | 115.31424 | 0.0020976E | 0.0064439 | 0.5407984 |
| 265.63745 | 142.55551 | 0.0019520E | 0.0061201 | 0.5314314 |
| 315.37891 | 168.72205 | 0.00185024 | 0.0058658 | 0.5285262 |
| 362.50706 | 193.57210 | 0.00176919 | 0.0056620 | 0.5225787 |
| 451.88647 | 240.86383 | 0.00165012 | 0.0053493 | 0.4982729 |
| 535.03198 | 285.34180 | 0.00156007 | 0.0051087 | 0.4807866 |
| 615.27148 | 328.46411 | 0.00149346 | 0.0049185 | 0.4444761 |
| 692.78540 | 369.45972 | 0.00143969 | 0.0047717 | 0.4275557 |
| 767.53540 | 409.36865 | 0.00139443 | 0.0046436 | 0.4127043 |
| 792.63867 | 421.93506 | 0.00137853 | 0.0046113 | 0.4102182 |

| XIN | PRESSURE DROP (KPA) | PRANDTL NO | U/UW | DOTMS(KG/SEC) |
|---|---|---|---|---|
| 0.28023736-03 | 1.71268 | 5.14975 | 1.05683 | 0.1177993 |
| 0.20639586-03 | 3.52454 | 5.38646 | 1.05490 | 0.1766167 |
| 0.16621036-03 | 6.05854 | 5.55143 | 1.05237 | 0.2358615 |
| 0.14024336-03 | 9.12524 | 5.64485 | 1.04981 | 0.2948965 |
| 0.12219386-03 | 12.83053 | 5.72517 | 1.04683 | 0.3539453 |
| 0.98226306-04 | 22.61676 | 5.83685 | 1.04199 | 0.4720519 |
| 0.83095136-04 | 36.48749 | 5.92586 | 1.03617 | 0.5901853 |
| 0.72324156-04 | 52.44830 | 5.97675 | 1.03218 | 0.7083027 |
| 0.64297226-04 | 72.00645 | 6.03403 | 1.02998 | 0.8264572 |
| 0.58079336-04 | 94.82741 | 6.07707 | 1.02743 | 0.9446105 |
| 0.56280116-04 | 103.21783 | 6.11803 | 1.02713 | 0.9860229 |

| RES | AR AT | RESR | AR ATR |
|---|---|---|---|
| 20021.69 | 0.8707 | 18457.55 | 0.6933 |
| 28566.20 | 0.8593 | 26752.75 | 0.7152 |
| 37374.35 | 0.8619 | 35996.56 | 0.7758 |
| 46109.28 | 0.8614 | 45012.48 | 0.8053 |
| 54382.02 | 0.8631 | 53589.90 | 0.8074 |
| 73525.19 | 0.8765 | 71908.88 | 0.8236 |
| 94029.38 | 0.9008 | 93026.50 | 0.8741 |
| 113809.44 | 0.9116 | 114744.75 | 0.9328 |
| 134126.44 | 0.9242 | 137670.69 | 0.9966 |
| 154640.31 | 0.9357 | 160353.56 | 1.0321 |
| 161126.38 | 0.9372 | 167826.21 | 1.0505 |

Table XXII. TURBOTEC Medium Pitch Results (Tube No. T-2), Run 5

| VELOCITY M/SEC | UN W/(C*M**2) | UC W/(C*M**2) | HI W/(C*M**2) | HO W/(C*M**2) |
|---|---|---|---|---|
| 0.72 | 5669.016 | 5740.492 | 11643.020 | 12521.657 |
| 1.08 | 6784.199 | 6886.816 | 15810.492 | 13204.633 |
| 1.45 | 7545.875 | 7673.043 | 19643.055 | 13439.512 |
| 1.81 | 7967.895 | 8109.820 | 23287.336 | 13133.632 |
| 2.17 | 8206.039 | 8356.656 | 26721.203 | 12729.383 |
| 2.89 | 8753.852 | 8925.461 | 33152.770 | 12673.152 |
| 3.61 | 9217.707 | 9408.180 | 39317.199 | 12762.738 |
| 4.34 | 9677.176 | 9887.328 | 45123.391 | 13021.344 |

| REYNOLDS NO | PLAIN END REYN NO | FLOW RATE PER AREA KG/(SEC*M**2) | FRICTION FACTOR | SIEDER TATE CONSTANT |
|---|---|---|---|---|
| 12927.06 | 12927.06 | 718.22 | 0.03385161 | 0.07303506 |
| 18634.64 | 18634.65 | 1078.05 | 0.03550368 | 0.07337445 |
| 24120.38 | 24120.37 | 1438.10 | 0.03550179 | 0.07362926 |
| 29573.42 | 29573.41 | 1798.17 | 0.03952480 | 0.07379621 |
| 34910.25 | 34910.23 | 2158.35 | 0.04017805 | 0.07393849 |
| 45630.64 | 45630.64 | 2878.67 | 0.03825636 | 0.07411146 |
| 56426.27 | 56426.24 | 3598.92 | 0.03791236 | 0.07420558 |
| 67037.88 | 67037.88 | 4319.34 | 0.03795416 | 0.07429302 |

# Table XXII. Page 2

| NUSSELT NO | NU/PR1/3(U/UW)0.14 | STANTON NO | J FACTOR | PERFORM FACTOR |
|---|---|---|---|---|
| 261.80835 | 142.14476 | 0.00387665 | 0.0116715 | 0.6895911 |
| 357.17136 | 191.33801 | 0.00350619 | 0.0108805 | 0.5508596 |
| 445.25257 | 236.02461 | 0.00326481 | 0.0103624 | 0.5246545 |
| 529.10278 | 278.45435 | 0.00309502 | 0.0099689 | 0.5044367 |
| 608.25321 | 318.59009 | 0.00295838 | 0.0096484 | 0.4882844 |
| 756.46548 | 395.63013 | 0.00275156 | 0.0091106 | 0.4762546 |
| 898.26709 | 469.48389 | 0.00260990 | 0.0087128 | 0.4596278 |
| 1032.13403 | 539.51465 | 0.00249553 | 0.0083946 | 0.4423521 |

| XIA | PRESSURE DROP (KPA) | PRANDTL NO | U/UW | COTMS(KG/SEC) |
|---|---|---|---|---|
| 0.28050500-03 | 2.22413 | 5.22429 | 1.06148 | 0.1178252 |
| 0.20659840-03 | 5.84379 | 5.46663 | 1.05967 | 0.1768569 |
| 0.16630760-03 | 10.39247 | 5.65462 | 1.05898 | 0.2355229 |
| 0.14025210-03 | 16.25418 | 5.78063 | 1.05875 | 0.2949538 |
| 0.12227110-03 | 23.79889 | 5.88988 | 1.05725 | 0.3540822 |
| 0.98558260-04 | 40.29771 | 6.02498 | 1.05075 | 0.4722518 |
| 0.83109010-04 | 62.40901 | 6.09958 | 1.04717 | 0.5904058 |
| 0.72417650-04 | 89.98145 | 6.16955 | 1.04307 | 0.7085964 |

| RES | ARAT | RESR | ARATR |
|---|---|---|---|
| 17376.97 | 0.4684 | 18049.66 | 0.5209 |
| 28002.56 | 0.5097 | 29015.37 | 0.5630 |
| 37128.51 | 0.5178 | 39038.70 | 0.5955 |
| 46420.60 | 0.5248 | 49558.77 | 0.6446 |
| 56118.82 | 0.5338 | 61697.56 | 0.7024 |
| 73433.25 | 0.5331 | 83906.88 | 0.7743 |
| 92278.94 | 0.5393 | 108057.31 | 0.8390 |
| 111534.94 | 0.5461 | 132811.75 | 0.8904 |

Table XXIII. TURBOTEC Low Pitch Results (Tube No. T-3a), Run 6

| VELOCITY M/SEC | UA W/(C*M**2) | UC W/(C*M**2) | HI W/(C*M**2) | HO W/(C*M**2) |
|---|---|---|---|---|
| 0.72 | 8137.406 | 8285.492 | 19EC4.E71 | 1533C.168 |
| 1.08 | 9417.445 | 9616.352 | 2EE36.E16 | 15857.914 |
| 1.45 | 1C239.64E | 10475.23E | 33282.734 | 16010.105 |
| 1.81 | 1C620.418 | 10874.070 | 39263.E52 | 15628.297 |
| 2.17 | 1C816.137 | 11079.344 | 44918.496 | 15196.547 |

| REYNOLDS NO | PLAIN END REYN NO | FLOW RATE PER AREA KG/(SEC*M**2) | FRICTION FACTOR | SIEDER TATE CONSTANT |
|---|---|---|---|---|
| 13760.59 | 13760.59 | 717.41 | 0.12511581 | 0.12150186 |
| 19846.45 | 19846.46 | 1076.85 | C.11536783 | 0.12205565 |
| 25670.59 | 25670.58 | 1436.61 | C.10999535 | 0.12248725 |
| 31329.66 | 31329.85 | 1796.49 | 0.10927933 | C.12282926 |
| 36846.22 | 36846.19 | 2156.51 | 0.10350418 | 0.12311852 |

## Table XXIII. Page 2

| NUSSELT NO | NU/PR1/3(U/UW)0.14 | STANTON NO | J FACTOR | PERFORM FACTOR |
|---|---|---|---|---|
| 442.12183 | 248.59477 | 0.0066C415 | 0.0189616 | 0.3030953 |
| 6C1.E3276 | 334.73657 | 0.0059603E | 0.0176313 | 0.3056543 |
| 745.C2588 | 412.70386 | 0.00553955 | 0.0167704 | 0.3045202 |
| E86.C9741 | 485.36426 | 0.00522545 | 0.0161C85 | 0.2948141 |
| 1016.C9814 | 553.90674 | 0.00497930 | 0.0155866 | 0.3011777 |

| XIN | PRESSURE DROP (KPA) | PRANDTL NO | U/UW | DOTMS(KG/SEC) |
|---|---|---|---|---|
| 0.2762678D-03 | 8.21145 | 4.865C6 | 1.04955 | 0.1176929 |
| C.2C39C91C-03 | 17.C4794 | 5.08765 | 1.04536 | 0.1766658 |
| 0.1644366C-03 | 28.91216 | 5.26690 | 1.04313 | C.2356795 |
| 0.1394CC6C-03 | 44.89621 | 5.41282 | 1.03979 | 0.2947188 |
| 0.1218E69D-C3 | 61.25697 | 5.53827 | 1.03683 | C.3537801 |

| RES | ARAT | RESR | ARATR |
|---|---|---|---|
| 27744.18 | 0.3894 | 29144.75 | 0.4470 |
| 39766.26 | 0.3857 | 42934.77 | 0.4781 |
| 51443.33 | 0.3844 | 57099.95 | 0.5148 |
| 63748.82 | 0.3880 | 73049.50 | 0.5682 |
| 74071.31 | 0.3834 | 87839.44 | 0.6179 |

Table XXIV. TURBOTEC Variable Pitch Results (Tube No. T-4), Run 15

| VELOCITY M/SEC | UN W/(C*M**2) | UC W/(C*M**2) | HI W/(C*M**2) | HO W/(C*M**2) |
|---|---|---|---|---|
| 0.72 | 6817.508 | 6921.145 | 16353.715 | 12933.523 |
| 1.08 | 7934.602 | 8075.332 | 22188.113 | 13453.684 |
| 1.45 | 8719.398 | 8889.641 | 27607.883 | 13754.398 |
| 1.81 | 9333.645 | 9528.988 | 32755.023 | 14003.926 |
| 2.17 | 9827.422 | 9835.395 | 37619.941 | 13797.707 |
| 2.53 | 10023.648 | 10249.504 | 42321.691 | 13964.215 |
| 2.89 | 10102.074 | 10331.305 | 46833.070 | 13635.202 |
| 3.61 | 10210.152 | 10444.371 | 55511.547 | 13165.145 |
| 4.34 | 10436.324 | 10681.160 | 63858.746 | 13083.391 |
| 4.95 | 10491.711 | 10739.184 | 70903.375 | 12882.418 |

| REYNOLDS NO | PLAIN END REYN NO | FLOW RATE PER AREA KG/(SEC*M**2) | FRICTION FACTOR | SIEDER TATE CONSTANT |
|---|---|---|---|---|
| 13227.14 | 13227.14 | 717.08 | 0.07889372 | 0.10247058 |
| 19066.88 | 19066.88 | 1077.57 | 0.07422346 | 0.10294491 |
| 24878.93 | 24878.92 | 1437.28 | 0.07102144 | 0.10320425 |
| 30713.95 | 30713.94 | 1796.97 | 0.06416225 | 0.10335416 |
| 36398.04 | 36398.04 | 2156.80 | 0.06666815 | 0.10350531 |
| 42099.82 | 42099.82 | 2516.62 | 0.06510544 | 0.10360962 |
| 47861.77 | 47861.74 | 2876.38 | 0.06454861 | 0.10367334 |
| 59178.08 | 59178.05 | 3596.09 | 0.06295001 | 0.10380576 |
| 70754.94 | 70754.94 | 4315.55 | 0.06339252 | 0.10365013 |
| 80730.94 | 80730.94 | 4926.97 | 0.06333047 | 0.10385728 |

## Table XXIV. Page 2

| NUSSELT NO | NU/PR1/3(U/UW)0.14 | STANTON NO | J FACTOR | PERFORM FACTOR |
|---|---|---|---|---|
| 366.55546 | 203.12881 | 0.00544860 | 0.0161154 | 0.4085352 |
| 499.66530 | 273.41846 | 0.00492363 | 0.0150057 | 0.4044467 |
| 623.30713 | 339.12671 | 0.00455237 | 0.0142218 | 0.4007738 |
| 740.58838 | 401.97125 | 0.00435757 | 0.0136325 | 0.4249378 |
| 851.82861 | 461.13110 | 0.00416943 | 0.0131687 | 0.3950507 |
| 959.25586 | 518.58926 | 0.00401964 | 0.0127790 | 0.3925641 |
| 1062.16305 | 574.98623 | 0.00389163 | 0.0124216 | 0.3848765 |
| 1260.55668 | 682.25854 | 0.00368928 | 0.0118736 | 0.3770004 |
| 1451.67969 | 787.42944 | 0.00353862 | 0.0114205 | 0.3603120 |
| 1610.92529 | 875.12158 | 0.00343924 | 0.0111048 | 0.3506937 |

| XIN | PRESSURE DROP (KPA) | PRANDTL NO | U/UW | COTMS(KG/SEC) |
|---|---|---|---|---|
| 0.28103890-03 | 5.18108 | 5.08670 | 1.04935 | 0.1177655 |
| 0.20717050-03 | 10.97496 | 5.32270 | 1.04671 | 0.1767775 |
| 0.16651400-03 | 18.67610 | 5.45548 | 1.04407 | 0.2357850 |
| 0.14035450-03 | 26.36850 | 5.53346 | 1.04164 | 0.2947968 |
| 0.12221020-03 | 39.46162 | 5.61303 | 1.03943 | 0.3538275 |
| 0.10863670-03 | 52.45993 | 5.66848 | 1.03742 | 0.4128566 |
| 0.98173830-04 | 67.93677 | 5.70257 | 1.03557 | 0.4718754 |
| 0.82829060-04 | 103.60895 | 5.77356 | 1.02952 | 0.5899461 |
| 0.71956160-04 | 150.15885 | 5.79803 | 1.02620 | 0.7079756 |
| 0.64849450-04 | 195.52775 | 5.80193 | 1.02443 | 0.8062795 |

| RES | ARAT | RESR | ARATR |
|---|---|---|---|
| 22968.65 | 0.4097 | 24782.84 | 0.5065 |
| 33233.57 | 0.4091 | 36716.16 | 0.5456 |
| 43507.43 | 0.4091 | 49146.00 | 0.5756 |
| 52100.98 | 0.3987 | 60256.19 | 0.5951 |
| 63966.06 | 0.4095 | 75640.13 | 0.6548 |
| 74151.06 | 0.4099 | 89105.81 | 0.6855 |
| 84956.44 | 0.4123 | 104707.06 | 0.7393 |
| 105975.25 | 0.4145 | 136334.50 | 0.8353 |
| 129374.88 | 0.4213 | 171091.44 | 0.9215 |
| 149457.00 | 0.4256 | 202682.63 | 0.9980 |

## Table XXV. TURBOTEC Low Pitch "supported" Results (Tube No. T-3b), Run 17

| VELOCITY M/SEC | UA W/(C*M**2) | UC W/(C*M**2) | HI W/(C*M**2) | HJ W/(C*M**2) |
|---|---|---|---|---|
| 0.72 | 8221.465 | 8372.652 | 20625.078 | 15104.402 |
| 1.08 | 9631.402 | 9839.591 | 27973.867 | 16034.695 |
| 1.45 | 10453.996 | 10699.666 | 34862.805 | 16141.035 |
| 1.81 | 11134.688 | 11413.824 | 41422.941 | 16367.725 |
| 2.17 | 11440.375 | 11735.250 | 47755.512 | 16073.653 |
| 2.53 | 11652.484 | 11958.543 | 53777.309 | 15823.563 |
| 2.89 | 11882.695 | 12201.133 | 59683.809 | 15734.250 |
| 3.25 | 12098.879 | 12429.168 | 65527.684 | 15700.258 |
| 3.61 | 12180.340 | 12515.152 | 71249.000 | 15507.117 |
| 4.12 | 12130.766 | 12462.820 | 79125.313 | 15070.086 |

| REYNOLDS NO | PLAIN END REYN NO | FLOW RATE PER AREA KG/(SEC*M**2) | FRICTION FACTOR | SIEDER TATE CONSTANT |
|---|---|---|---|---|
| 14012.51 | 14012.51 | 717.12 | 0.11084348 | 0.12630755 |
| 20236.98 | 20236.99 | 1076.44 | 0.08994156 | 0.12686116 |
| 26474.89 | 26474.88 | 1435.74 | 0.10638664 | 0.12714034 |
| 32810.00 | 32809.97 | 1794.95 | 0.10298234 | 0.12726724 |
| 39266.18 | 39266.15 | 2154.05 | 0.10106218 | 0.12730700 |
| 45533.38 | 45533.35 | 2513.32 | 0.10069597 | 0.12729604 |
| 51932.75 | 51932.72 | 2872.47 | 0.09764057 | 0.12742656 |
| 58404.72 | 58404.69 | 3231.55 | 0.09673011 | 0.12743157 |
| 64945.20 | 64945.17 | 3590.56 | 0.09614348 | 0.12741595 |
| 74279.50 | 74279.38 | 4093.00 | 0.09403992 | 0.12737167 |

## Table XXV. Page 2

| NUSSELT NO | NU/PR1/3(U/UW)0.14 | STANTON NO | J FACTOR | PERFORM FACTOR |
|---|---|---|---|---|
| 459.49780 | 262.20508 | 0.00688465 | 0.0194897 | 0.3516614 |
| 625.64673 | 353.38257 | 0.00621637 | 0.0181120 | 0.4027514 |
| 781.43634 | 439.08569 | 0.00580776 | 0.0171676 | 0.3227388 |
| 929.40576 | 521.81958 | 0.00551935 | 0.0164221 | 0.3185299 |
| 1071.82446 | 602.65112 | 0.00530226 | 0.0158085 | 0.3126465 |
| 1207.82788 | 678.92358 | 0.00511714 | 0.0153270 | 0.3044223 |
| 1340.60151 | 754.41821 | 0.00496903 | 0.0149064 | 0.3053318 |
| 1472.14258 | 828.77148 | 0.00484935 | 0.0145511 | 0.3006595 |
| 1600.53174 | 902.14014 | 0.00474557 | 0.0142312 | 0.2960400 |
| 1776.75179 | 1004.07617 | 0.00462332 | 0.0138302 | 0.2941351 |

| XIN | PRESSURE DROP (KPA) | PRANDTL NO | C/UW | DCTNS(KG/SEC) |
|---|---|---|---|---|
| 0.27631550-03 | 7.27152 | 4.76306 | 1.04155 | 0.1176445 |
| 0.20385500-03 | 13.28513 | 4.97332 | 1.03721 | 0.1765918 |
| 0.16356460-03 | 27.94595 | 5.08218 | 1.03513 | 0.2355366 |
| 0.13768220-03 | 42.27470 | 5.13229 | 1.03256 | 0.2944659 |
| 0.11942610-03 | 59.74336 | 5.14806 | 1.03001 | 0.3533757 |
| 0.10605580-03 | 81.03131 | 5.18380 | 1.02794 | 0.4123156 |
| 0.95560930-04 | 102.62909 | 5.19579 | 1.02613 | 0.4712344 |
| 0.87038740-04 | 128.67958 | 5.19778 | 1.02544 | 0.5301418 |
| 0.80049200-04 | 157.89804 | 5.19312 | 1.02450 | 0.5890365 |
| 0.72079550-04 | 200.70287 | 5.17384 | 1.02313 | 0.6714645 |

| RES | ARAT | RESR | ARATR |
|---|---|---|---|
| 28128.16 | 0.3515 | 28566.82 | 0.4518 |
| 35166.65 | 0.3313 | 39656.04 | 0.4630 |
| 51371.16 | 0.3609 | 58686.42 | 0.5235 |
| 62962.67 | 0.3615 | 74615.00 | 0.5570 |
| 77154.94 | 0.3642 | 92505.50 | 0.6045 |
| 90654.44 | 0.3677 | 111293.69 | 0.6525 |
| 103150.63 | 0.3669 | 129313.38 | 0.6905 |
| 118825.19 | 0.3685 | 148547.19 | 0.7284 |
| 130901.54 | 0.3712 | 170387.13 | 0.7728 |
| 150956.13 | 0.3721 | 200922.50 | 0.8420 |

## Table XXVI. KORODENSE CuNi-LPD Results (Tube No. K-1), Run 9

| VELOCITY M/SEC | UN W/(C*M**2) | LC W/(C*M**2) | HI W/(C*M**2) | HO W/(C*M**2) |
|---|---|---|---|---|
| 0.84 | 3449.565 | 3852.432 | 6970.258 | 11181.824 |
| 1.26 | 4115.902 | 4702.680 | 9495.578 | 11356.176 |
| 1.69 | 4619.316 | 5371.523 | 11877.922 | 11584.625 |
| 2.11 | 4930.691 | 5797.516 | 14088.590 | 11330.008 |
| 2.53 | 5236.695 | 6224.914 | 16207.367 | 11432.391 |
| 3.37 | 5577.262 | 6712.129 | 20216.207 | 11071.711 |
| 4.21 | 5924.813 | 7221.973 | 24022.469 | 11223.645 |
| 5.06 | 6310.086 | 7832.680 | 27775.582 | 11700.941 |
| 5.90 | 6426.695 | 7981.762 | 31481.777 | 11413.652 |
| 6.74 | 6650.141 | 8329.348 | 35138.105 | 11586.676 |
| 7.49 | 6623.977 | 8288.344 | 38304.125 | 11149.551 |

| REYNOLDS NO | PLAIN END REYN NO | FLOW RATE PER AREA KG/(SEC*M**2) | FRICTION FACTOR | SIEDER TATE CONSTANT |
|---|---|---|---|---|
| 13010.39 | 13010.39 | 838.19 | 0.01341556 | 0.04026243 |
| 19077.74 | 19077.75 | 1257.73 | 0.01214029 | 0.04036942 |
| 25315.76 | 25315.74 | 1677.10 | 0.01177227 | 0.04039202 |
| 31317.43 | 31317.41 | 2096.71 | 0.01117707 | 0.04044124 |
| 37220.58 | 37220.58 | 2516.42 | 0.01076251 | 0.04048696 |
| 48911.50 | 48911.47 | 3355.96 | 0.00997351 | 0.04055607 |
| 60513.92 | 60513.92 | 4195.58 | 0.00917143 | 0.04066508 |
| 72813.94 | 72813.94 | 5034.50 | 0.00871721 | 0.04059215 |
| 85364.31 | 85364.31 | 5873.16 | 0.00819452 | 0.04056893 |
| 98432.06 | 98432.13 | 6711.29 | 0.00779372 | 0.04052652 |
| 110356.00 | 110356.00 | 7456.92 | 0.00742333 | 0.04048440 |

AD-A062 204 NAVAL POSTGRADUATE SCHOOL MONTEREY CALIF F/G 13/11
AN EXPERIMENTAL COMPARISON OF ENHANCED HEAT TRANSFER CONDENSER --ETC(U)
SEP 78 J H FENNER
UNCLASSIFIED NPS69-78-015 NL

2 OF 2
AD A062204

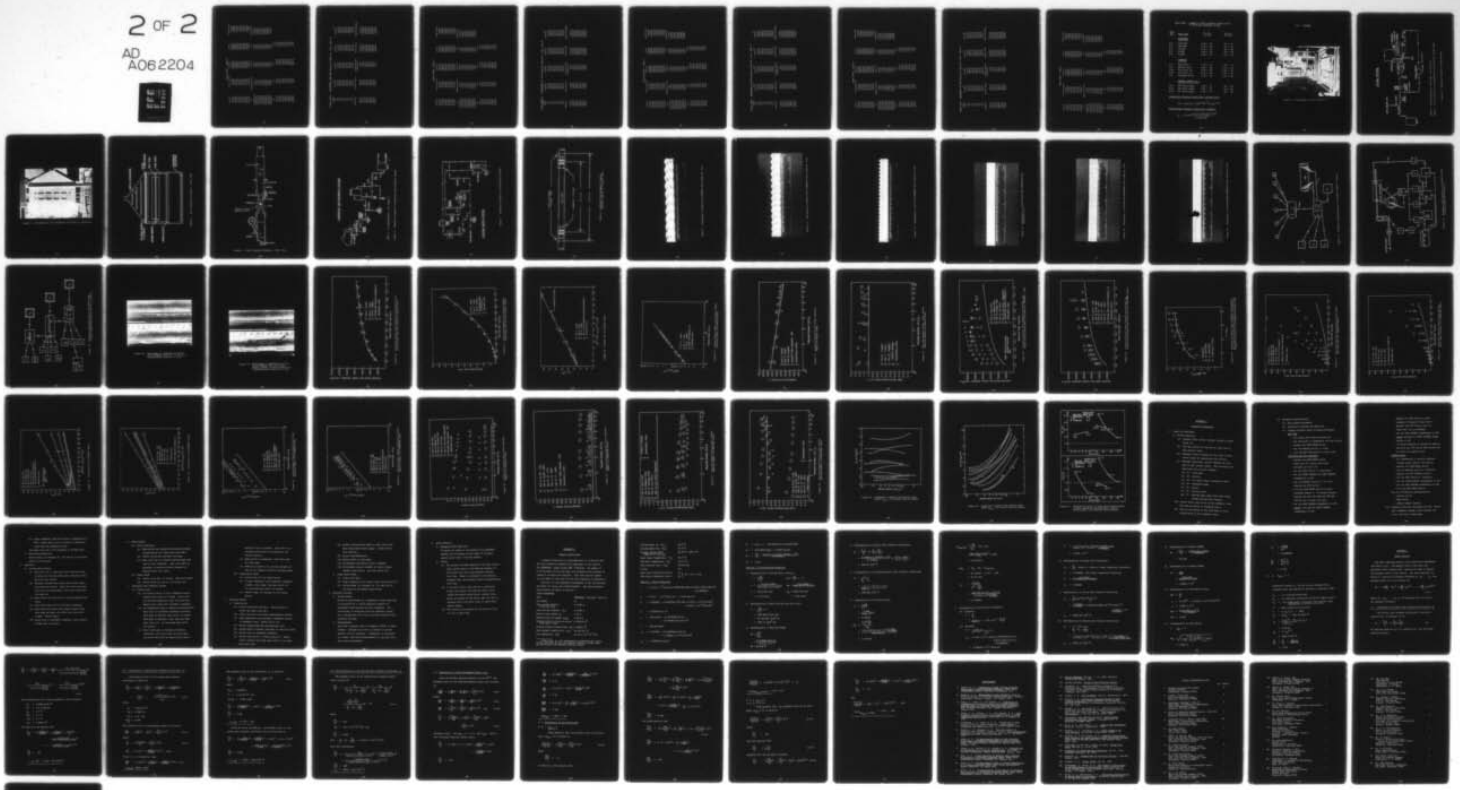

END
DATE FILMED
3-79
DDC

## Table XXVI. Page 2

| NUSSELT NO | NU/PR1/3(U/Uw)0.14 | STANTON NO | J FACTOR | PERFORM FACTOR |
|---|---|---|---|---|
| 144.29463 | 78.76468 | 0.00196772 | 0.0063107 | 0.9408027 |
| 199.62661 | 107.26891 | 0.00180430 | 0.0058280 | 0.9601094 |
| 250.10101 | 134.58833 | 0.00169254 | 0.0054869 | 0.9321786 |
| 296.84155 | 159.75432 | 0.00160474 | 0.0052436 | 0.9382735 |
| 342.06372 | 183.62897 | 0.00153853 | 0.0050655 | 0.9413223 |
| 427.40336 | 228.86746 | 0.00143921 | 0.0047899 | 0.9605172 |
| 506.48413 | 271.68335 | 0.00136782 | 0.0045880 | 1.0004588 |
| 587.73901 | 314.92896 | 0.00131801 | 0.0044118 | 1.0122128 |
| 665.78223 | 357.44849 | 0.00128061 | 0.0042708 | 1.0223546 |
| 742.33308 | 400.17334 | 0.00125093 | 0.0041437 | 1.0333335 |
| 808.37451 | 438.05005 | 0.00122738 | 0.0040383 | 1.0380127 |

| XIA | PRESSURE DROP (KPA) | PRANDTL NO | L/Uh | DOTMS (KG/SEC) |
|---|---|---|---|---|
| 0.27688086E-03 | 1.29473 | 5.65694 | 1.04240 | 0.1179556 |
| 0.20320595E-03 | 2.63717 | 5.80522 | 1.03651 | 0.1769969 |
| 0.16245510-03 | 4.54651 | 5.83693 | 1.03208 | 0.2360135 |
| 0.13704720-03 | 6.74584 | 5.90653 | 1.02792 | 0.2950642 |
| 0.11906800-03 | 9.35509 | 5.97178 | 1.02675 | 0.3541288 |
| 0.95462180-04 | 15.41536 | 6.07156 | 1.02365 | 0.4722747 |
| 0.80339700-04 | 22.15285 | 6.14318 | 1.02192 | 0.5904332 |
| 0.69483240-04 | 30.31905 | 6.12421 | 1.02005 | 0.7084917 |
| 0.61302230-04 | 38.79030 | 6.09029 | 1.01993 | 0.8265139 |
| 0.54921500-04 | 48.18045 | 6.02874 | 1.01923 | 0.9444621 |
| 0.50380200-04 | 56.66183 | 5.96813 | 1.01736 | 1.0493927 |

| RES | ARAT | RESR | ARATR |
|---|---|---|---|
| 14837.93 | 0.7449 | 14709.39 | 0.7270 |
| 21476.86 | 0.7353 | 21595.28 | 0.7467 |
| 28861.05 | 0.7423 | 29340.42 | 0.7774 |
| 35515.42 | 0.7383 | 36884.27 | 0.8208 |
| 42117.08 | 0.7362 | 44368.55 | 0.8517 |
| 54707.69 | 0.7281 | 59828.09 | 0.9354 |
| 66262.50 | 0.7150 | 74237.81 | 0.9866 |
| 79196.38 | 0.7114 | 90008.44 | 1.0160 |
| 91488.94 | 0.7035 | 106845.31 | 1.0863 |
| 104412.69 | 0.6984 | 123752.69 | 1.1250 |
| 115620.19 | 0.6923 | 140663.81 | 1.1986 |

## Table XXVII. KORODENSE CuNi-MHT Results (Tube No. K-2), Run 12

| VELOCITY M/SEC | UN W/(C*M**2) | UC W/(C*M**2) | HI W/(C*M**2) | HO W/(C*M**2) |
|---|---|---|---|---|
| 0.84 | 4040.391 | 4172.492 | 8857.871 | 9400.336 |
| 1.26 | 4924.137 | 5121.762 | 12120.863 | 10266.848 |
| 1.69 | 5460.352 | 5704.430 | 15111.156 | 10328.441 |
| 2.11 | 5847.070 | 6127.832 | 17921.152 | 10307.859 |
| 2.53 | 6146.977 | 6458.047 | 20638.617 | 10268.785 |
| 3.37 | 6661.055 | 7027.883 | 25795.059 | 10382.688 |
| 4.21 | 6902.914 | 7297.656 | 30609.824 | 10174.398 |
| 5.06 | 7344.488 | 7792.988 | 35316.492 | 10555.250 |
| 5.90 | 6947.938 | 7347.996 | 39493.660 | 9428.406 |
| 6.74 | 6954.945 | 7355.832 | 43657.625 | 9192.730 |

| REYNOLDS NO | PLAIN END REYN NO | FLOW RATE PER AREA KG/(SEC*M**2) | FRICTION FACTOR | SIEDER TATE CONSTANT |
|---|---|---|---|---|
| 14252.58 | 14252.58 | 836.90 | 0.01253328 | 0.04865980 |
| 20984.25 | 20984.26 | 1255.76 | 0.01208469 | 0.04876507 |
| 27645.67 | 27645.66 | 1674.69 | 0.01152392 | 0.04883301 |
| 34256.02 | 34255.99 | 2093.67 | 0.01129129 | 0.04888270 |
| 40826.96 | 40826.96 | 2512.70 | 0.01114958 | 0.04892164 |
| 53933.54 | 53933.54 | 3350.79 | 0.01023959 | 0.04857449 |
| 66999.88 | 66999.88 | 4188.91 | 0.00986918 | 0.04900990 |
| 80021.13 | 80021.13 | 5027.09 | 0.00923088 | 0.04903689 |
| 90835.69 | 90835.69 | 5867.54 | 0.00898437 | 0.04919394 |
| 101990.31 | 101990.38 | 6707.64 | 0.00873101 | 0.04929592 |

## Table XXVII. Page 2

| NUSSELT NO | NU/PR1/3(U/UW)0.14 | STANTON NO | J FACTOR | PERFORM FACTOR |
|---|---|---|---|---|
| 184.78058 | 102.39630 | 0.00254251 | 0.0075337 | 1.2020350 |
| 252.25648 | 139.83742 | 0.00230831 | 0.0069353 | 1.1477776 |
| 314.52773 | 174.58806 | 0.00215772 | 0.0065421 | 1.1354036 |
| 373.87026 | 207.46458 | 0.00204674 | 0.0062471 | 1.1065273 |
| 430.90503 | 238.92329 | 0.00196353 | 0.0060256 | 1.0898601 |
| 535.14600 | 298.85205 | 0.00184055 | 0.0056870 | 1.1000357 |
| 640.24268 | 355.74780 | 0.00174702 | 0.0054235 | 1.0996782 |
| 739.09521 | 410.28516 | 0.00167952 | 0.0052327 | 1.1215868 |
| 829.16089 | 455.52905 | 0.00160883 | 0.0051179 | 1.1392870 |
| 918.48242 | 500.79175 | 0.00155551 | 0.0050153 | 1.1486514 |

| XIN | PRESSURE DROP (KPA) | PRANDTL NO | U/UW | DOTMS(KG/SEC) |
|---|---|---|---|---|
| 0.26477150-03 | 1.20772 | 5.09838 | 1.04848 | 0.1177741 |
| 0.19438170-03 | 2.62097 | 5.20782 | 1.04072 | 0.1767192 |
| 0.15592320-03 | 4.44420 | 5.27946 | 1.03594 | 0.2356745 |
| 0.13147900-03 | 6.80492 | 5.33235 | 1.03150 | 0.2946372 |
| 0.11417040-03 | 9.67719 | 5.37413 | 1.02964 | 0.3536053 |
| 0.91250870-04 | 15.95660 | 5.43125 | 1.02632 | 0.4715471 |
| 0.76983660-04 | 23.80032 | 5.46981 | 1.02144 | 0.5894945 |
| 0.66725130-04 | 32.40565 | 5.49933 | 1.02057 | 0.7074487 |
| 0.59674000-04 | 42.48856 | 5.67378 | 1.02054 | 0.8257240 |
| 0.53586050-04 | 53.94536 | 5.78948 | 1.02141 | 0.9439486 |

| RES | ARAT | RESR | ARATR |
|---|---|---|---|
| 14422.18 | 0.5601 | 18645.04 | 0.7035 |
| 21645.27 | 0.5677 | 23498.12 | 0.7141 |
| 28611.13 | 0.5663 | 31611.81 | 0.7514 |
| 35834.66 | 0.5726 | 40304.36 | 0.7958 |
| 43173.75 | 0.5771 | 49382.47 | 0.8407 |
| 50443.43 | 0.5717 | 66489.31 | 0.9044 |
| 65980.75 | 0.5704 | 85251.19 | 0.9913 |
| 82703.81 | 0.5653 | 102200.25 | 1.0226 |
| 93147.56 | 0.5600 | 122230.63 | 1.1984 |
| 104154.63 | 0.5572 | 140887.31 | 1.2966 |

Table XXVIII. KORODENSE Aℓ- LPD Results (Tube No. K-3), Run 13

| VELOCITY M/SEC | UN W/(C*M**2) | LC W/(C*M**2) | HI W/(C*M**2) | HO W/(C*M**2) |
|---|---|---|---|---|
| 0.84 | 4689.770 | 4868.688 | 11390.582 | 9673.945 |
| 1.26 | 5421.699 | 5662.258 | 15441.387 | 10019.629 |
| 1.69 | 5869.582 | 6142.676 | 19212.656 | 9894.375 |
| 2.11 | 6360.875 | 6694.559 | 22802.301 | 10270.676 |
| 2.53 | 6511.008 | 6861.066 | 26232.176 | 9946.297 |
| 3.37 | 6852.707 | 7286.246 | 32784.305 | 9854.102 |
| 4.21 | 7312.711 | 7757.219 | 39061.176 | 10147.074 |
| 5.06 | 7598.727 | 8079.832 | 45086.234 | 10260.543 |
| 5.90 | 7585.160 | 8064.492 | 50875.078 | 9931.555 |
| 6.74 | 7563.785 | 8062.941 | 56582.828 | 9702.660 |

| REYNOLDS NO | PLAIN END REYN NO | FLOW RATE PER AREA KG/(SEC*M**2) | FRICTION FACTOR | SIEDER TATE CONSTANT |
|---|---|---|---|---|
| 12583.05 | 12583.05 | 838.21 | 0.02143038 | 0.06561226 |
| 18720.30 | 18720.30 | 1258.10 | 0.02024282 | 0.06591642 |
| 24403.00 | 24403.00 | 1678.03 | 0.01966798 | 0.06609136 |
| 30101.49 | 30101.49 | 2097.95 | 0.01852071 | 0.06619453 |
| 35700.71 | 35700.68 | 2517.97 | 0.01801943 | 0.06628585 |
| 46992.19 | 46992.16 | 3357.91 | 0.01649238 | 0.06638640 |
| 58450.04 | 58450.04 | 4197.69 | 0.01515549 | 0.06642514 |
| 70101.44 | 70101.38 | 5037.25 | 0.01419308 | 0.06642544 |
| 81626.94 | 81627.00 | 5876.97 | 0.01317564 | 0.06644458 |
| 93314.13 | 93314.13 | 6716.50 | 0.01265517 | 0.06644237 |

## Table XXVIII. Page 2

| NUSSELT NC | NU/PR1/3(U/UW))0.14 | STANTON NC | J FACTOR | PERFORM FACTOR |
|---|---|---|---|---|
| 239.12886 | 128.14040 | 0.00324812 | 0.0103287 | 0.9659339 |
| 325.67212 | 172.52151 | 0.00293260 | 0.0096104 | 0.9455072 |
| 406.28687 | 213.84485 | 0.00273539 | 0.0091187 | 0.9272628 |
| 482.94922 | 253.33315 | 0.00259638 | 0.0087431 | 0.9441419 |
| 556.36035 | 290.77759 | 0.00248844 | 0.0084546 | 0.9383910 |
| 626.37915 | 362.82568 | 0.00233181 | 0.0080004 | 0.9701909 |
| 830.19165 | 432.27441 | 0.00222236 | 0.0076536 | 1.0100107 |
| 958.30859 | 499.56655 | 0.00213760 | 0.0073648 | 1.0378008 |
| 1081.59717 | 564.64082 | 0.00206729 | 0.0071334 | 1.0624833 |
| 1202.90308 | 628.64063 | 0.00201153 | 0.0069405 | 1.0968676 |

| XIN | PRESSURE DROP (KPA) | PRANDTL NC | U/UW | DOTMS(KG/SEC) |
|---|---|---|---|---|
| 0.2759721D-03 | 2.06831 | 5.67053 | 1.04650 | 0.1179556 |
| 0.2036057D-03 | 4.29852 | 5.93178 | 1.04282 | 0.1770486 |
| 0.1636538D-03 | 7.60010 | 6.08653 | 1.04058 | 0.2361451 |
| 0.1376976D-03 | 11.18467 | 6.17938 | 1.03887 | 0.2952392 |
| 0.1198725D-03 | 15.67265 | 6.26256 | 1.03803 | 0.3543472 |
| 0.9592068D-04 | 25.50603 | 6.35517 | 1.03619 | 0.4725503 |
| 0.8050750D-04 | 36.62520 | 6.39116 | 1.03469 | 0.5907291 |
| 0.6974543D-04 | 49.39148 | 6.39518 | 1.03263 | 0.7088902 |
| 0.6181344D-04 | 62.42877 | 6.40930 | 1.03087 | 0.8270499 |
| 0.5557800D-04 | 76.29451 | 6.40725 | 1.03024 | 0.9451962 |

| RES | ARAT | RESR | ARATR |
|---|---|---|---|
| 14656.79 | 0.4534 | 16148.76 | 0.5948 |
| 21256.14 | 0.4534 | 24045.14 | 0.6404 |
| 28306.76 | 0.4561 | 32598.07 | 0.6976 |
| 34210.91 | 0.4519 | 40412.26 | 0.7204 |
| 40682.30 | 0.4522 | 49507.63 | 0.7836 |
| 52617.65 | 0.4452 | 66693.25 | 0.8646 |
| 64103.88 | 0.4376 | 83371.31 | 0.9134 |
| 75763.13 | 0.4325 | 101019.06 | 0.9679 |
| 88305.31 | 0.4249 | 119443.31 | 1.0554 |
| 97964.19 | 0.4226 | 139734.19 | 1.1416 |

Table XXIX. KORODENSE Aℓ-MIT Results (Tube No. K-4), Run 11

| VELOCITY M/SEC | UN W/(C*M**2) | UC W/(C*M**2) | HI W/(C*M**2) | HO W/(C*M**2) |
|---|---|---|---|---|
| 0.84 | 4046.648 | 4612.484 | 9627.851 | 10681.094 |
| 1.26 | 4759.902 | 5562.570 | 13130.684 | 11179.004 |
| 1.69 | 5224.180 | 6207.238 | 16310.172 | 11313.578 |
| 2.11 | 5444.910 | 6521.352 | 19294.754 | 10884.135 |
| 2.53 | 5702.129 | 6893.805 | 22186.188 | 10916.660 |
| 3.37 | 6106.473 | 7493.707 | 27736.938 | 11026.824 |
| 4.21 | 6262.539 | 7730.109 | 33016.395 | 10791.598 |
| 5.06 | 6646.410 | 8323.504 | 38080.664 | 11236.156 |
| 5.90 | 6717.094 | 8434.652 | 43039.434 | 10988.605 |
| 6.74 | 6788.648 | 8547.785 | 47968.168 | 10838.285 |

| REYNOLDS NO | PLAIN END REYN NO | FLOW RATE PER AREA KG/(SEC*M**2) | FRICTION FACTOR | SIEDER TATE CONSTANT |
|---|---|---|---|---|
| 14468.44 | 14468.44 | 836.67 | 0.01671752 | 0.05201293 |
| 21015.03 | 21015.04 | 1255.72 | 0.01737395 | 0.05220737 |
| 27370.57 | 27370.56 | 1674.97 | 0.01641210 | 0.05234984 |
| 33584.81 | 33584.81 | 2094.37 | 0.01594628 | 0.05246294 |
| 39826.17 | 39826.17 | 2513.74 | 0.01518683 | 0.05253560 |
| 52288.95 | 52288.95 | 3352.49 | 0.01375036 | 0.05263028 |
| 64678.30 | 64678.27 | 4191.31 | 0.01274708 | 0.05269491 |
| 77188.00 | 77187.94 | 5030.01 | 0.01189908 | 0.05272682 |
| 89694.06 | 89694.13 | 5868.72 | 0.01120712 | 0.05275345 |
| 102266.63 | 102266.69 | 6707.36 | 0.01049045 | 0.05276796 |

## Table XXIX. Page 2

| NUSSELT NO | NU/PR1/3(U/UW)0.14 | STANTON NO | J FACTOR | PERFORM FACTOR |
|---|---|---|---|---|
| 199.59317 | 110.77664 | 0.00275254 | 0.0080611 | 0.9643640 |
| 273.22607 | 149.88394 | 0.00250070 | 0.0075050 | 0.8639322 |
| 340.31177 | 185.66997 | 0.00232837 | 0.0071134 | 0.8668520 |
| 403.45483 | 219.16261 | 0.00220259 | 0.0068246 | 0.8558444 |
| 464.55737 | 251.52890 | 0.00210996 | 0.0065969 | 0.8687621 |
| 581.83154 | 313.30176 | 0.00197767 | 0.0062562 | 0.9073264 |
| 693.42798 | 371.85547 | 0.00188282 | 0.0060039 | 0.9419984 |
| 800.30493 | 426.63379 | 0.00180945 | 0.0057941 | 0.9738727 |
| 904.94092 | 483.57178 | 0.00175276 | 0.0056256 | 1.0046473 |
| 1008.84912 | 537.22485 | 0.00170920 | 0.0054955 | 1.0484819 |

| XIA | PRESSURE DROP (KPA) | PRANDTL NO | U/UW | DOTMS(KG/SEC) |
|---|---|---|---|---|
| 0.26195830-03 | 1.61052 | 5.01177 | 1.05288 | 0.1177423 |
| 0.19213020-03 | 3.76803 | 5.19912 | 1.05226 | 0.1767147 |
| 0.15465010-03 | 6.33041 | 5.34000 | 1.04863 | 0.2357147 |
| 0.13077150-03 | 9.61473 | 5.45405 | 1.04582 | 0.2947252 |
| 0.11373370-03 | 13.18675 | 5.52837 | 1.04453 | 0.3537514 |
| 0.90978470-04 | 21.29282 | 5.62644 | 1.04413 | 0.4717868 |
| 0.76433570-04 | 30.75821 | 5.69422 | 1.04428 | 0.5898323 |
| 0.66270250-04 | 41.34888 | 5.73007 | 1.04340 | 0.7078605 |
| 0.58635940-04 | 53.01096 | 5.75619 | 1.04419 | 0.8258892 |
| 0.52611520-04 | 64.81354 | 5.77165 | 1.04650 | 0.9439084 |

| RES | APAT | RESR | APATR |
|---|---|---|---|
| 16379.42 | 0.5733 | 17170.55 | 0.6542 |
| 25128.54 | 0.5967 | 26661.46 | 0.7043 |
| 32616.65 | 0.5934 | 35436.32 | 0.7485 |
| 40224.29 | 0.5945 | 45068.73 | 0.8175 |
| 47314.50 | 0.5899 | 54149.88 | 0.8607 |
| 60774.35 | 0.5786 | 72132.56 | 0.9348 |
| 72783.13 | 0.5693 | 91192.25 | 1.0303 |
| 86564.50 | 0.5612 | 108744.75 | 1.0630 |
| 99074.94 | 0.5542 | 128391.69 | 1.1452 |
| 110719.31 | 0.5452 | 147430.88 | 1.2157 |

Table XXX. KORODENSE Ti-MHT Results (Tube No. K-5), Run 14

| VELOCITY M/SEC | UN W/(C*M**2) | UC W/(C*M**2) | HI W/(C*M**2) | HO W/(C*M**2) |
|---|---|---|---|---|
| 0.72 | 4120.527 | 5008.004 | 8687.680 | 13611.307 |
| 1.08 | 4801.230 | 6050.602 | 11910.293 | 13659.281 |
| 1.44 | 5142.234 | 6602.367 | 14856.074 | 12877.766 |
| 1.80 | 5767.867 | 7670.648 | 17772.121 | 14562.434 |
| 2.16 | 5888.797 | 7886.012 | 20582.086 | 13599.379 |
| 2.88 | 6224.777 | 8500.430 | 25866.285 | 13288.977 |
| 3.60 | 6605.590 | 9226.816 | 30857.152 | 13727.727 |
| 4.32 | 6705.023 | 9421.984 | 35690.219 | 13260.445 |
| 5.04 | 6882.063 | 9775.355 | 40360.090 | 13310.207 |
| 5.76 | 7302.133 | 10645.195 | 44907.672 | 14383.836 |

| REYNOLDS NO | PLAIN END REYN NO | FLOW RATE PER AREA KG/(SEC*M**2) | FRICTION FACTOR | SIEDER TATE CONSTANT |
|---|---|---|---|---|
| 12691.84 | 12691.84 | 715.86 | 0.03259499 | 0.05461306 |
| 18545.20 | 18545.20 | 1074.26 | 0.03462725 | 0.05478032 |
| 24065.34 | 24065.33 | 1432.68 | 0.03507061 | 0.05495308 |
| 30176.50 | 30176.48 | 1791.13 | 0.03541131 | 0.05493348 |
| 36363.79 | 36363.79 | 2149.21 | 0.03530702 | 0.05490662 |
| 48282.38 | 48282.35 | 2865.81 | 0.03420818 | 0.05493348 |
| 60051.23 | 60051.17 | 3582.55 | 0.03354866 | 0.05496568 |
| 72061.38 | 72061.31 | 4299.06 | 0.03276976 | 0.05496568 |
| 83983.19 | 83983.19 | 5015.66 | 0.03203691 | 0.05497244 |
| 96081.81 | 96081.81 | 5732.08 | 0.03097348 | 0.05496568 |

## Table XXX. Page 2

| REYNOLDS NO | NU/PR1/3(U/UW)0.14 | STANTON NO | J FACTOR | PERFORM FACTOR |
|---|---|---|---|---|
| 155.58678 | 104.74065 | 0.00290154 | 0.0088450 | 0.5427245 |
| 265.51025 | 142.30058 | 0.00265061 | 0.0082416 | 0.4760174 |
| 337.23413 | 175.83665 | 0.00247806 | 0.0078656 | 0.4485561 |
| 403.28027 | 210.65482 | 0.00237175 | 0.0075101 | 0.4241663 |
| 466.81494 | 244.43263 | 0.00228919 | 0.0072256 | 0.4093037 |
| 586.55117 | 306.80811 | 0.00215747 | 0.0068316 | 0.3954141 |
| 700.61230 | 365.51685 | 0.00205876 | 0.0065435 | 0.3801154 |
| 810.34790 | 422.91431 | 0.00198435 | 0.0063074 | 0.3849534 |
| 916.49023 | 478.07715 | 0.00192337 | 0.0061185 | 0.3819651 |
| 1019.63037 | 532.35742 | 0.00187262 | 0.0059523 | 0.3843474 |

| XIN | PRESSURE DROP (KPA) | PRANDTL NO | U/UW | DOTMS(KG/SEC) |
|---|---|---|---|---|
| 0.28021050-03 | 2.12332 | 5.32131 | 1.07179 | 0.1178511 |
| 0.20441350-03 | 5.07757 | 5.48274 | 1.07408 | 0.1768546 |
| 0.16386750-03 | 9.14638 | 5.65493 | 1.07650 | 0.2359101 |
| 0.13700360-03 | 14.42935 | 5.63467 | 1.07584 | 0.2948729 |
| 0.11825750-03 | 20.71565 | 5.60782 | 1.07495 | 0.3538233 |
| 0.94131960-04 | 35.68410 | 5.63467 | 1.07509 | 0.4717563 |
| 0.78500560-04 | 54.68568 | 5.66697 | 1.07511 | 0.5897930 |
| 0.66222910-04 | 76.91930 | 5.66697 | 1.07474 | 0.7077511 |
| 0.60325430-04 | 102.35619 | 5.67378 | 1.07483 | 0.8257240 |
| 0.54219930-04 | 129.24959 | 5.66697 | 1.07429 | 0.9436683 |

| RES | ARAT | RESR | ARATR |
|---|---|---|---|
| 19324.43 | 0.6920 | 18157.49 | 0.5813 |
| 30182.27 | 0.7277 | 28766.45 | 0.6362 |
| 40392.61 | 0.7435 | 39675.64 | 0.7071 |
| 52070.38 | 0.7604 | 50881.54 | 0.7128 |
| 63849.09 | 0.7715 | 64171.51 | 0.7824 |
| 85825.31 | 0.7787 | 89512.13 | 0.8761 |
| 106010.19 | 0.7856 | 115088.38 | 0.9364 |
| 130456.25 | 0.7897 | 143567.06 | 1.0326 |
| 152638.75 | 0.7921 | 171667.50 | 1.1007 |
| 174042.50 | 0.7961 | 196455.56 | 1.1091 |

Table XXXI. Summary of Heat Transfer Capabilities of Enhanced Condenser Tubing.

| Tube No. | Tube Type | $\overline{Ci}_a/\overline{Ci}_s$ | $\overline{ho}_a/\overline{ho}_s$ |
|---|---|---|---|
| | KORODENSE | | |
| K-1 | CuNi-LPD | 1.60 ± .18 | .97 ± .11 |
| K-2 | CuNi-MHT | 2.12 ± .21 | .93 ± .09 |
| K-3 | Aℓ-LPD | 2.60 ± .47 | .85 ± .09 |
| K-4 | Aℓ-MHT | 2.60 ± .29 | .85 ± .09 |
| K-5 | Ti-MHT | 2.20 ± .27 | 1.15 ± .12 |
| | TURBOTEC | | |
| T-1 | High Pitch | 1.76 ± .24 | 1.03 ± .13 |
| T-2 | Medium Pitch | 2.92 ± .33 | 1.10 ± .10 |
| T-3a | Low Pitch (u) | 4.88 ± .82 | 1.32 ± .12 |
| T-3b | Low Pitch (s) | 5.12 ± .90 | 1.34 ± .13 |
| T-4 | Variable Pitch | 4.12 ± .72 | 1.14 ± .09 |
| | GENERAL ATOMIC [11] | | |
| GA-1 | 30° Helix Angle | 3.28 ± .51 | .94 ± .06 |
| GA-2 | 45° Helix Angle | 3.24 ± .50 | .94 ± .06 |
| GA-3 | 60° Helix Angle | 3.28 ± .51 | .99 ± .09 |

Inside Heat Transfer Coefficient (Sieder-Tate)

$$Nu_i = h_i D_i / k_b = C_i Re^{0.8} Pr^{1/3} (\mu/\mu_w)^{0.14}$$

Outside Heat Transfer Coefficient (Nusselt)

$$h_o = 0.725 \left[\frac{\rho_f(\rho_f-\rho_v)g\, h_{fg} k_f^3}{\mu_f D_o (T_s-T_w)}\right]^{0.25}$$

# VIII. FIGURES

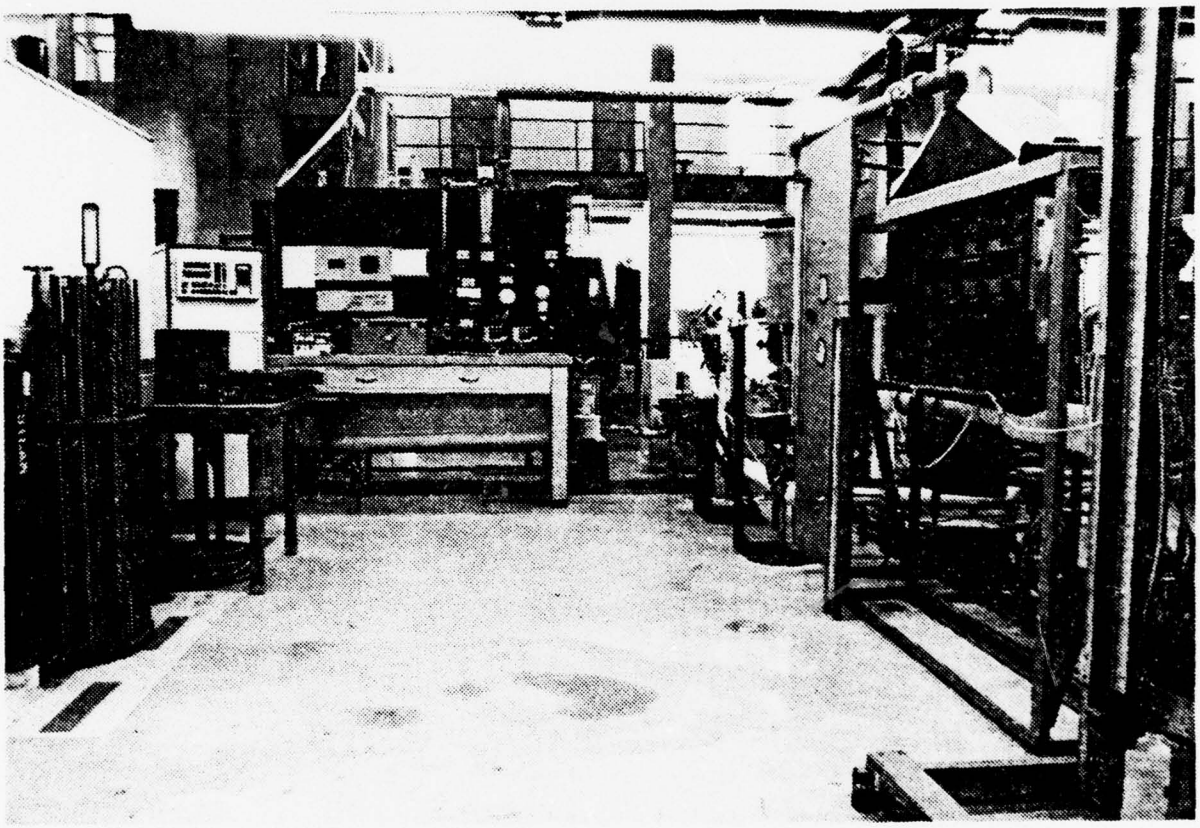

Figure 1. Photograph of Test Facility

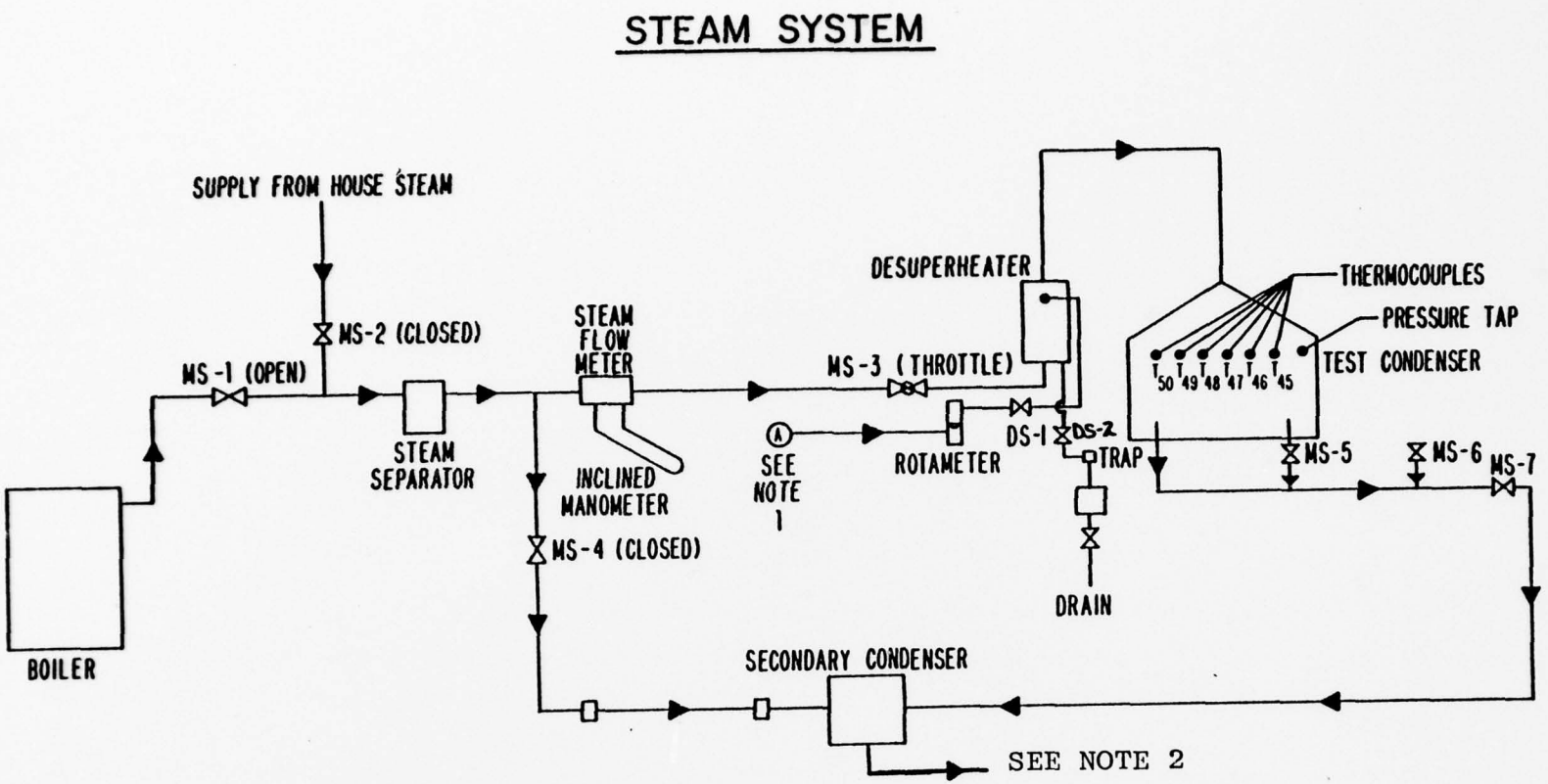


NOTE 1: From discharge of feed pump, see Figure 6

NOTE 2: To air ejector via refrigerated cold trap and vacuum pump

Figure 2. Schematic Diagram of Steam System

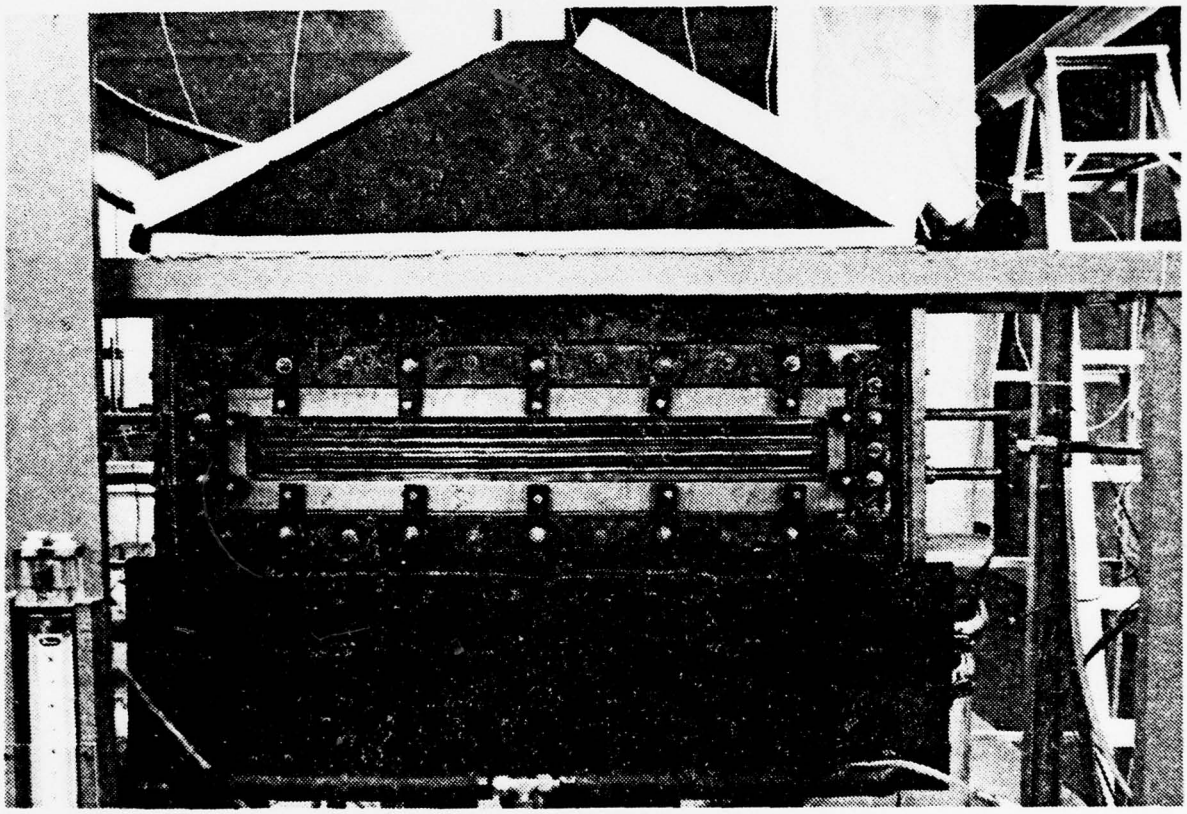

Figure 3. Photograph of Test Condenser with Partial Insulation

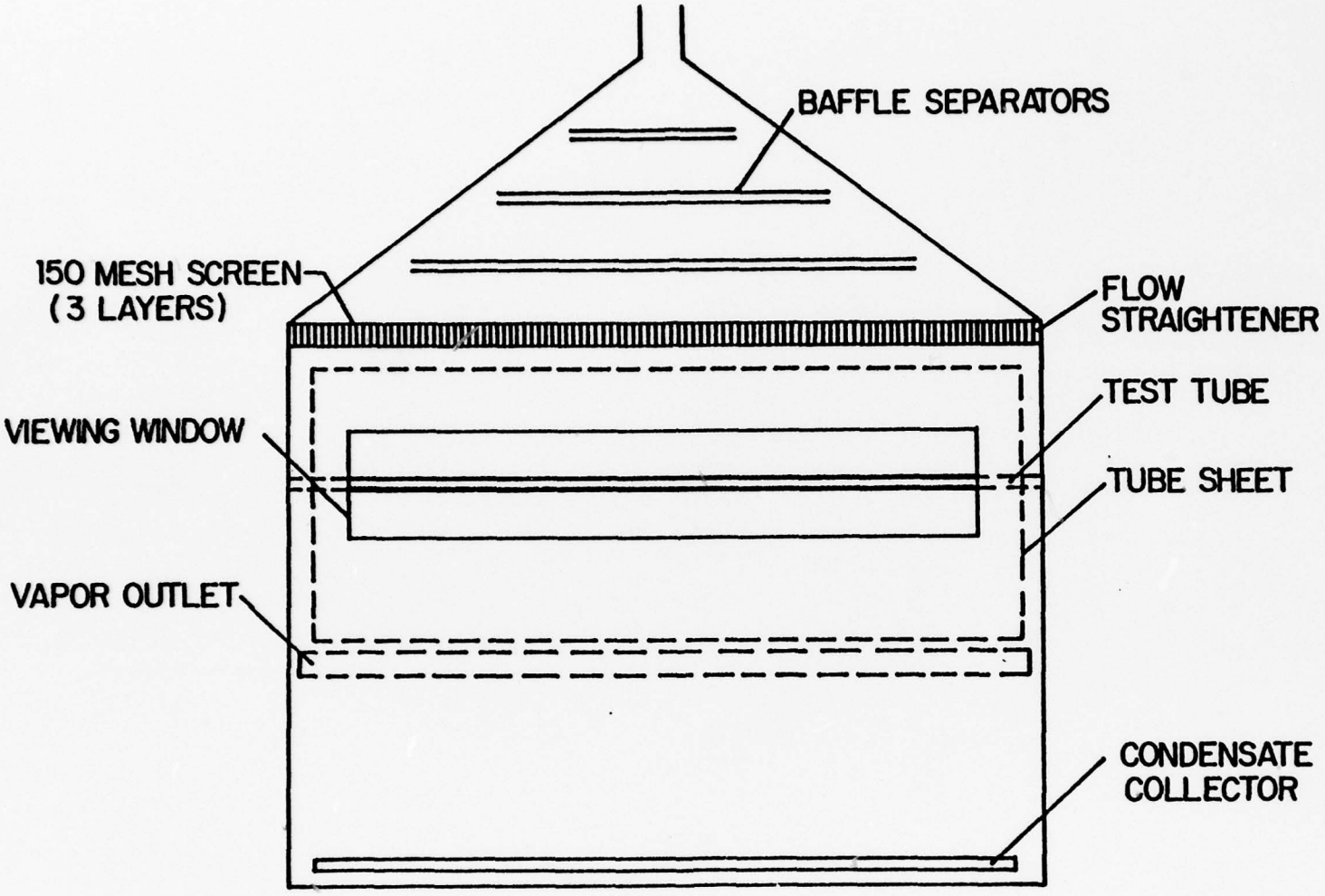


Figure 4. Test Condenser Schematic, Front View

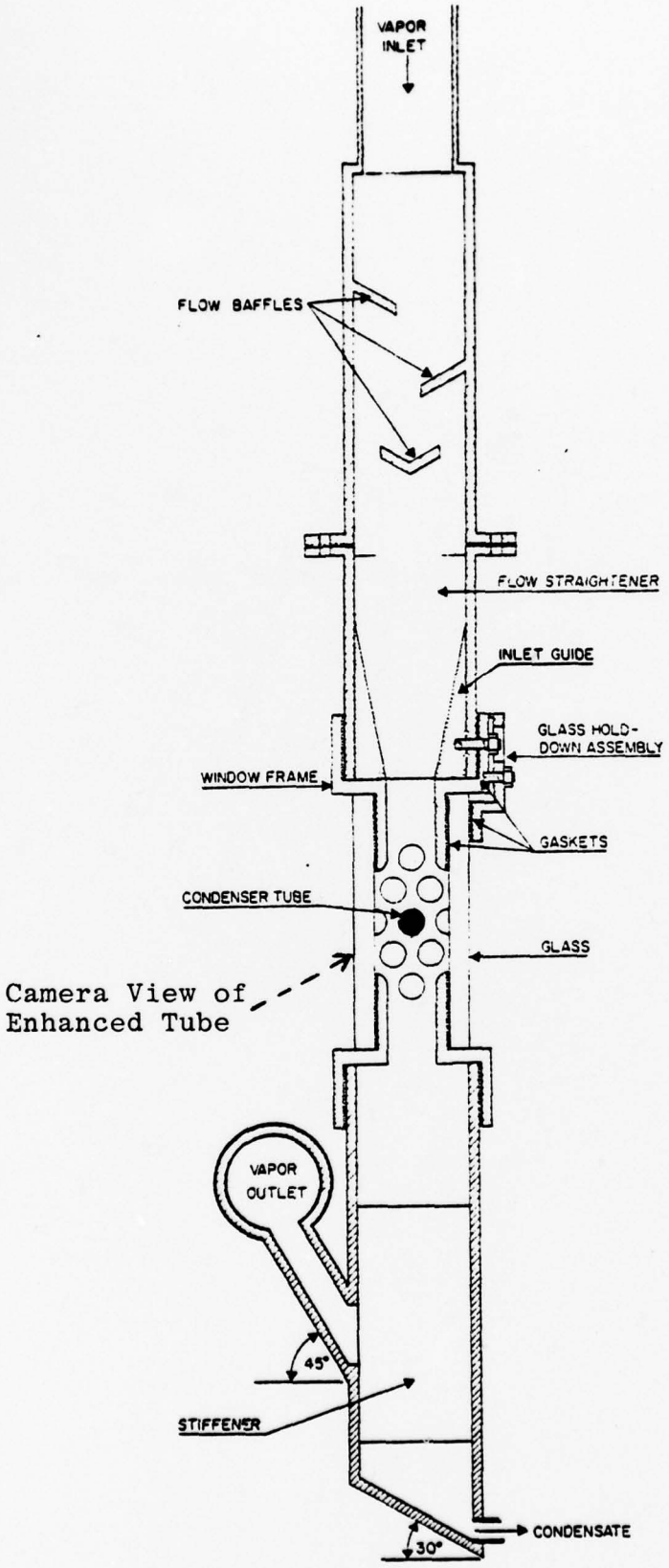


Figure 5. Test Condenser Schematic, Side View

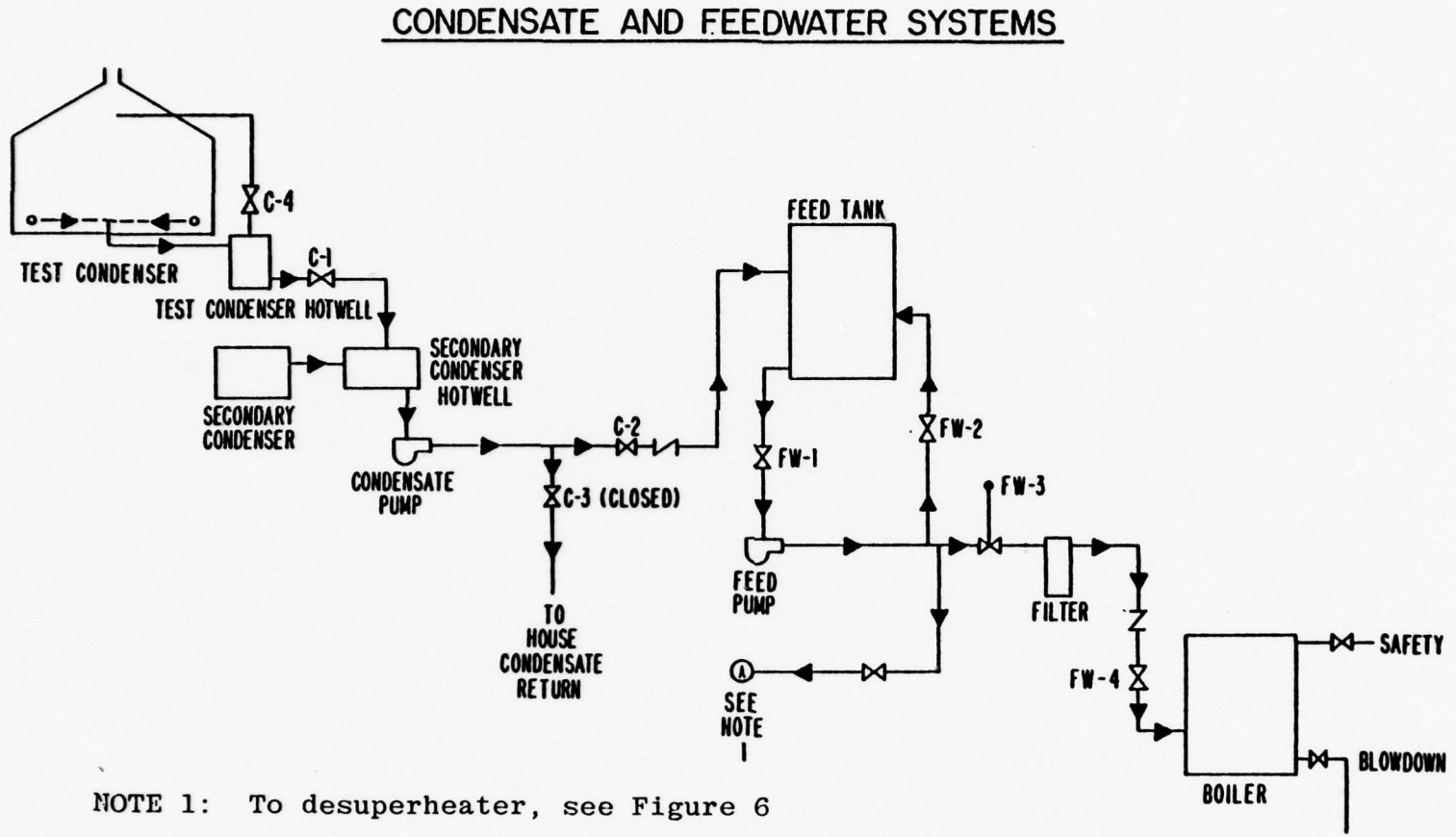


NOTE 1: To desuperheater, see Figure 6

Figure 6. Schematic Diagram of Condensate and Feedwater System

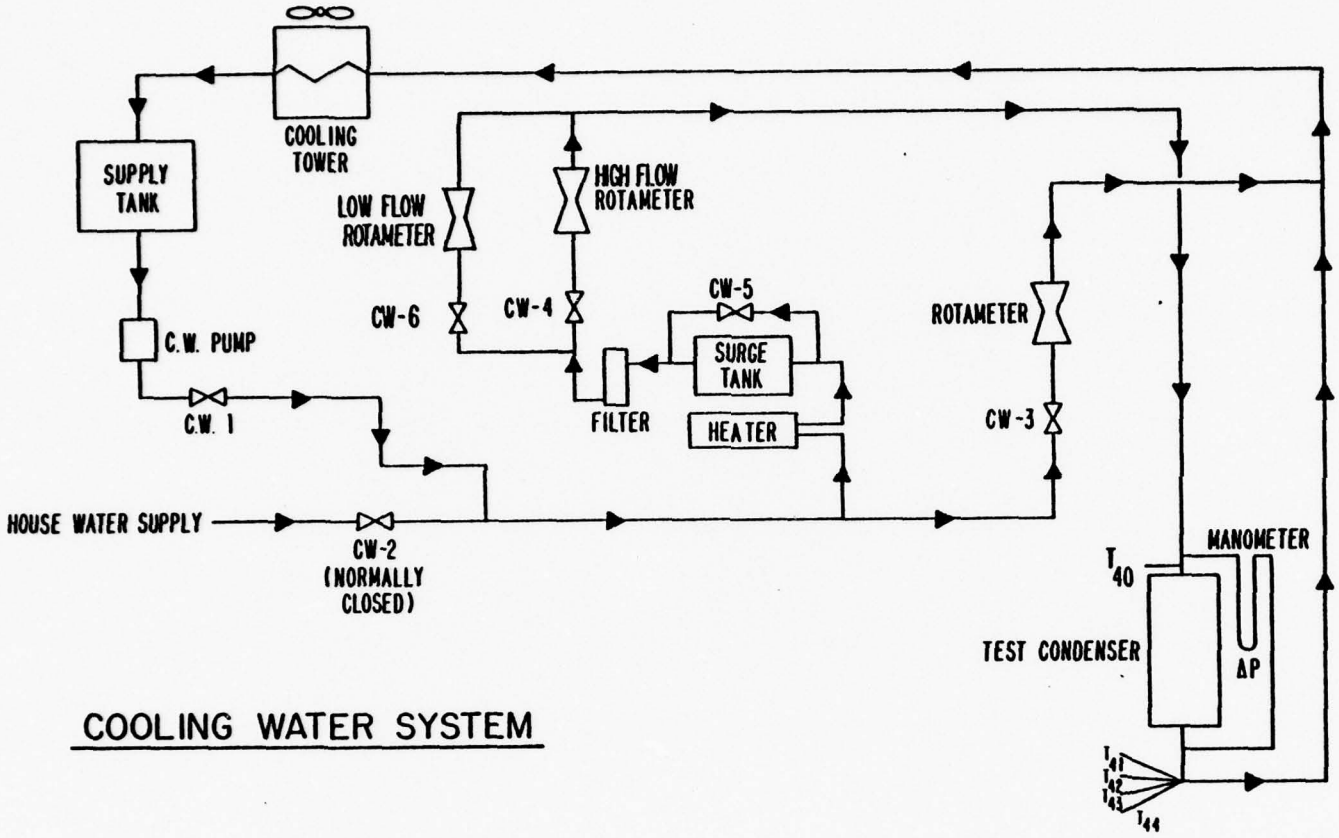


COOLING WATER SYSTEM

Figure 7. Schematic Diagram of Cooling Water System

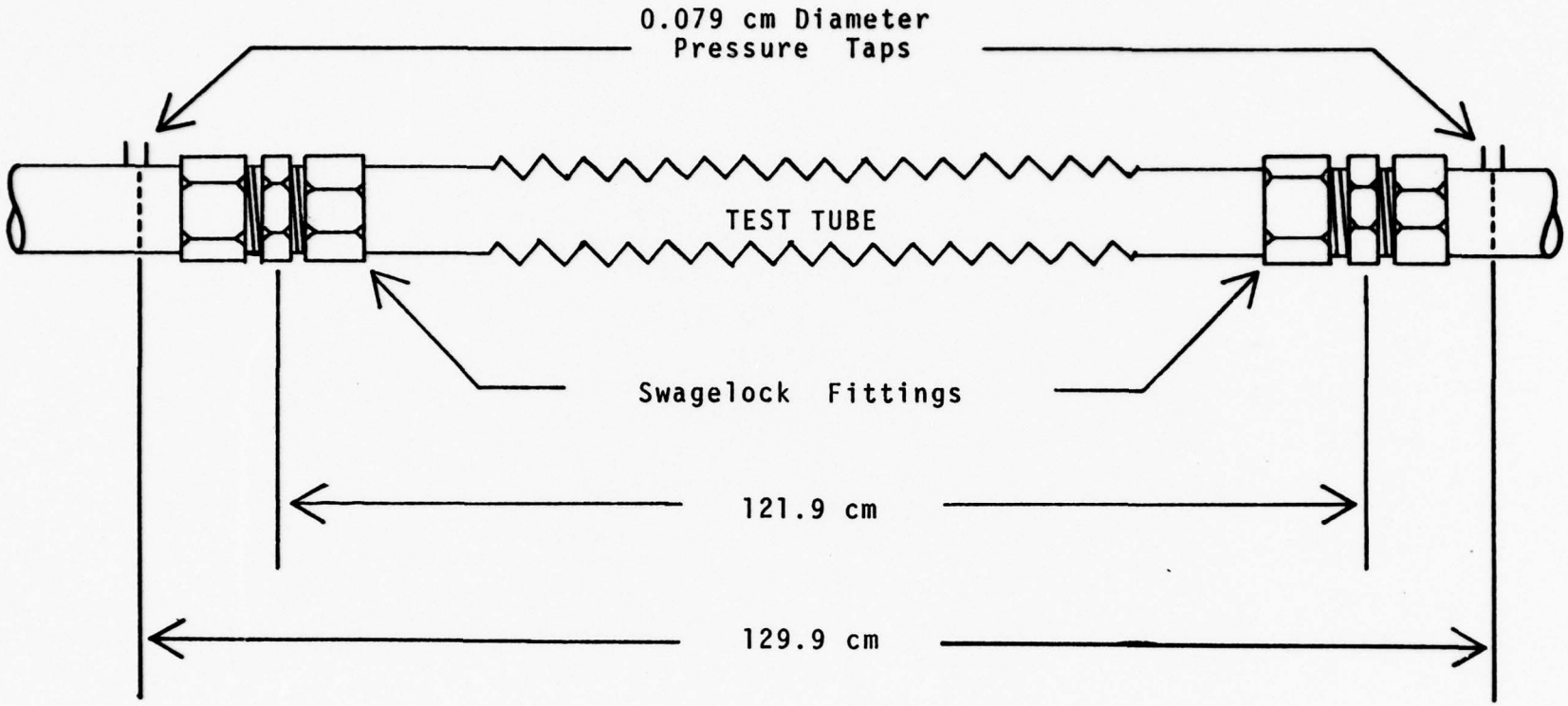


Figure 8. Enhanced Tube Schematic Drawing Showing Location of Pressure Taps.

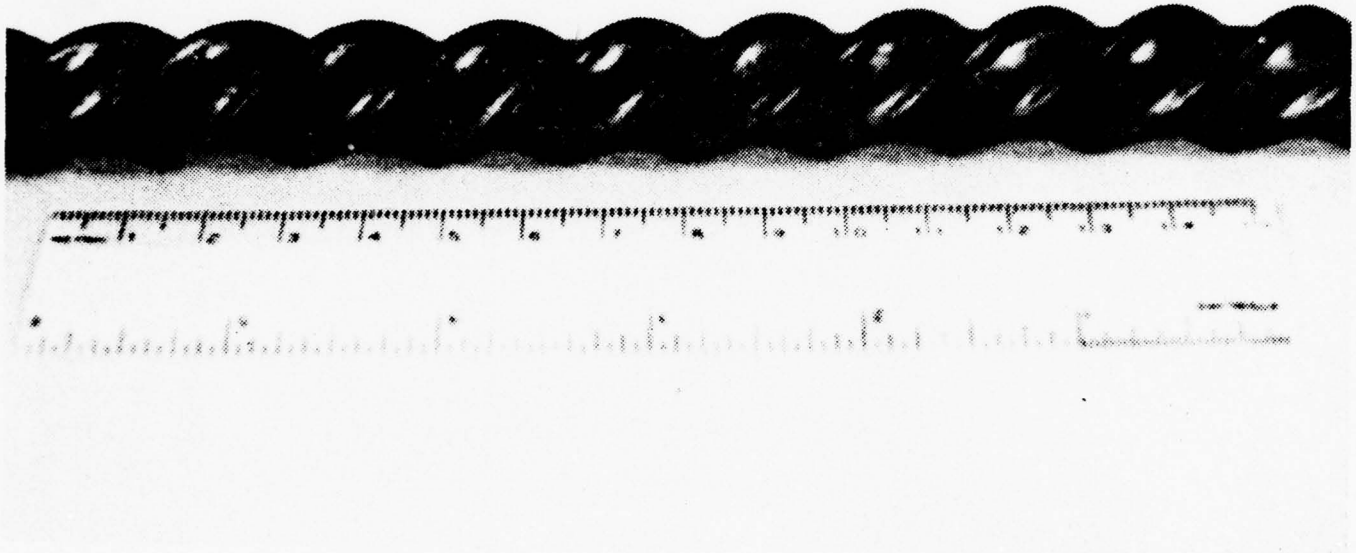

Figure 9. Photograph of High Pitch TURBOTEC Tube (Tube No. T-1)

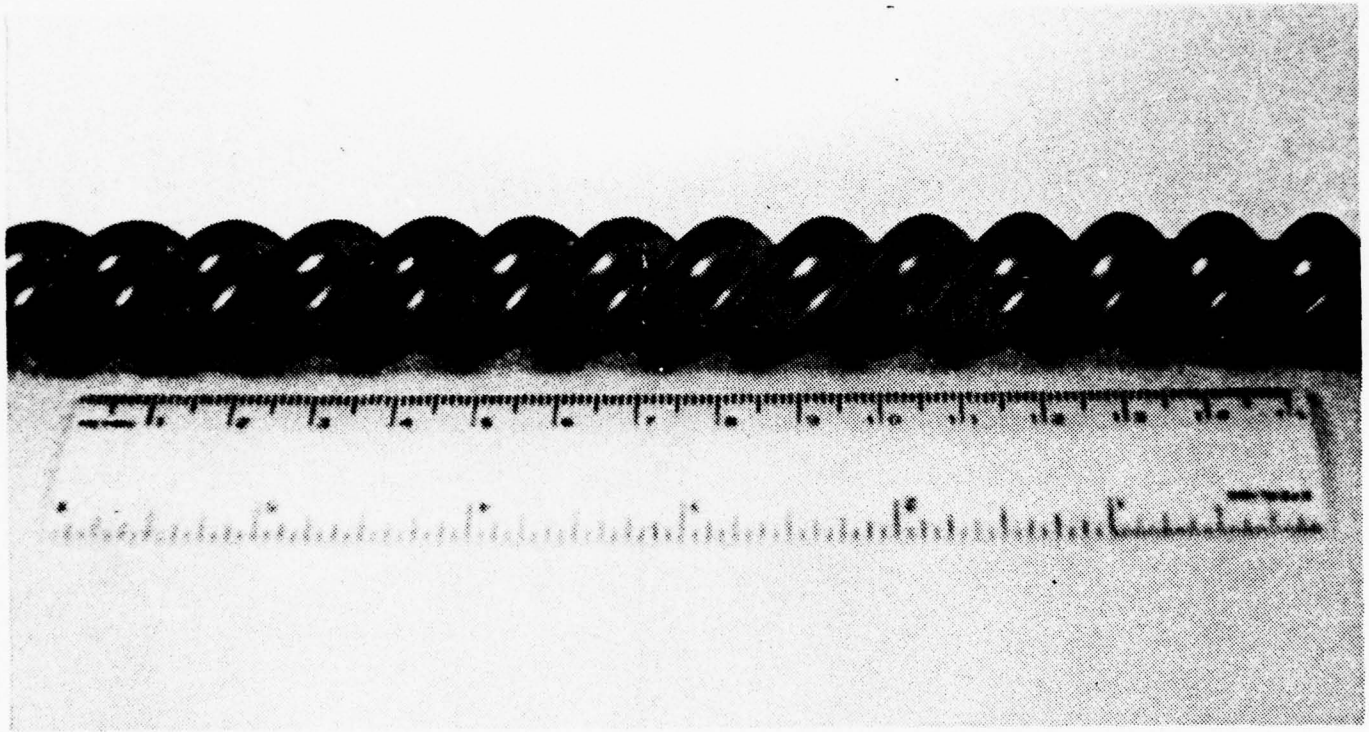

Figure 10. Photograph of Medium Pitch TURBOTEC Tube (Tube No. T-2)

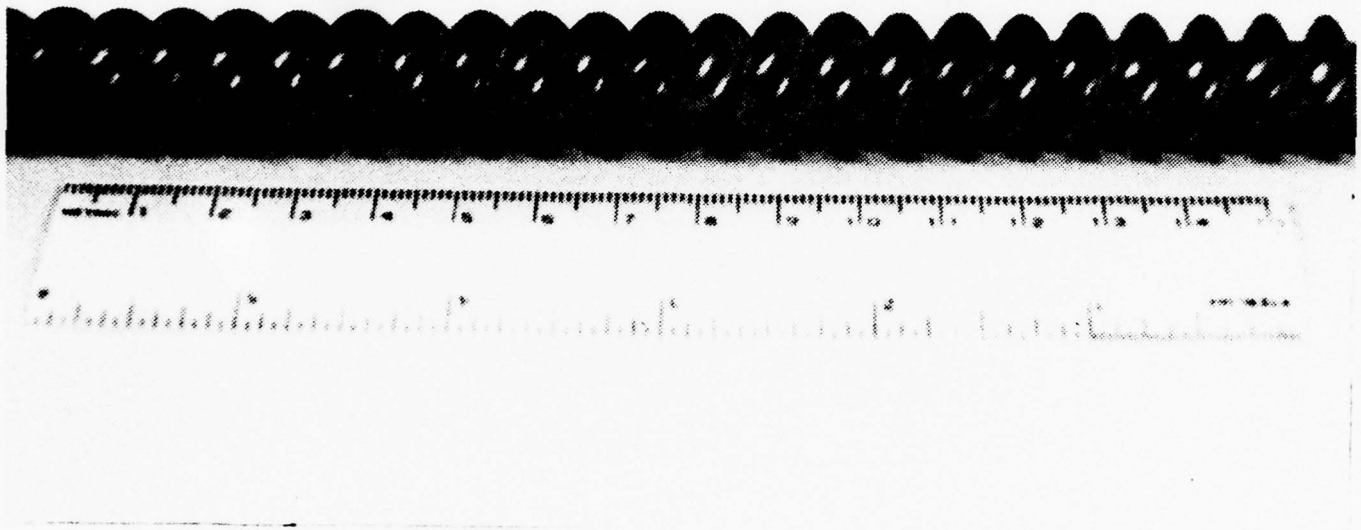

Figure 11. Photograph of Low Pitch TURBOTEC Tube (Tube No. T-3)

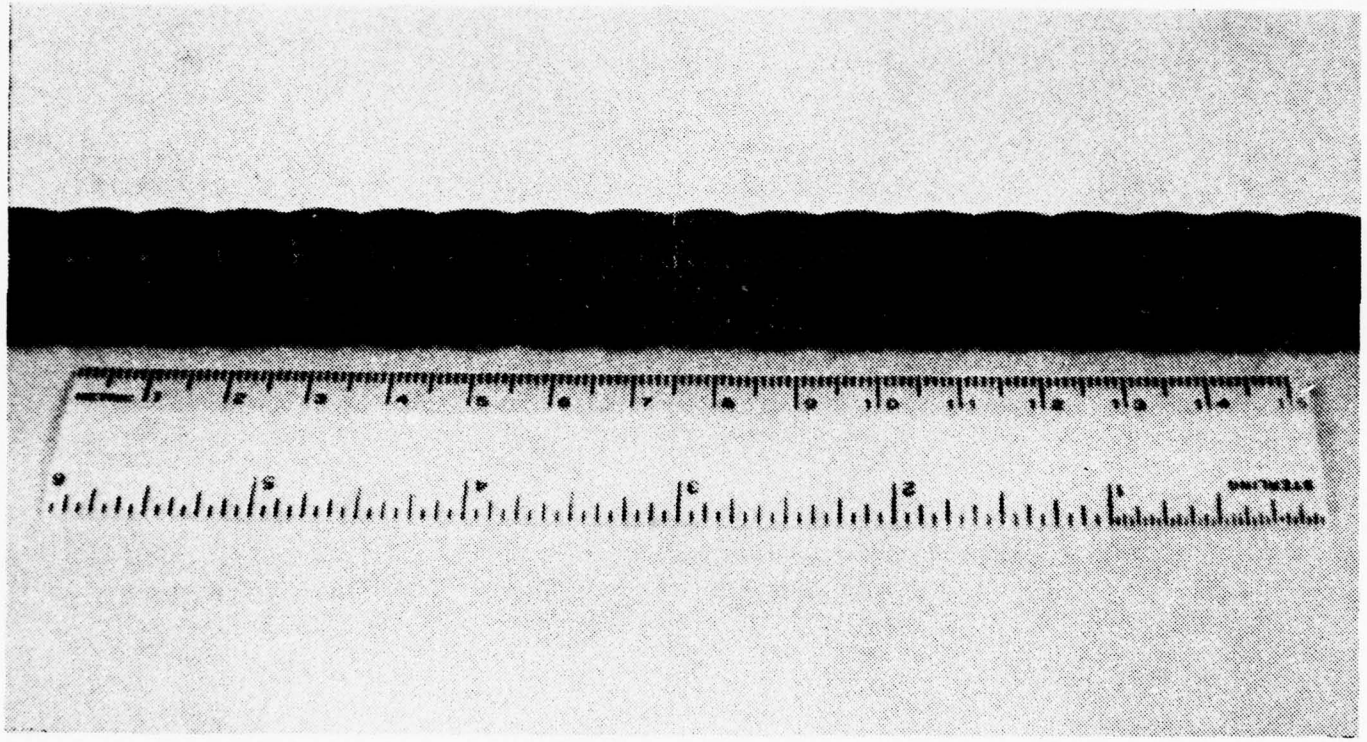

Figure 12. Photograph of Copper-Nickel-MHT KORODENSE Tube (Tube No. K-2)

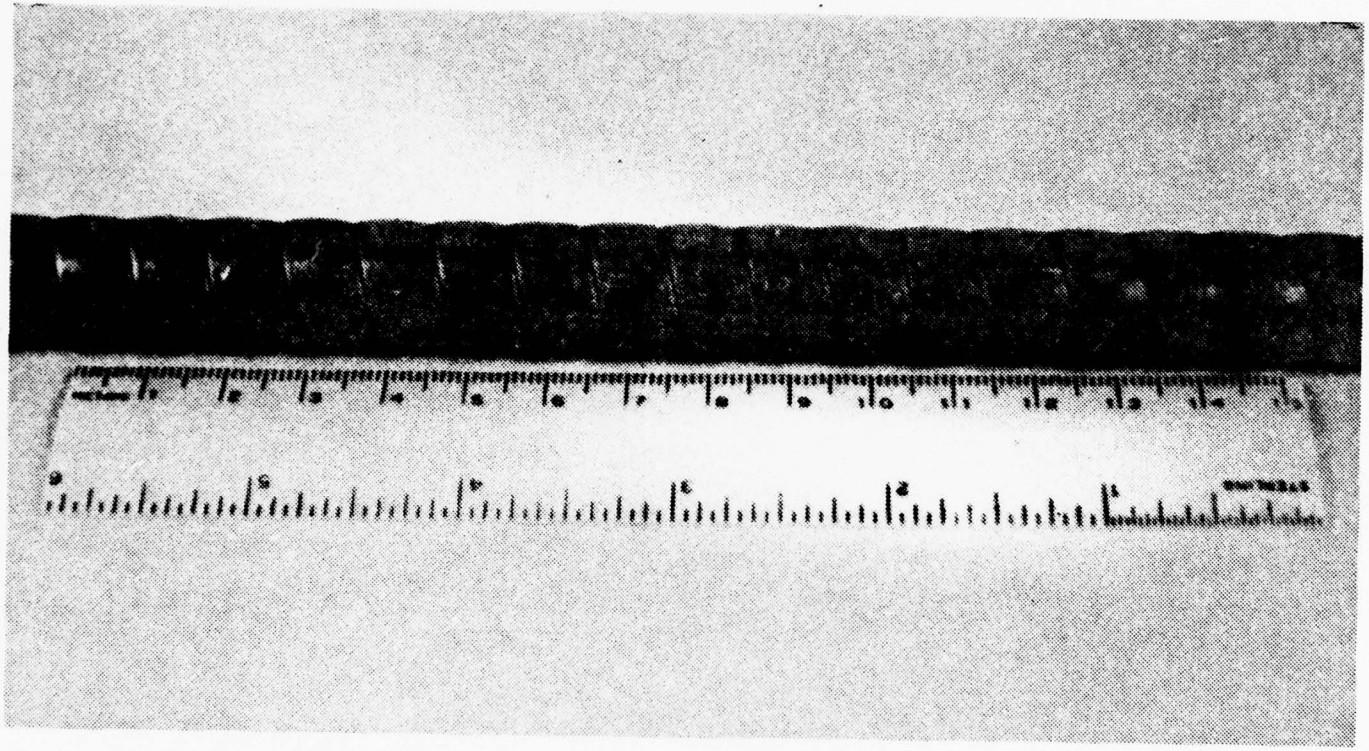

Figure 13. Photograph of Aluminum-MHT KORODENSE Tube (Tube No. K-4)

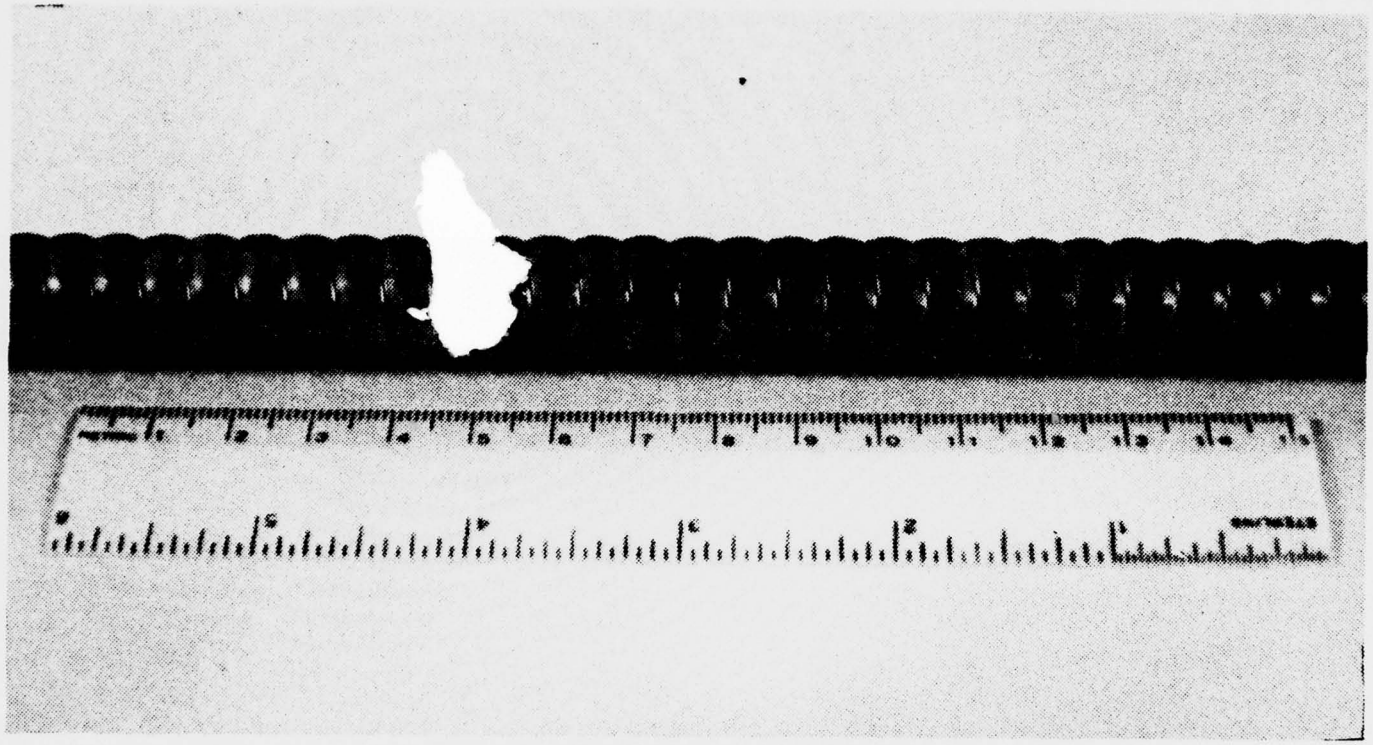

Figure 14. Photograph of Titanium-MHT KORODENSE Tube (Tube No. K-5)

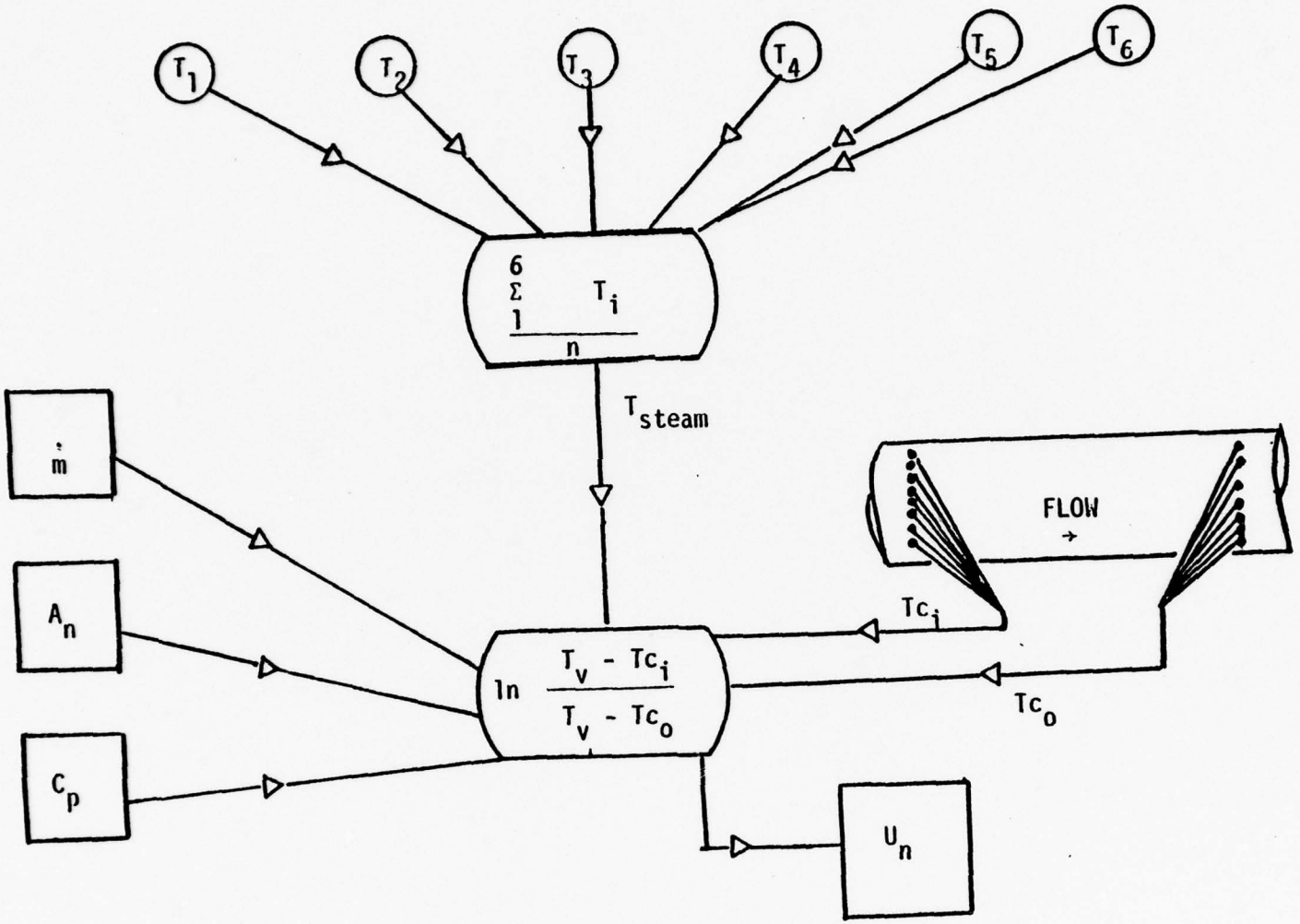


Figure 15. Schematic Representation of Procedure Used to Find $U_n$

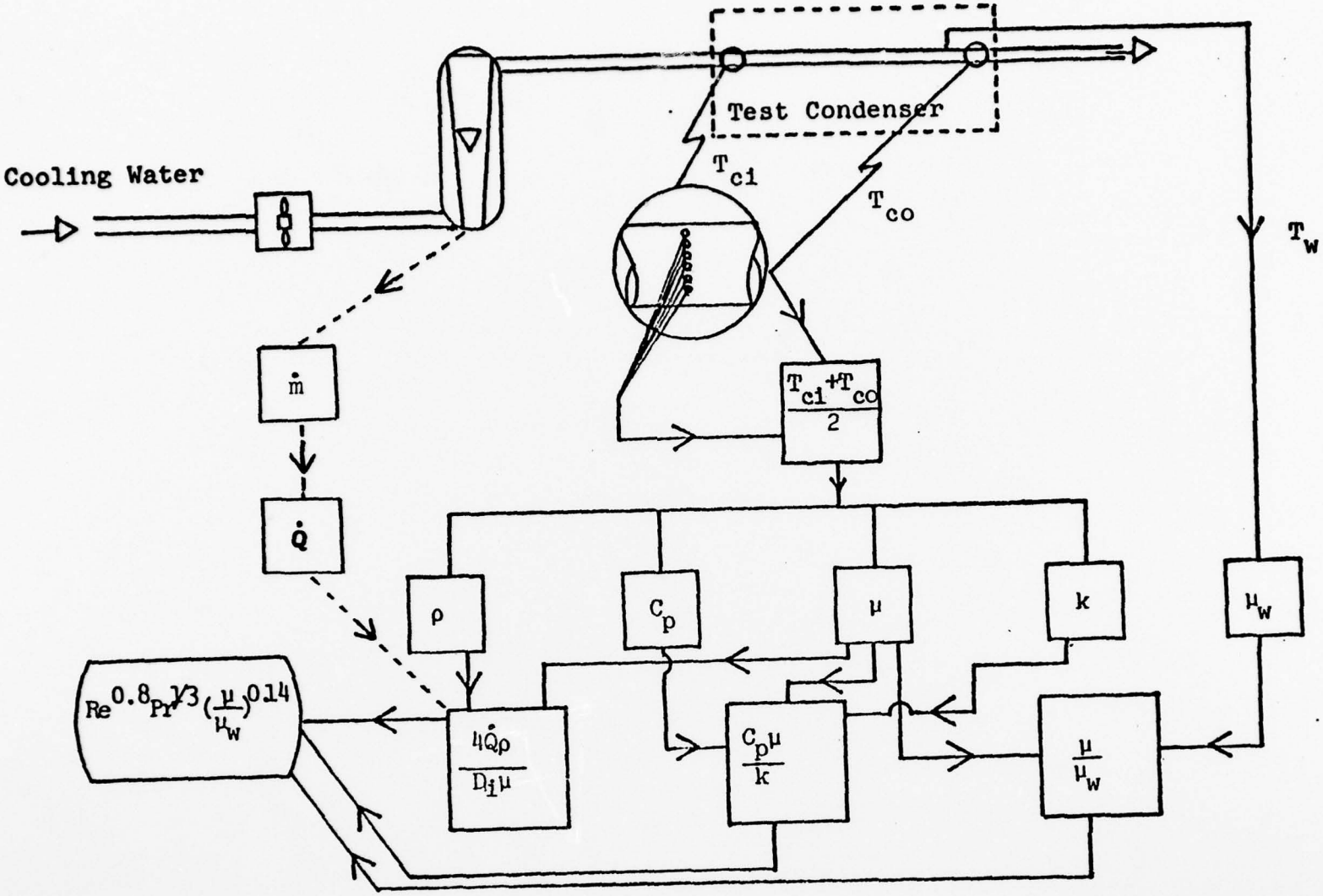


Figure 16. Schematic Representation of Procedure Used to Find Sieder-Tate Parameter

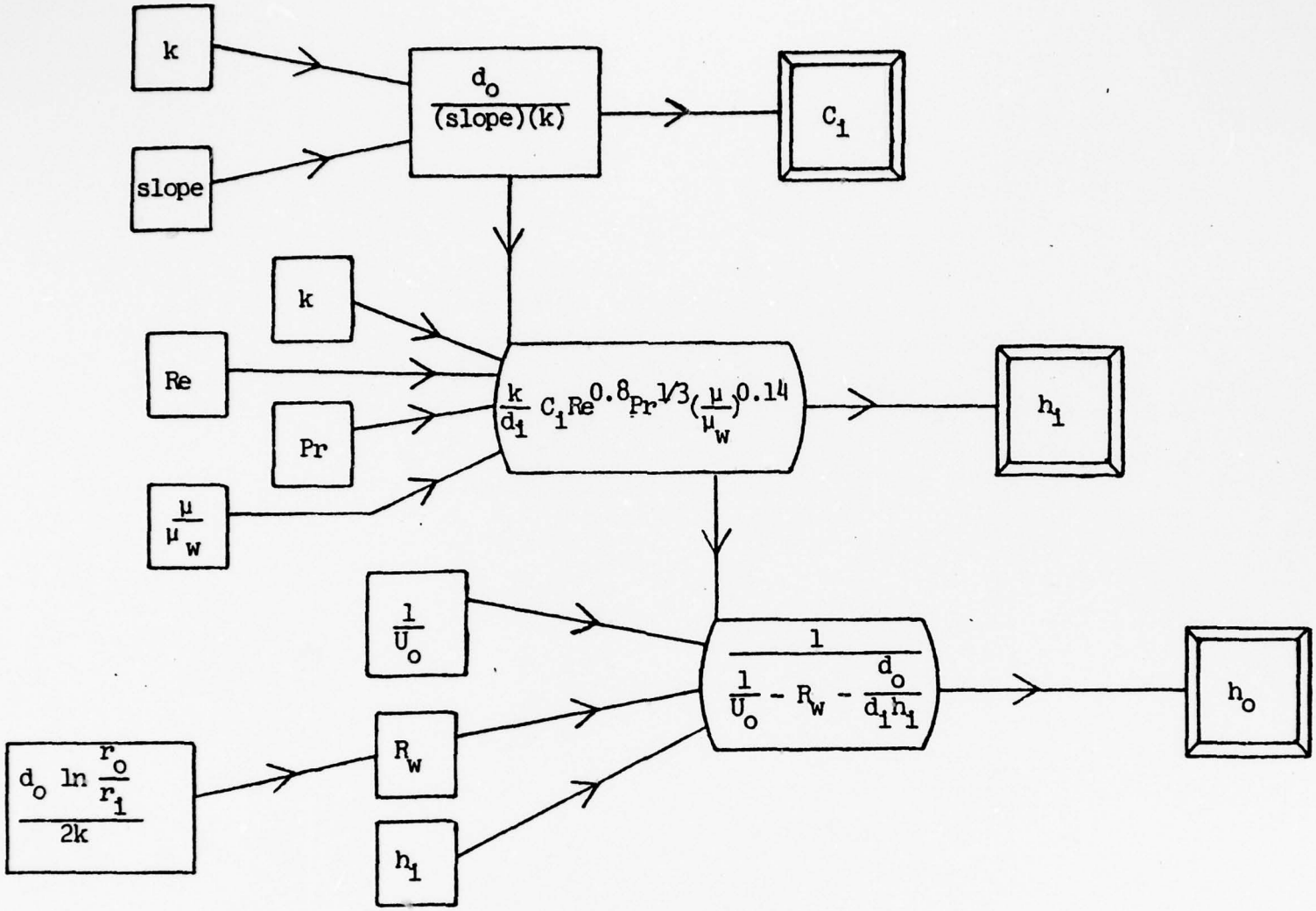


Figure 17. Schematic Representation of Procedure Used to Find Sieder-Tate Coefficient $C_i$, $h_i$ and $h_o$

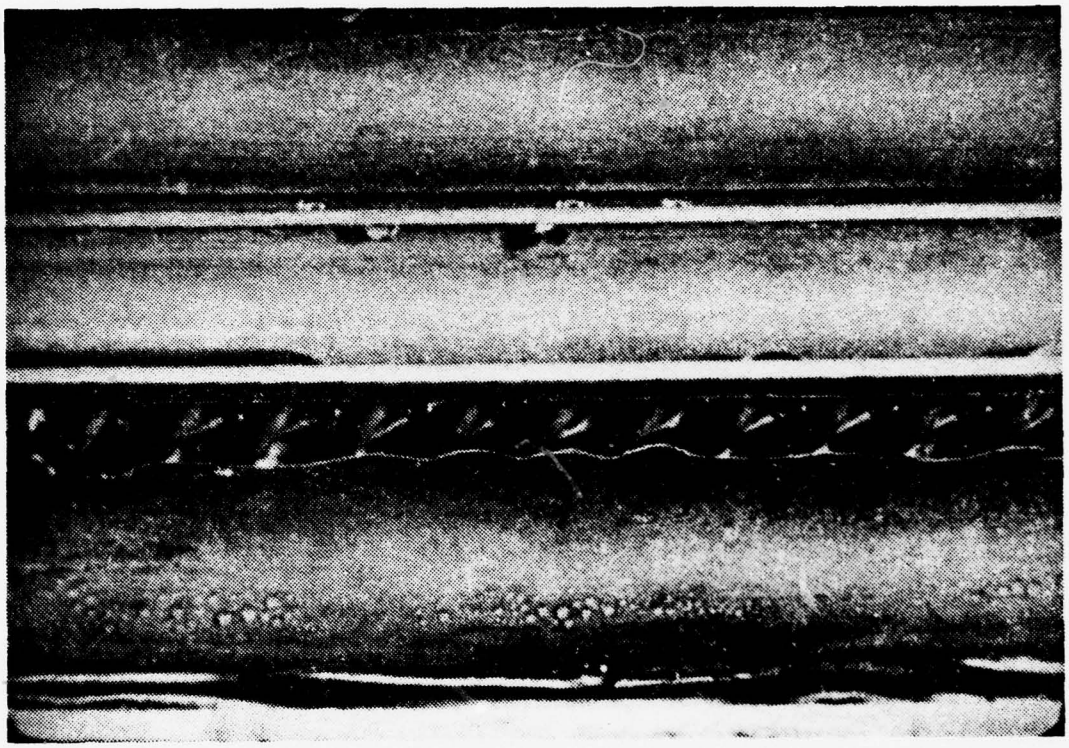

Figure 18. Photograph of Condensation on Low Pitch TURBOTEC Tube (No. T-3a) at a Cooling Water Velocity of 3 m/s

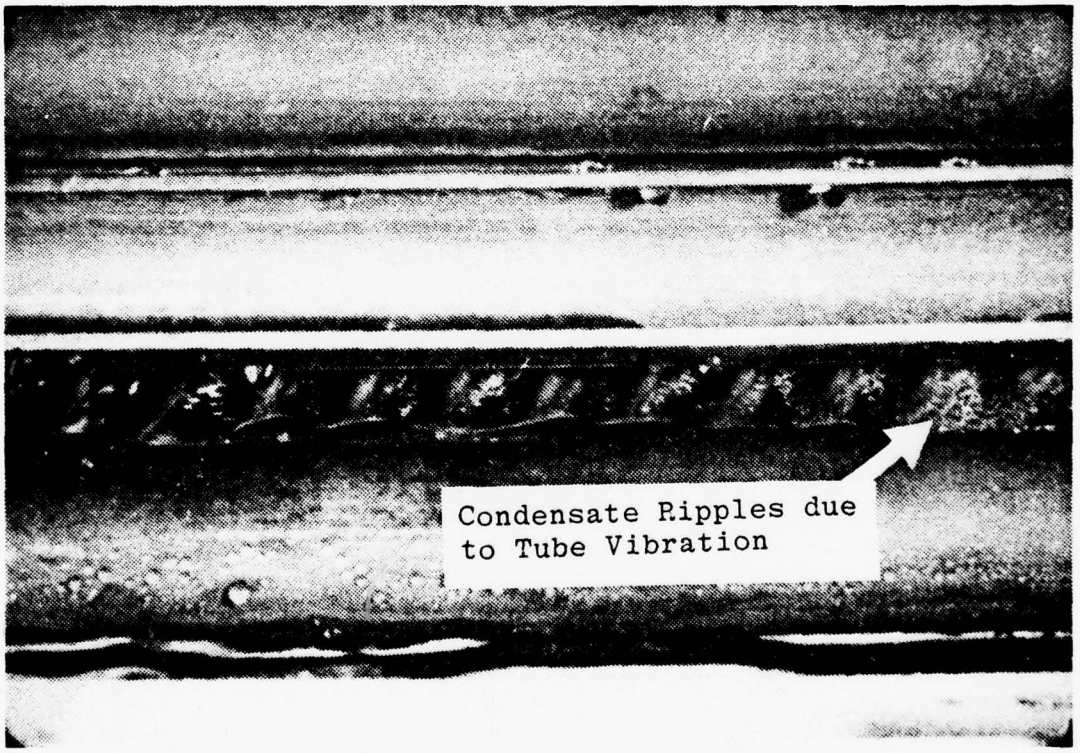


Figure 19. Photograph of Condensation on Low Pitch TURBOTEC Tube (No. T-3a) Showing Effect of Tube Vibration at a Cooling Water Velocity of 4 m/s

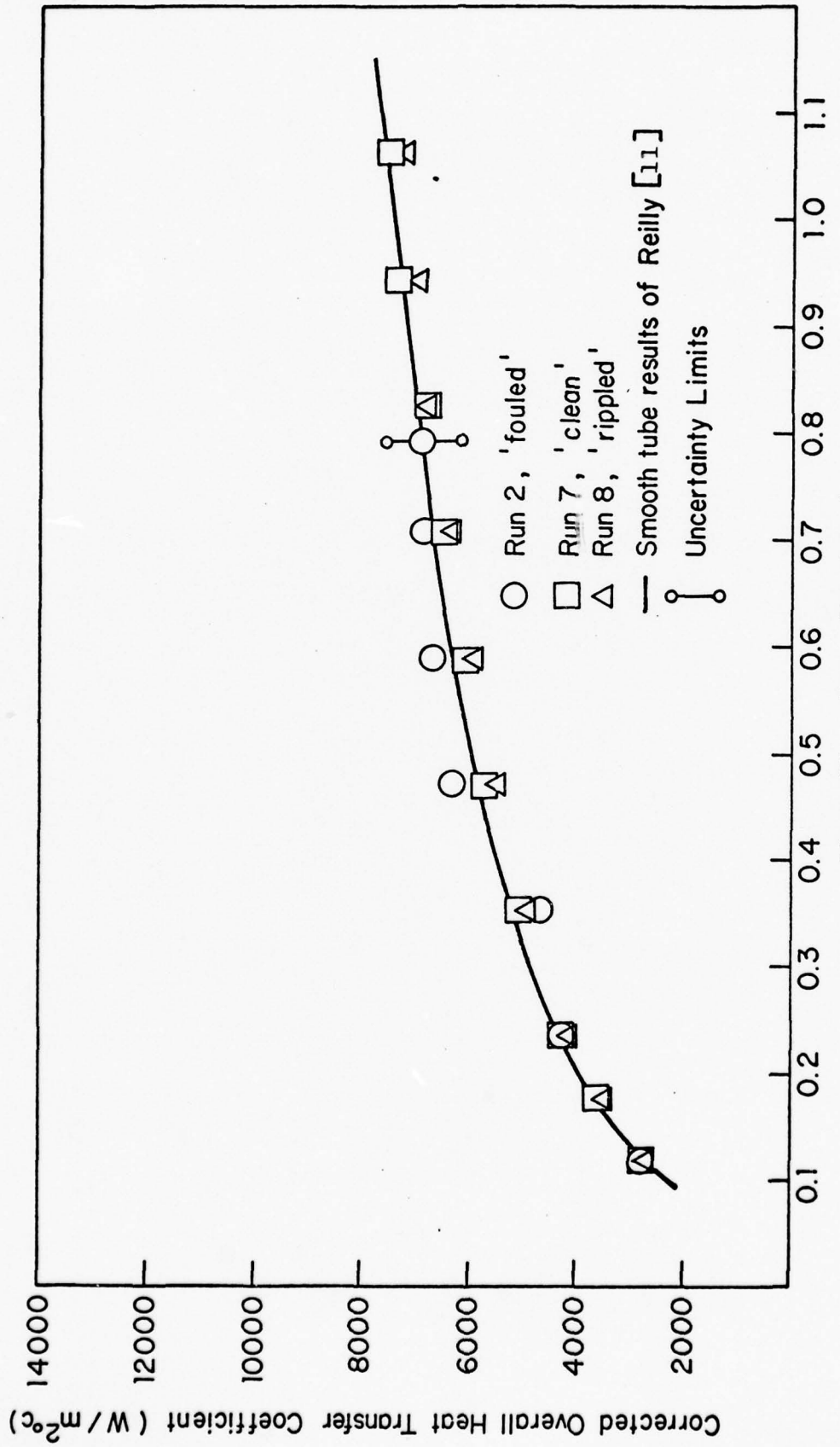


Figure 20. Corrected Overall Heat Transfer Coefficient Versus Cooling Water Mass Flow Rate for Smooth Tubes.

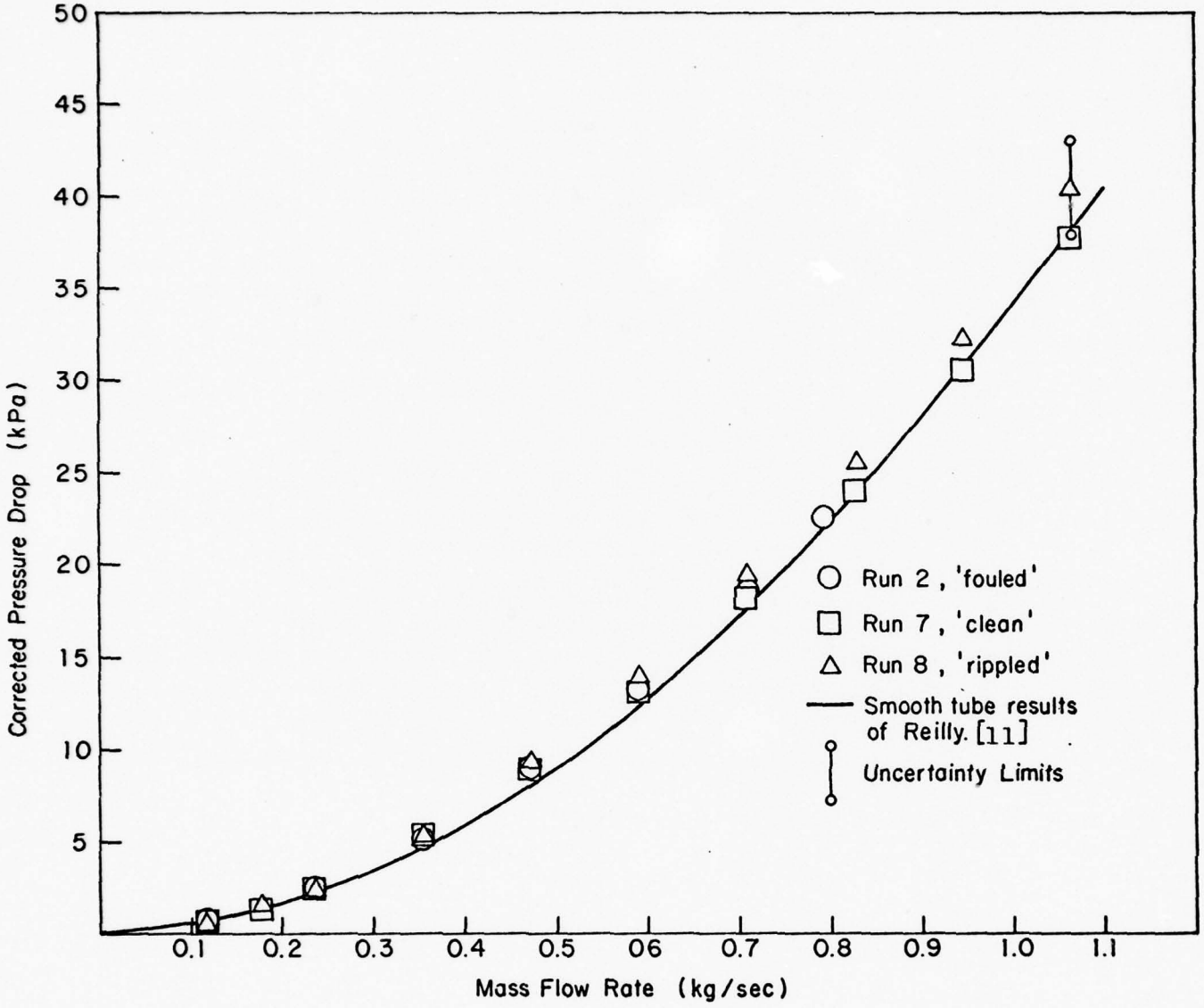


Figure 21. Corrected Pressure Drop Versus Cooling Water Mass Flow Rate for Smooth Tubes.

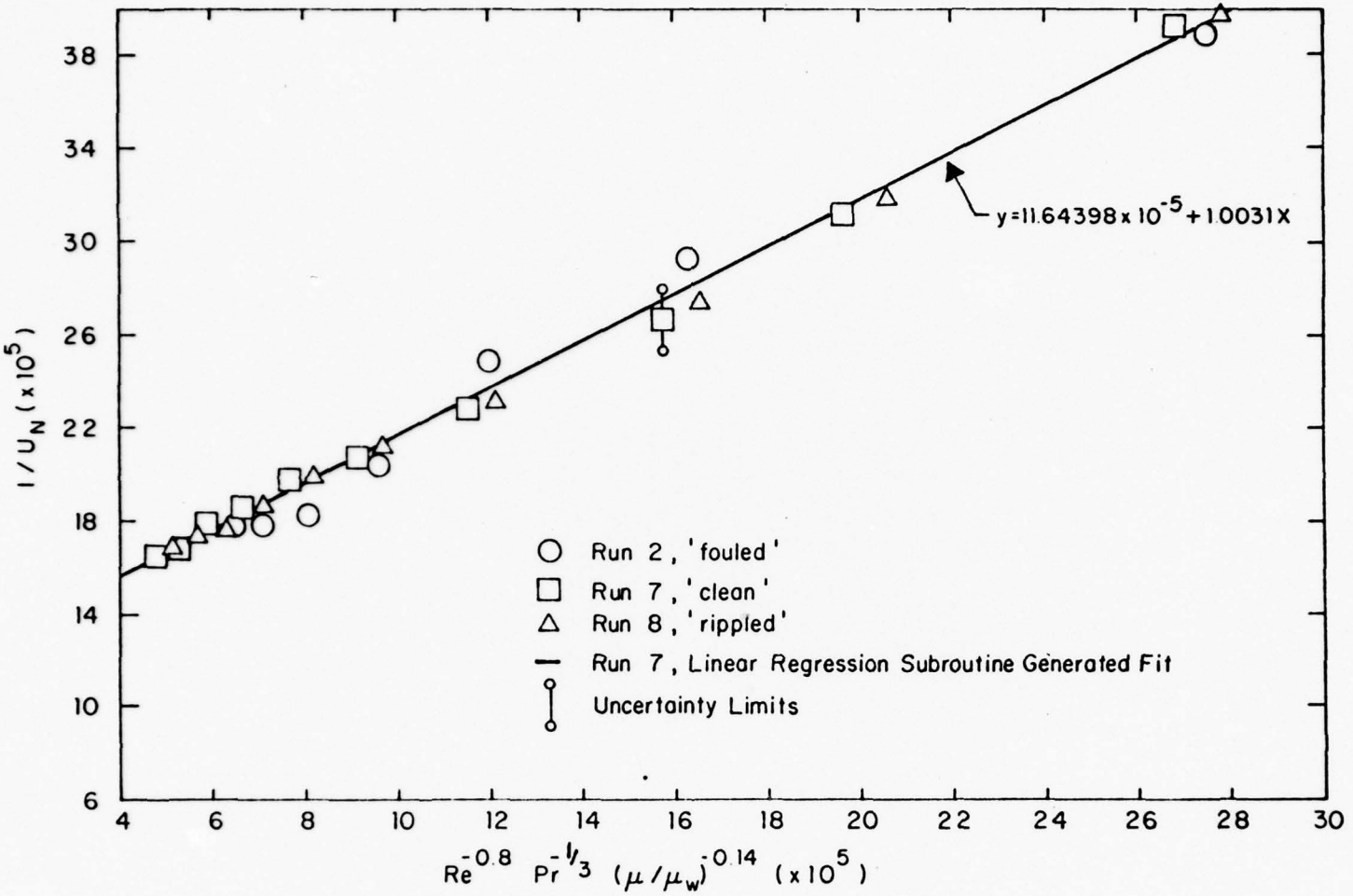


Figure 22. Wilson Plot for Smooth Tubes

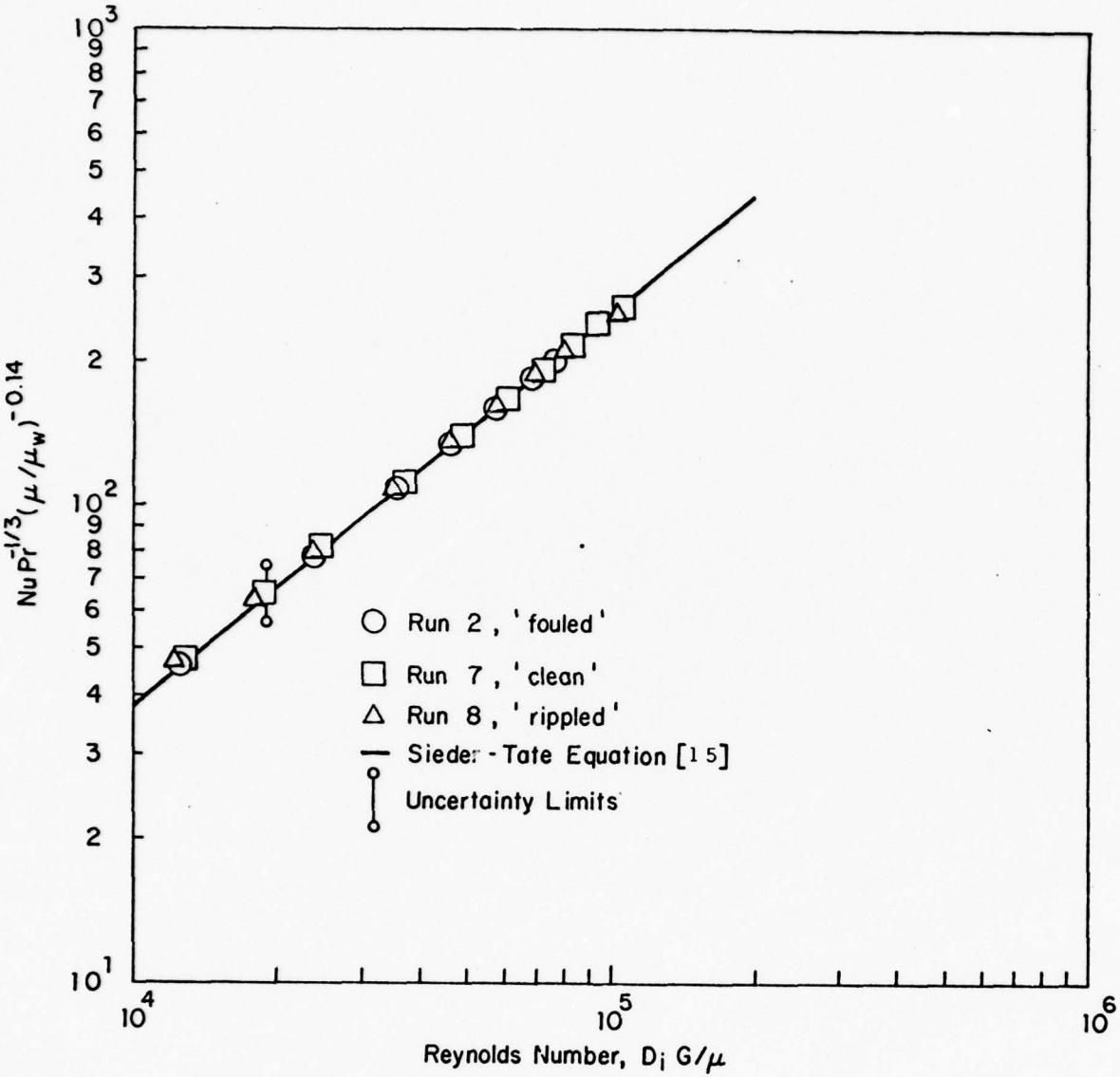


Figure 23. Inside Nusselt Number Correlation Versus Reynolds Number for Smooth Tubes.

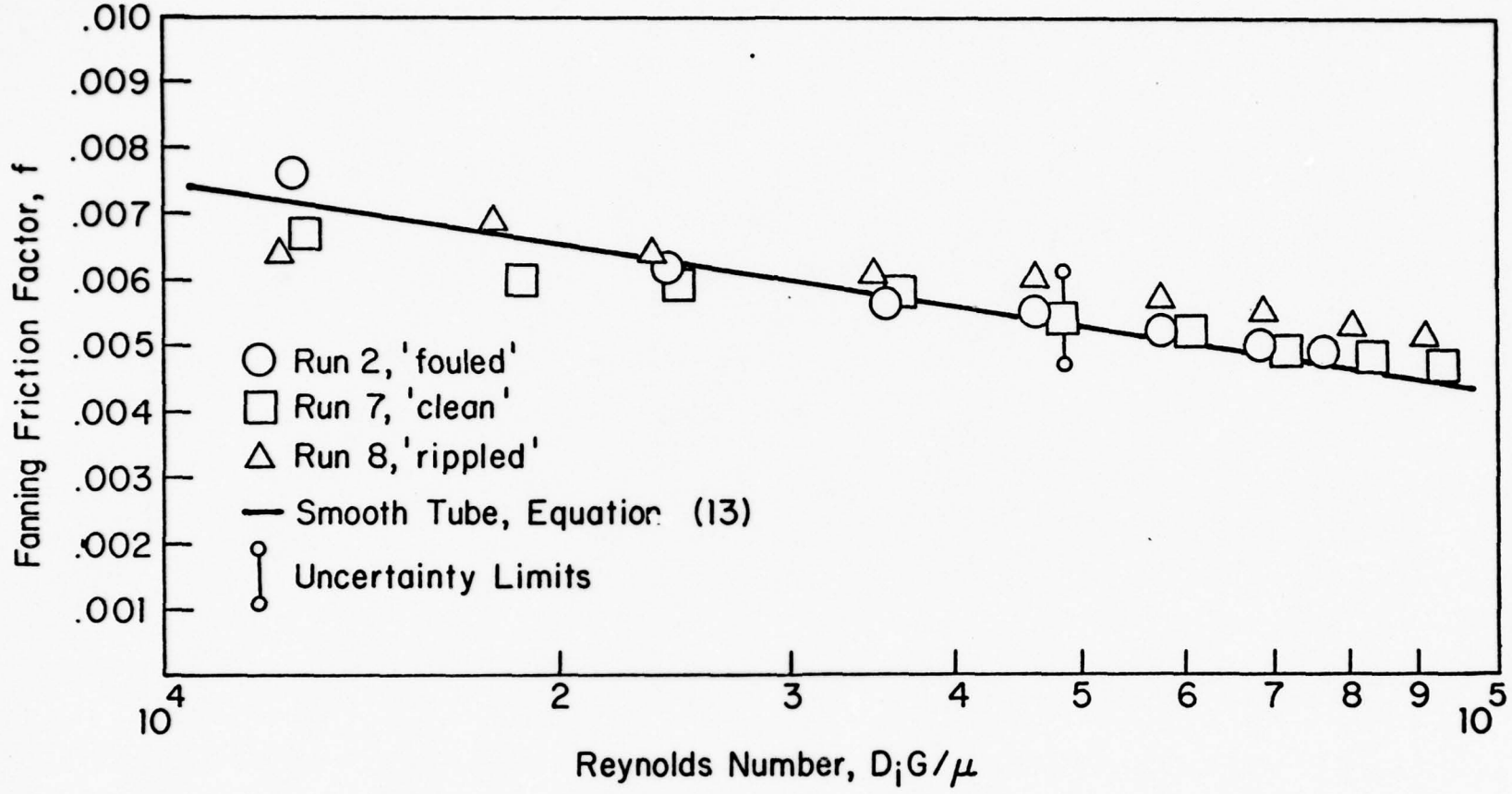


Figure 24. Fanning Friction Factor Versus Reynolds Number for Smooth Tubes.

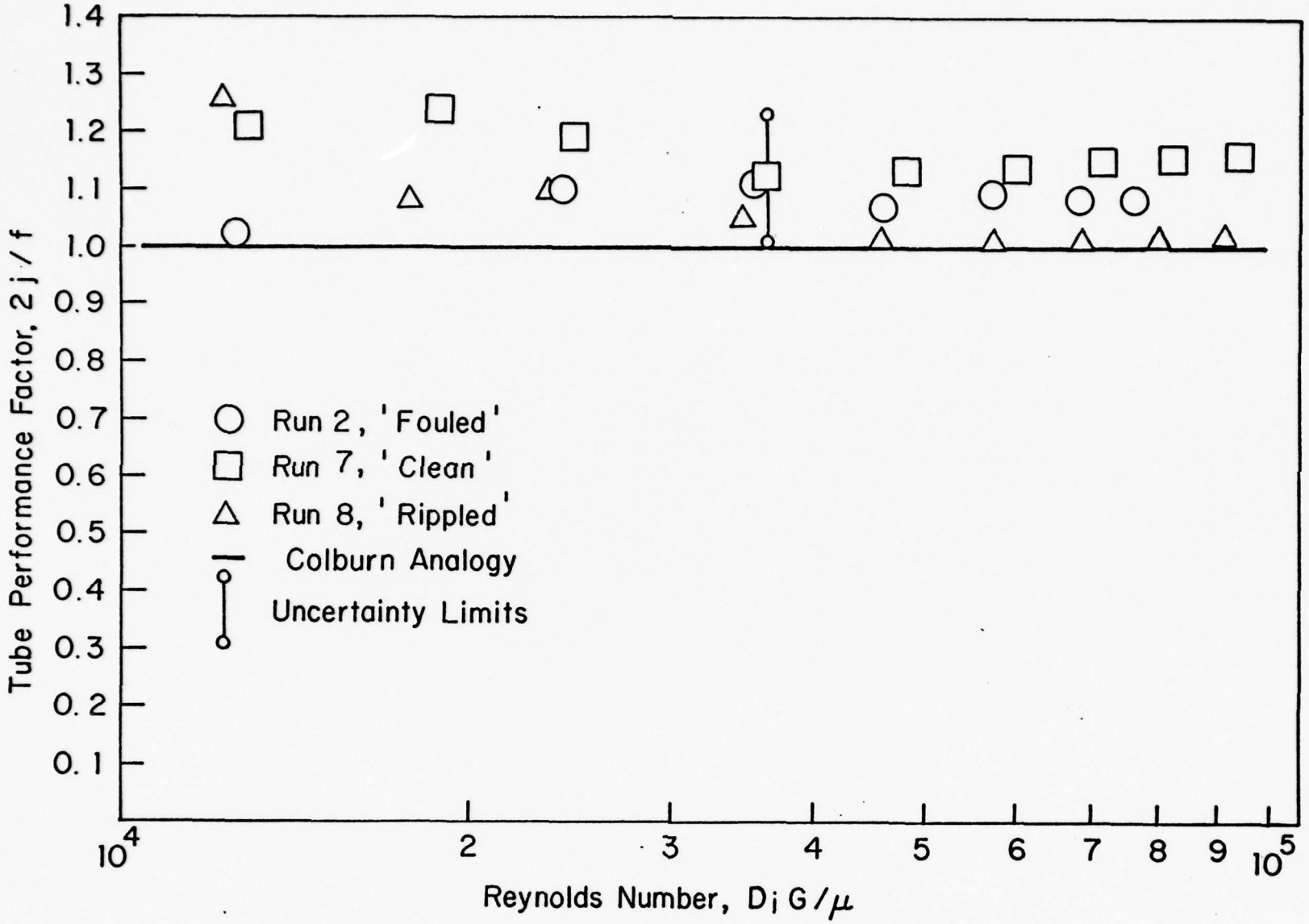


Figure 25. Tube Performance Factor, 2j/f, Versus Reynolds Number for Smooth Tubes.

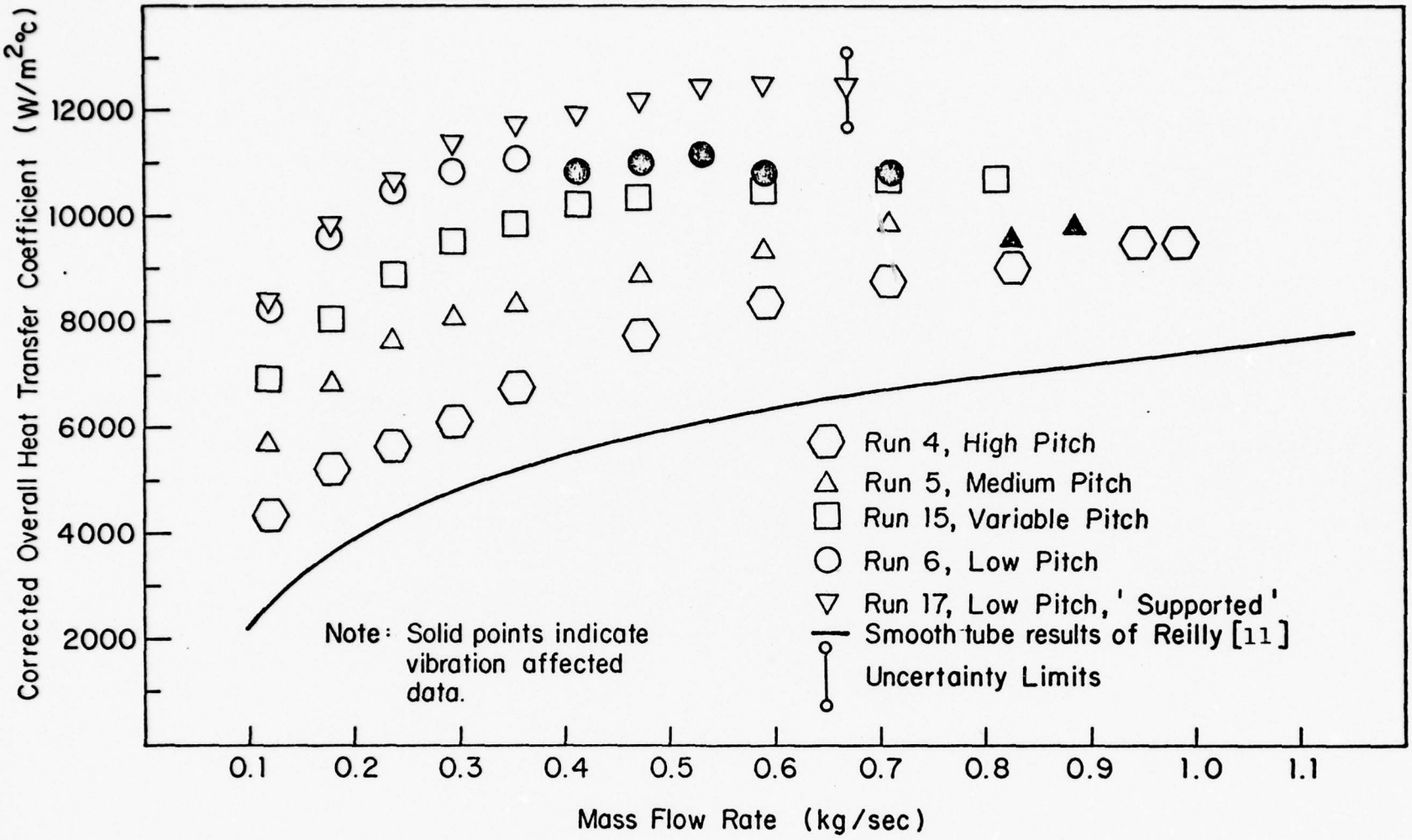


Figure 26. Corrected Overall Heat Transfer Coefficient, $U_c$, Versus Cooling Water Mass Flow Rate for TURBOTEC Tubes

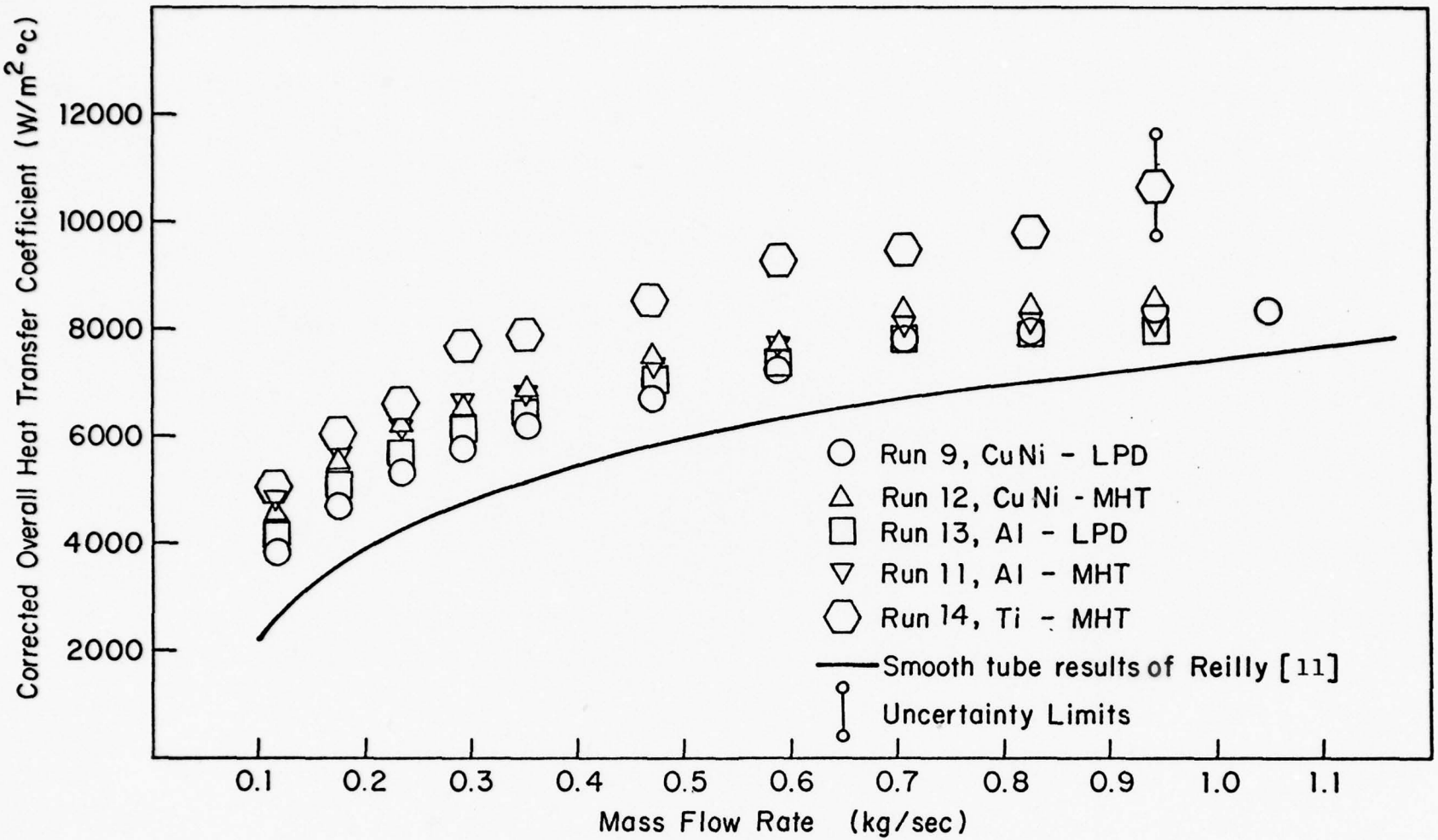


Figure 27. Corrected Overall Heat Transfer Coefficient, $U_c$, Versus Cooling Water Mass Flow Rate for KORODENSE Tubes.

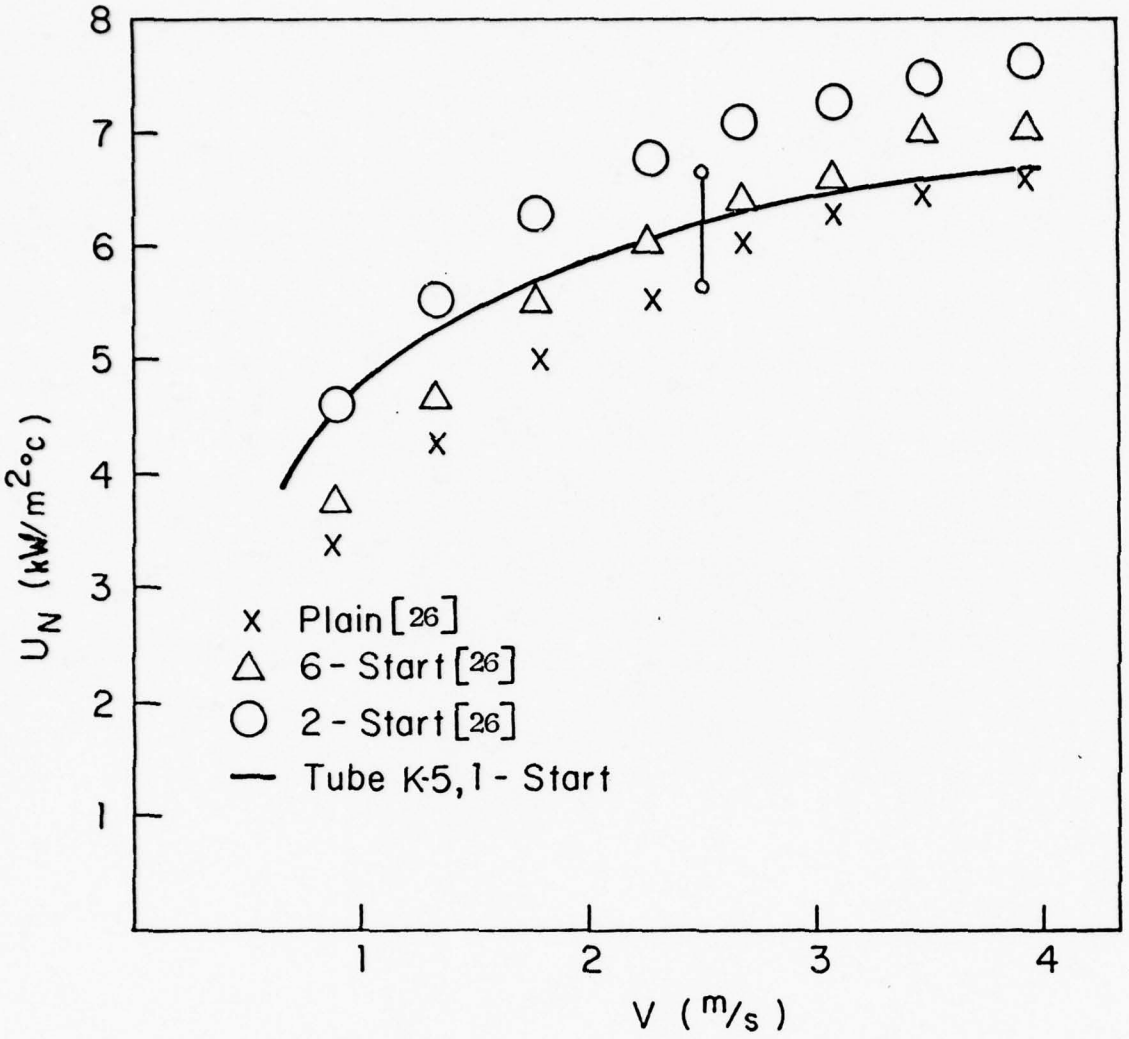


Figure 28. Uncorrected Overall Heat Transfer Coefficient, $U_n$, Versus Cooling Water Velocity for Tube K-5 Compared with Data of Cunningham and Milne [26]

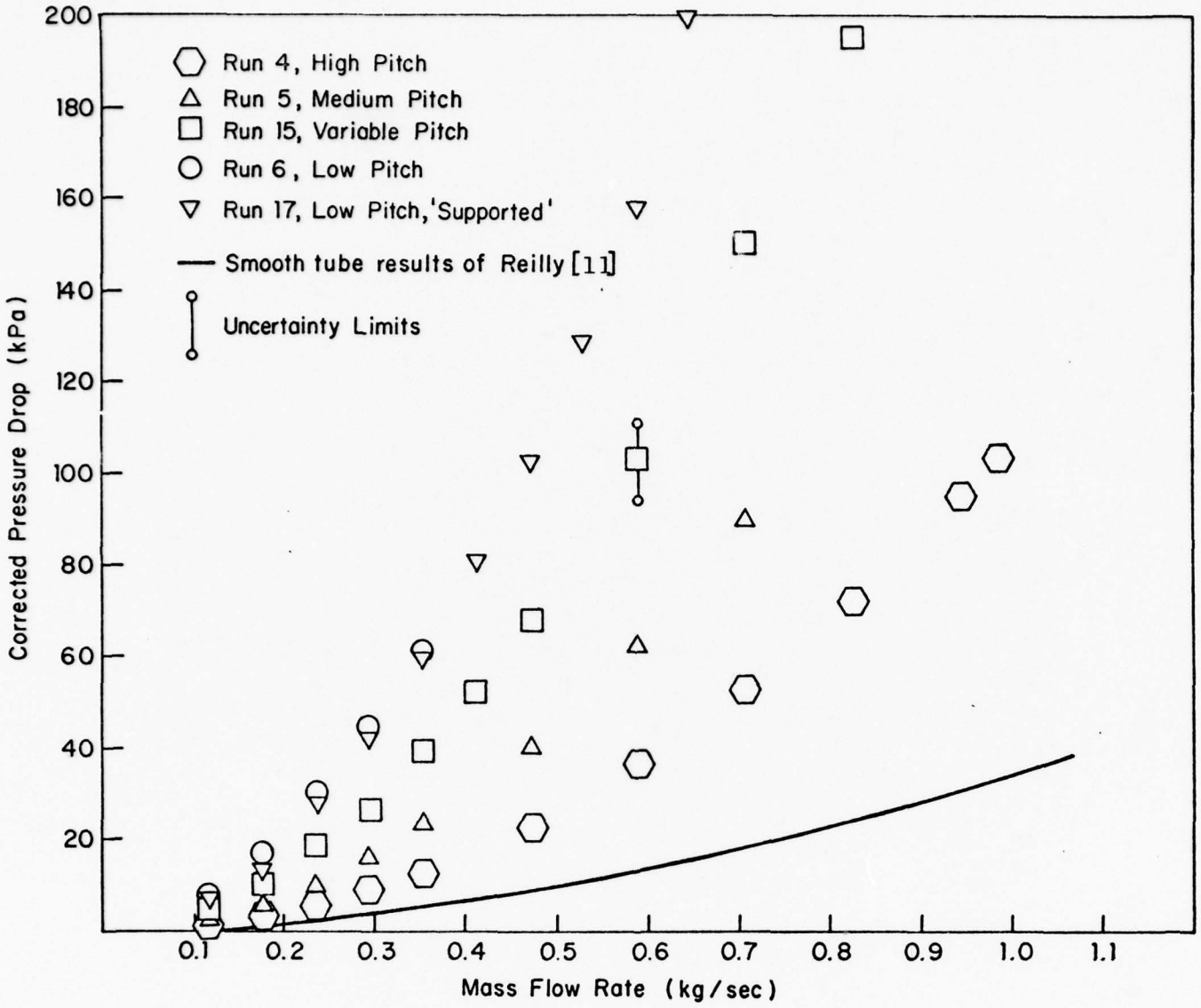


Figure 29. Corrected Pressure Drop Versus Cooling Water Mass Flow Rate for TURBOTEC Tubes.

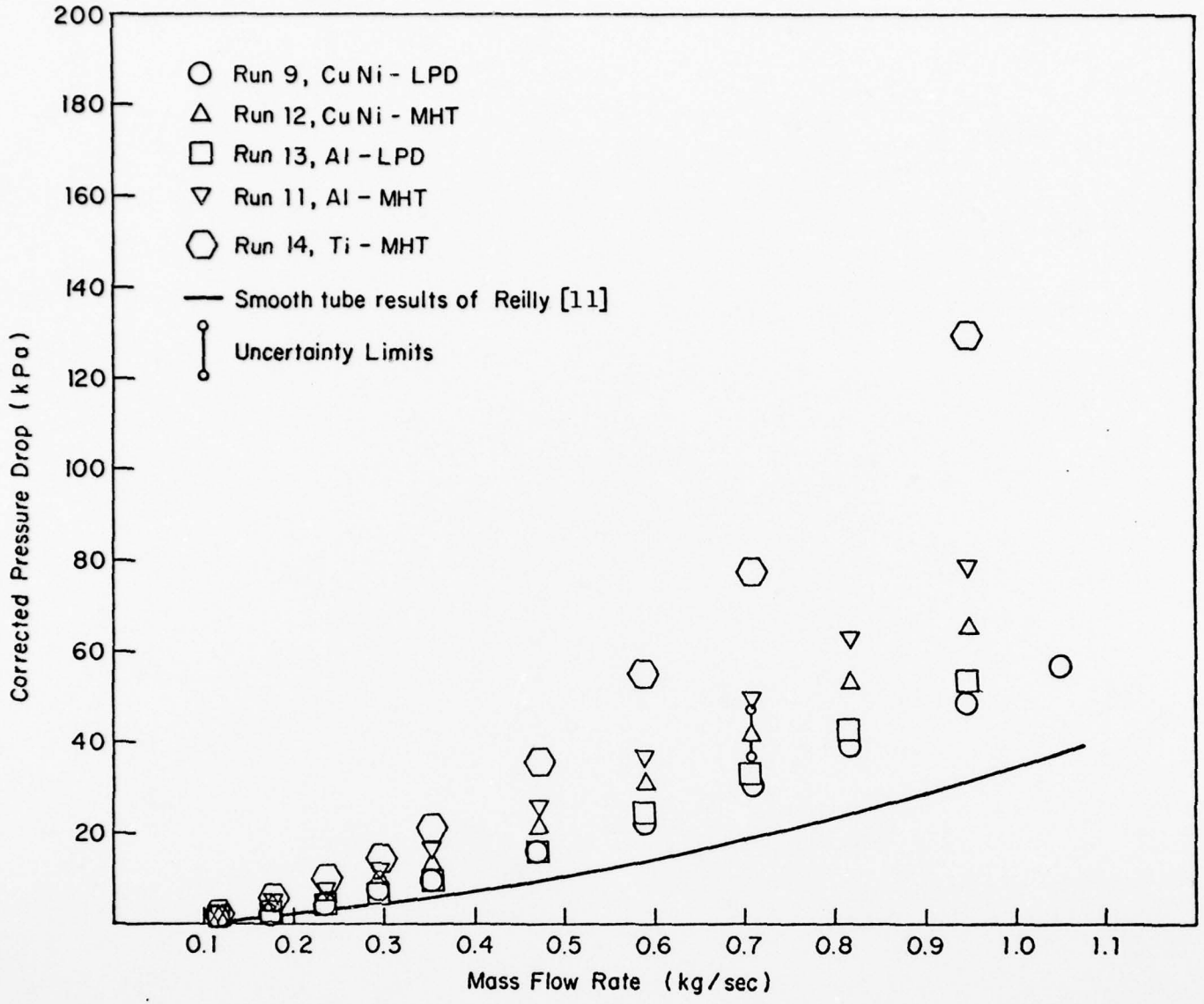


Figure 30. Corrected Pressure Drop Versus Cooling Water Mass Flow Rate for KORODENSE Tubes.

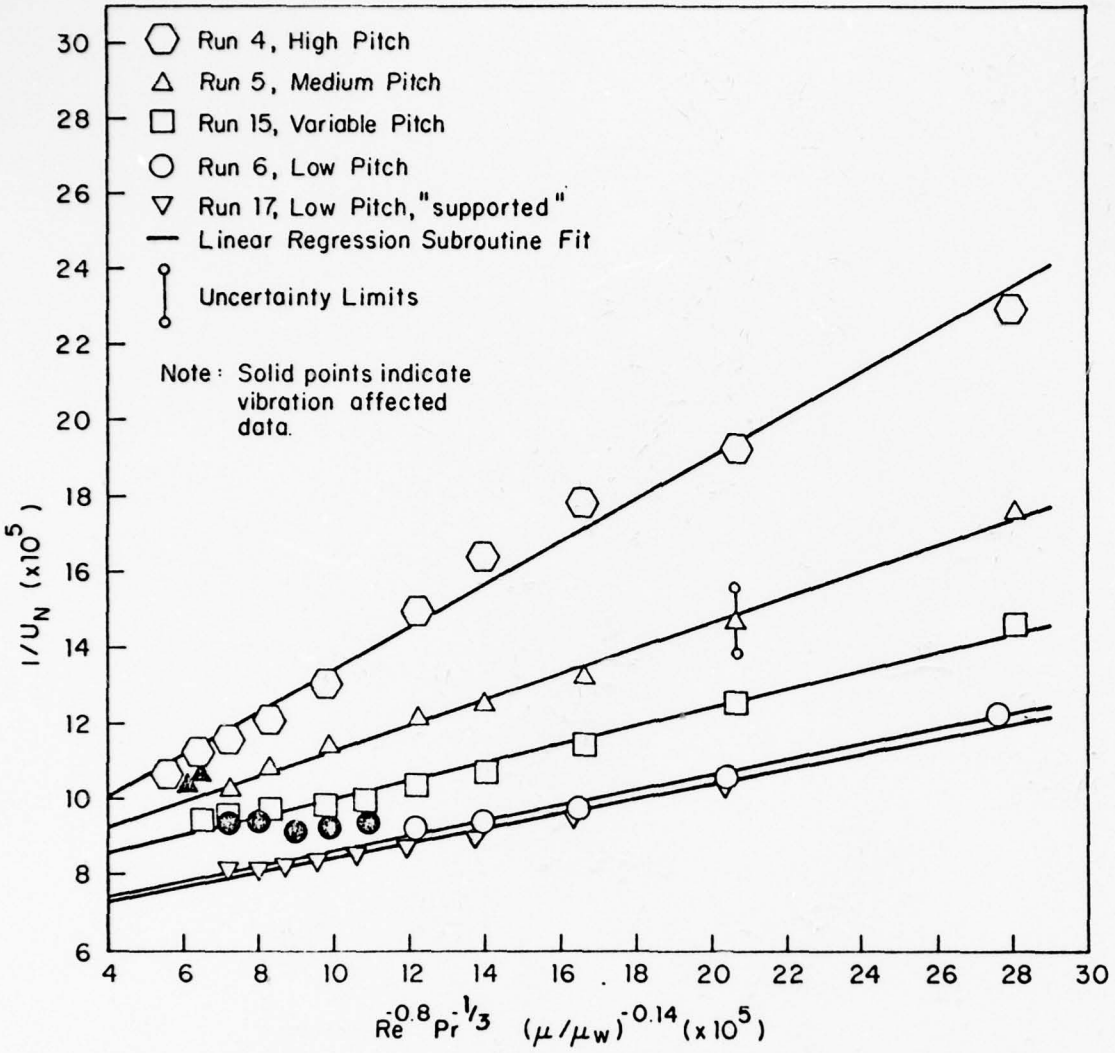


Figure 31. Wilson Plot for TURBOTEC Tubes.

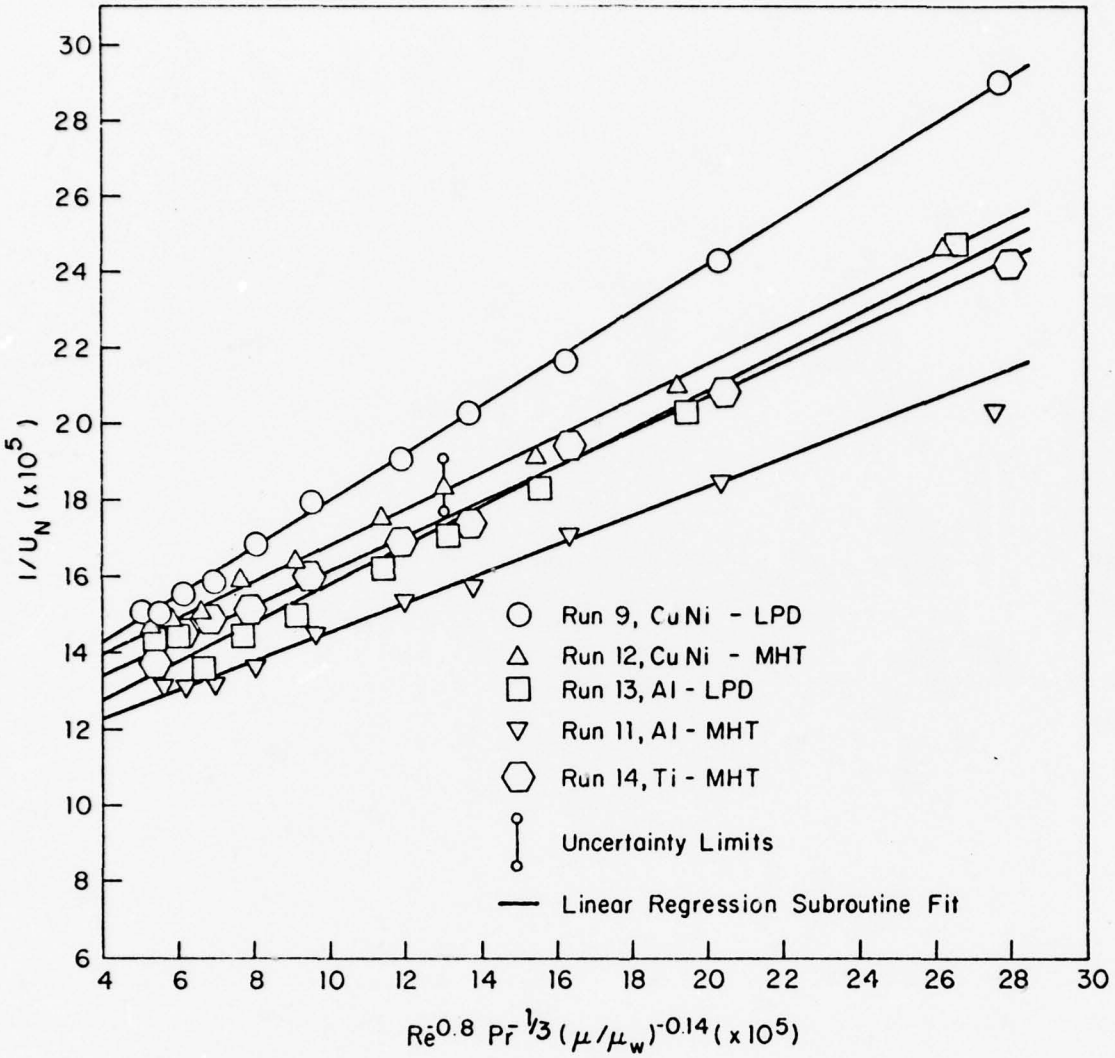


Figure 32. Wilson Plot for KORODENSE Tubes.

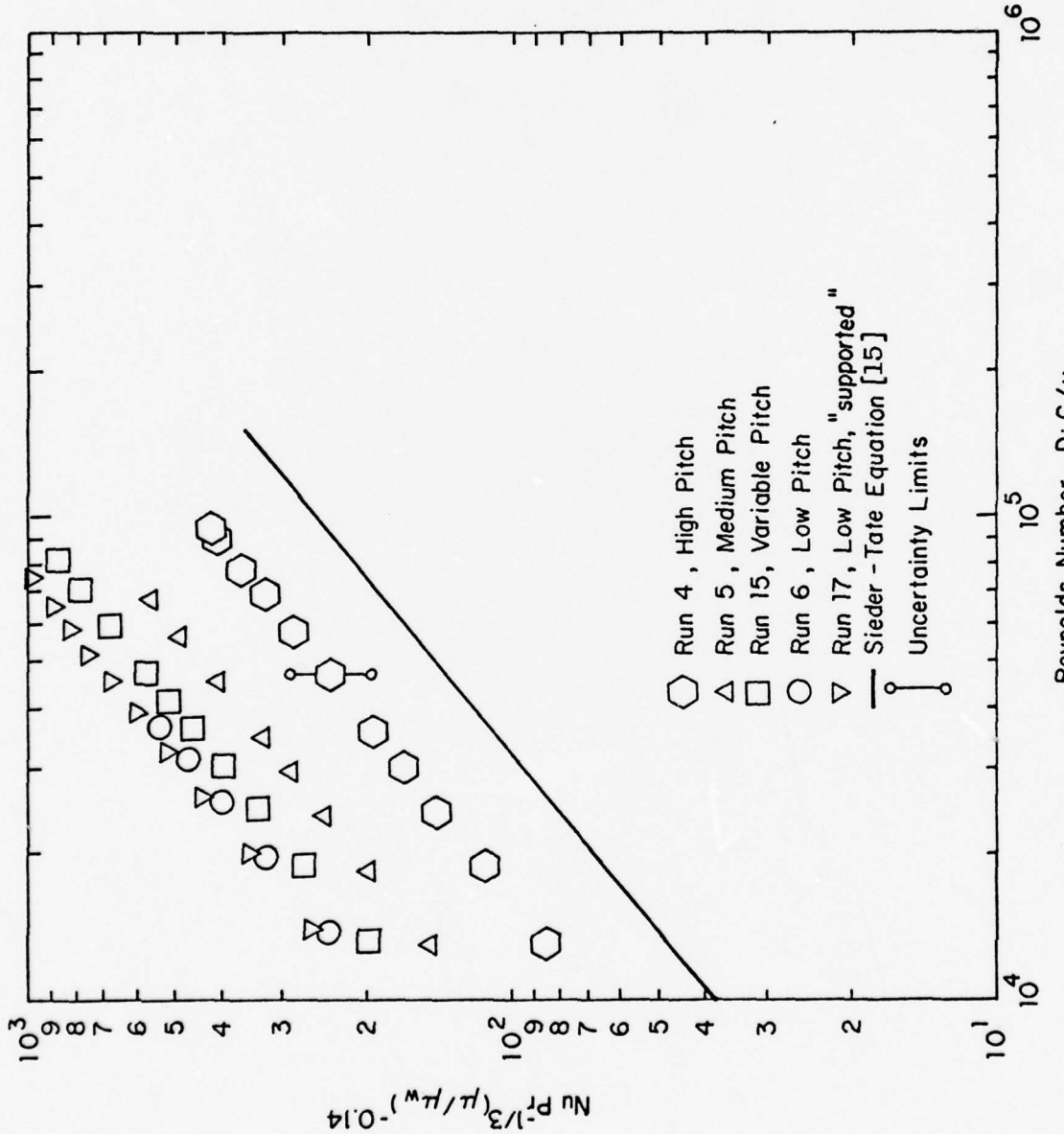


Figure 33. Inside Nusselt Number Correlation Versus Reynolds Number for TURBOTEC Tubes

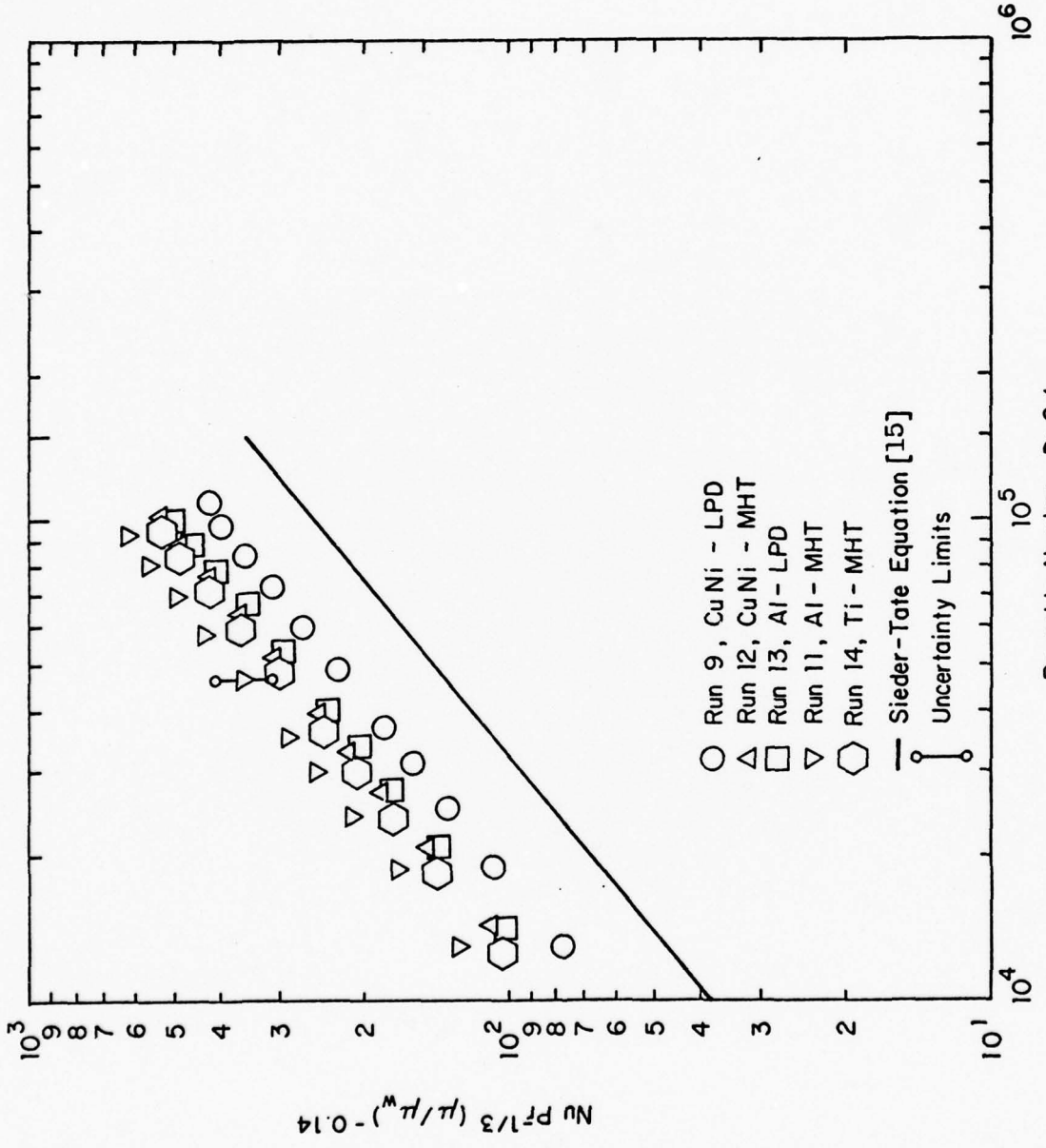


Figure 34. Inside Nusselt Number Correlation Versus Reynolds Number for KORODENSE Tubes

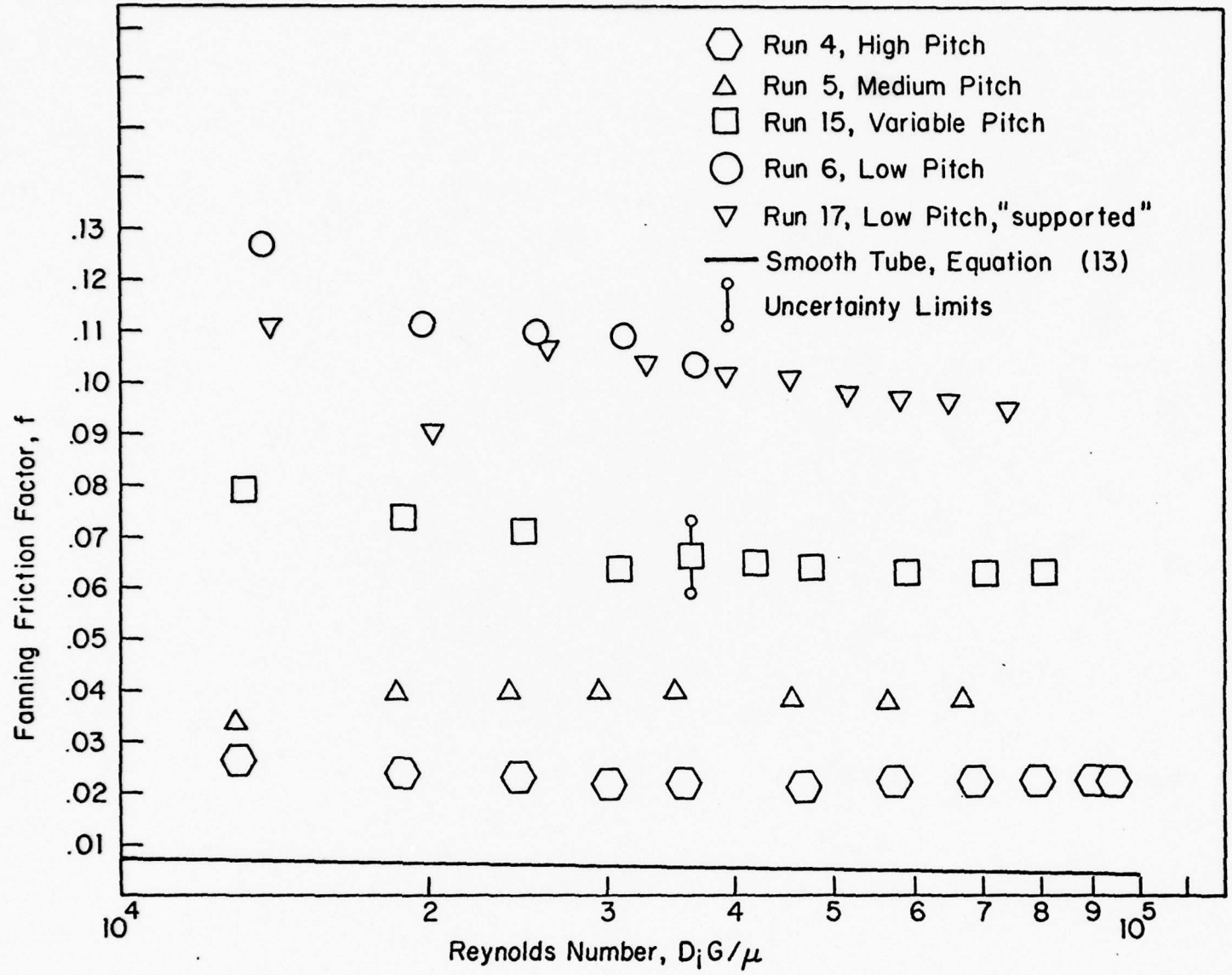


Figure 35. Fanning Friction Factor Versus Reynolds Number for TURBOTEC Tubes.

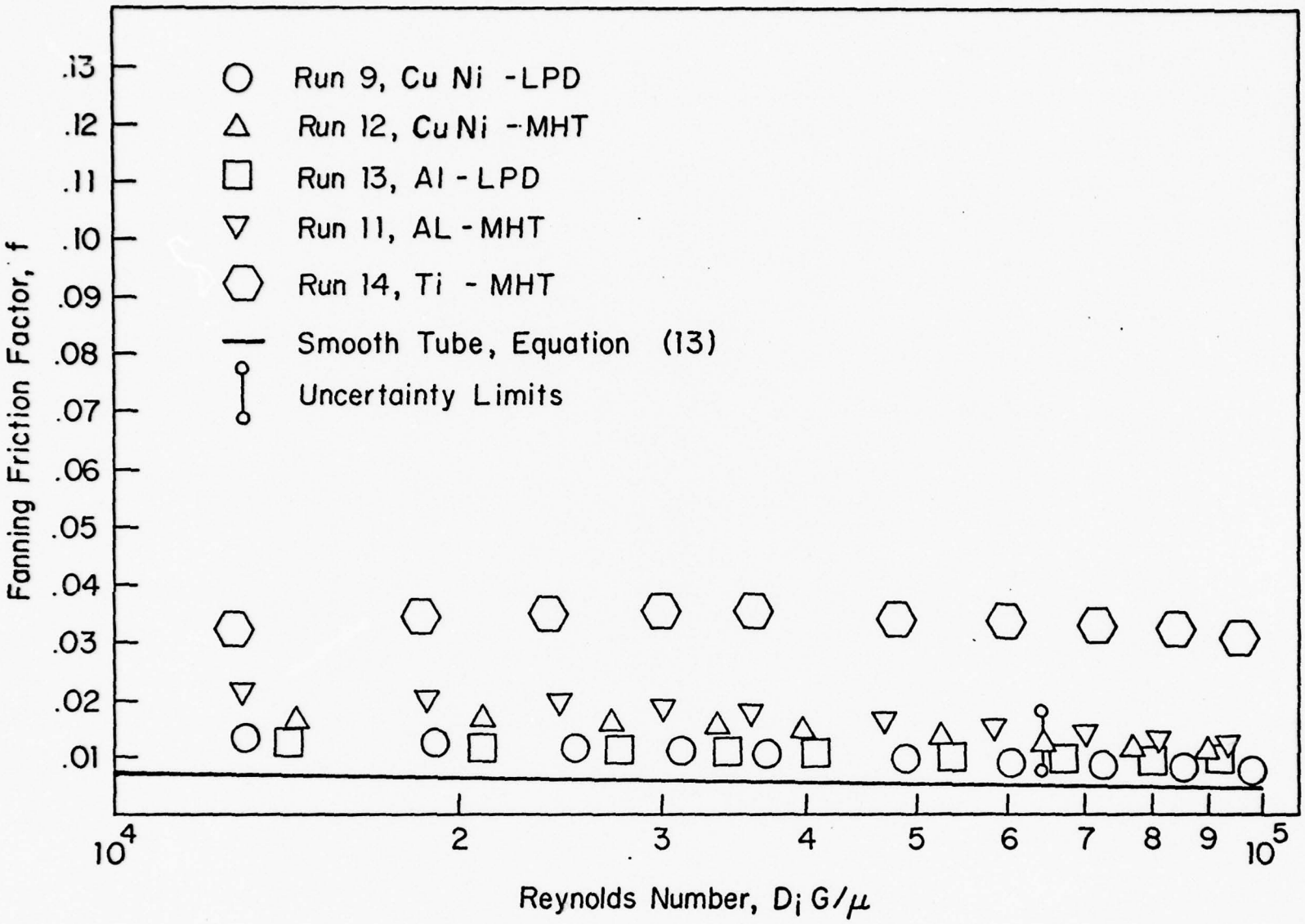


Figure 36. Fanning Friction Factor Versus Reynolds Number for KORODENSE Tubes.

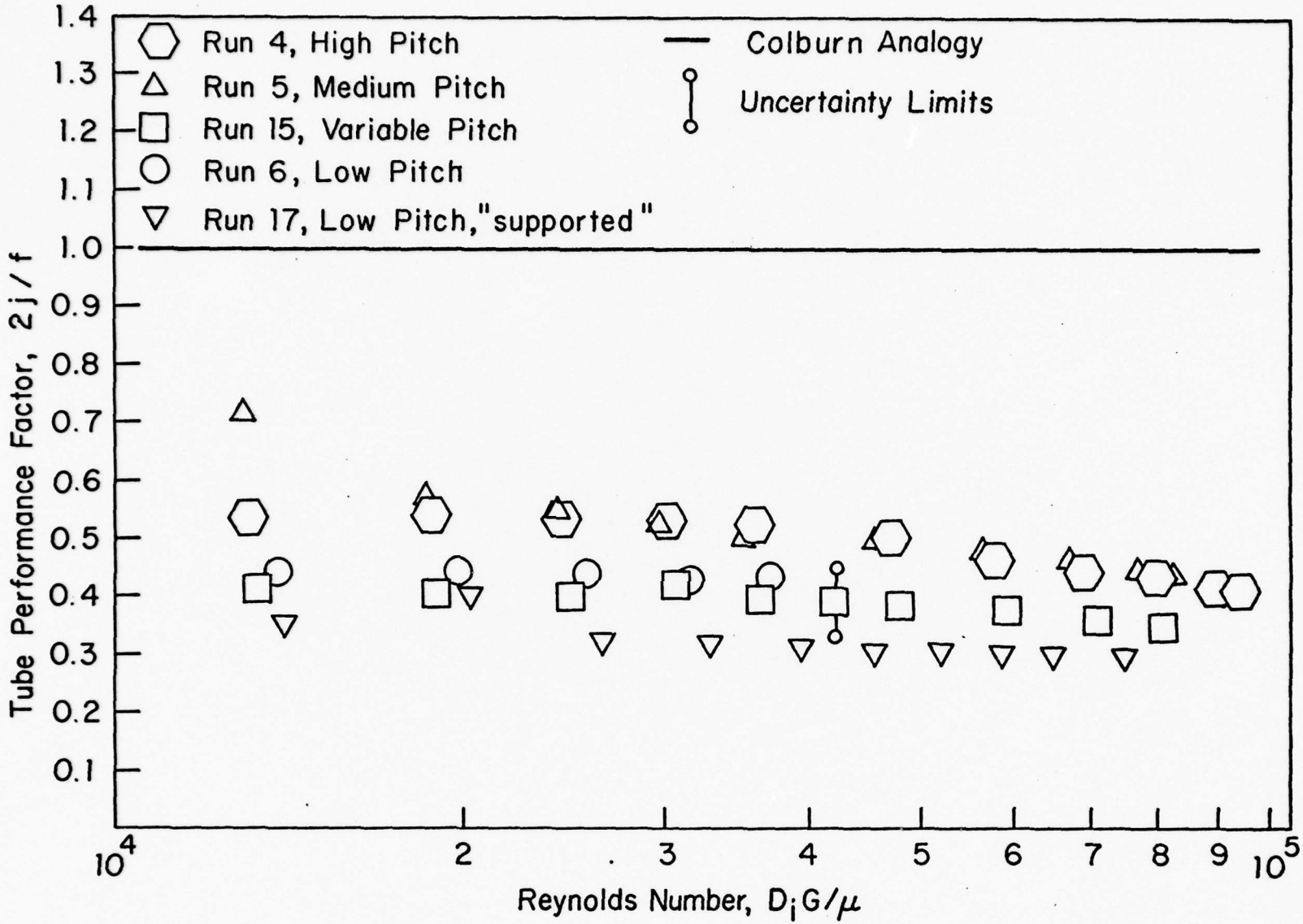


Figure 37. Tube Performance Factor, 2j/f, Versus Reynolds Number for TURBOTEC Tubes.

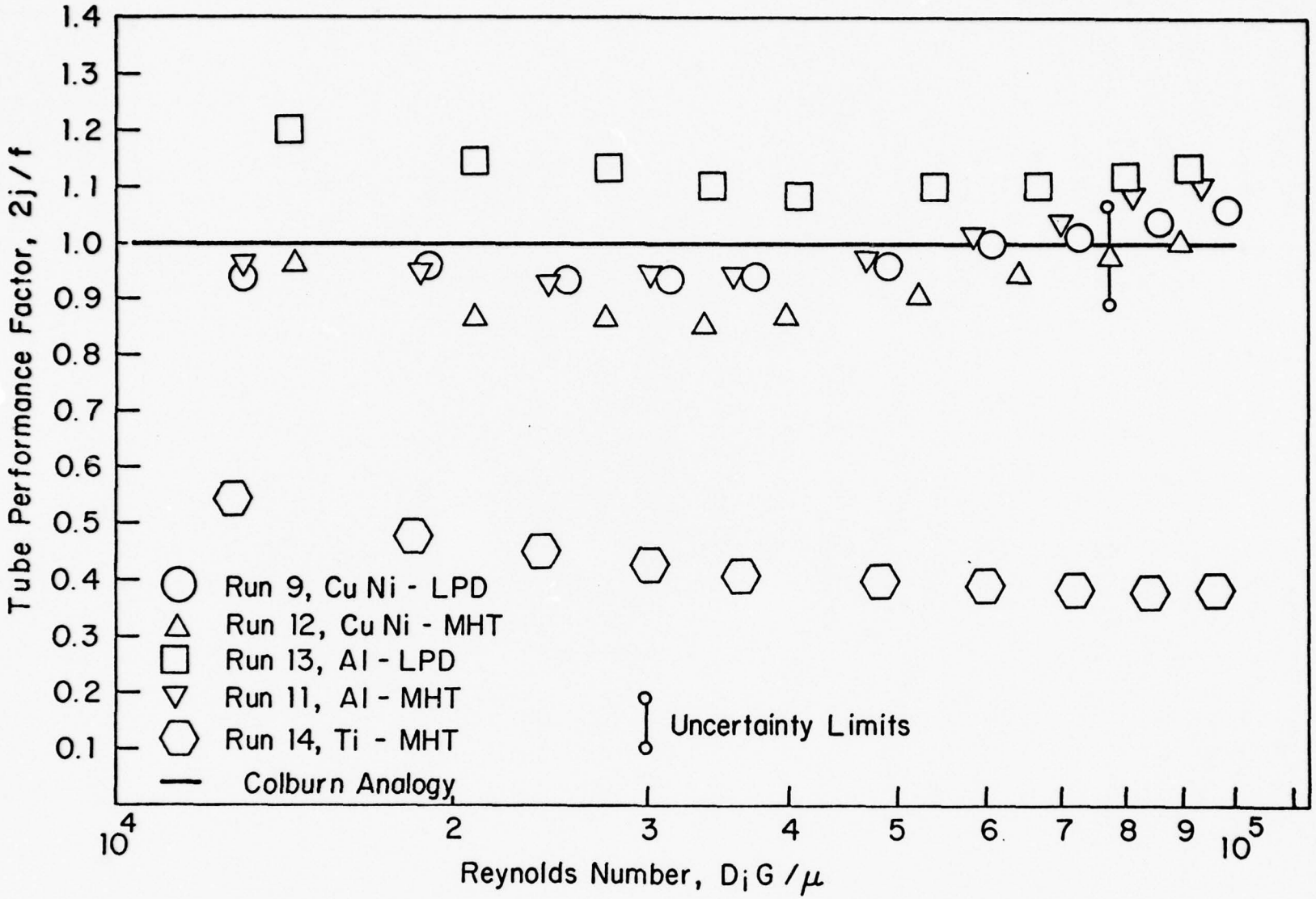


Figure 38. Tube Performance Factor, 2j/f, Versus Reynolds Number for KORODENSE Tubes.

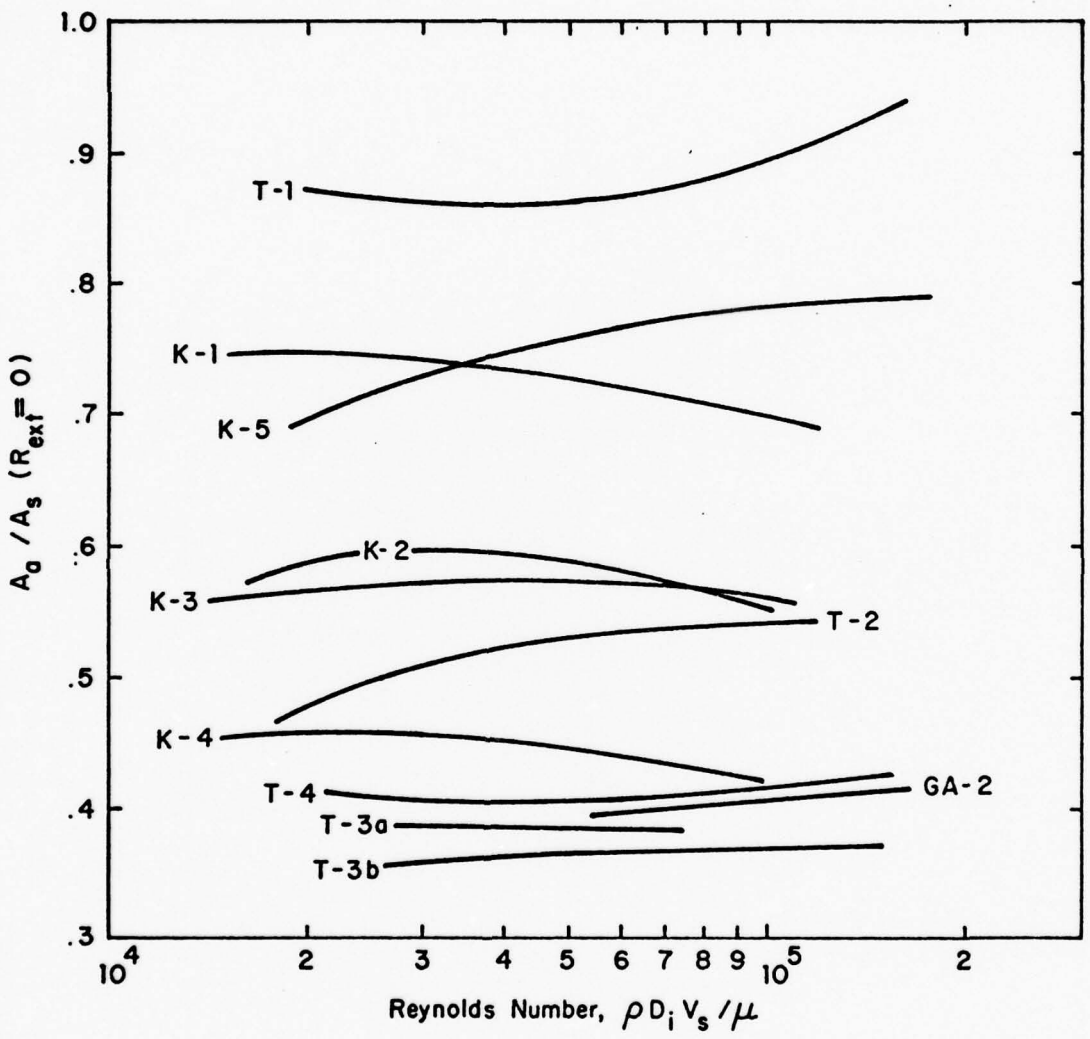


Figure 39. Augmented to Smooth Tube Surface Area Ratio ($R_{ext}$ = 0) Versus Reynolds Number.

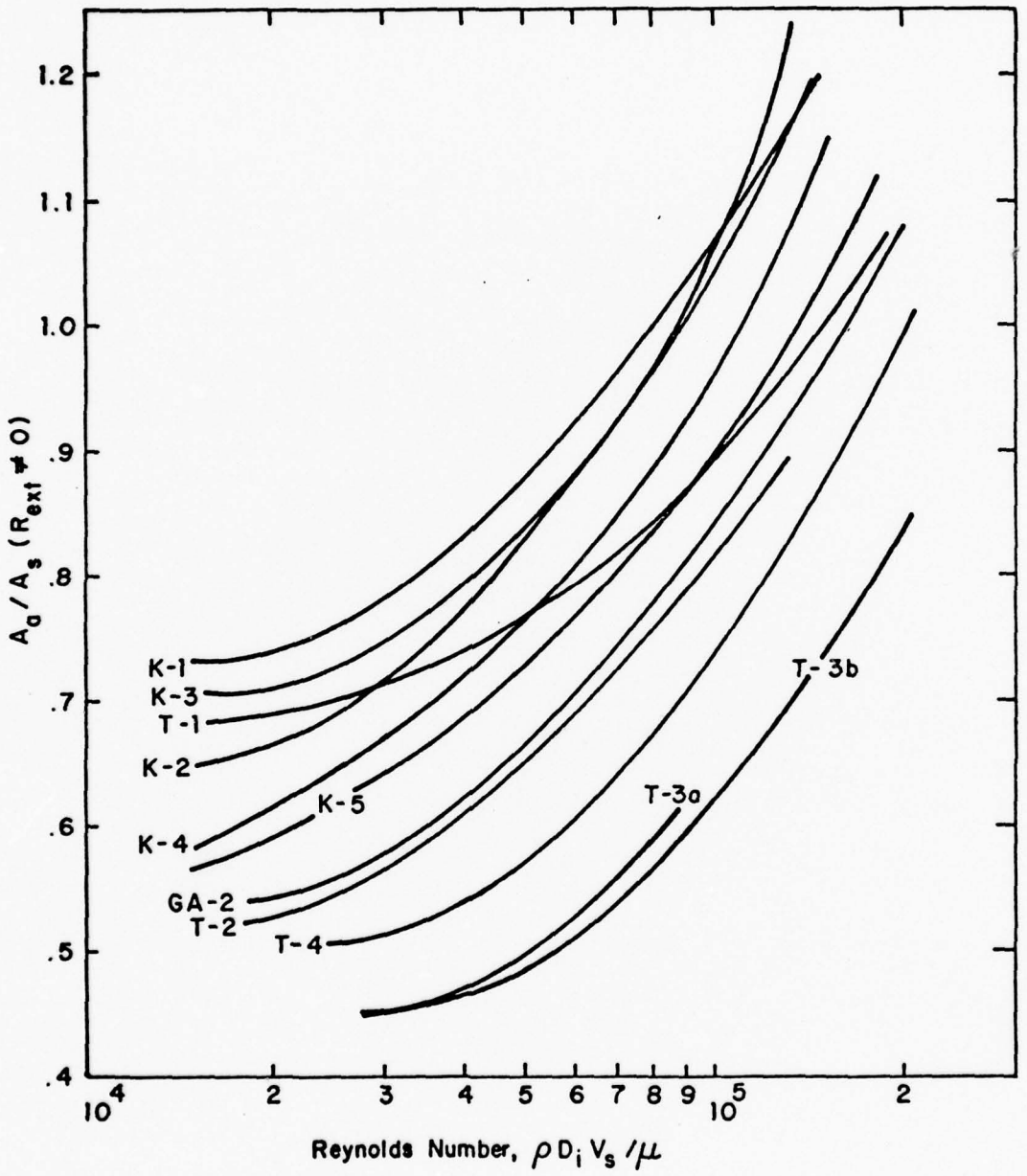


Figure 40. Augmented to Smooth Tube Surface Area Ratio ($R_{ext} \neq 0$) Versus Reynolds Number.

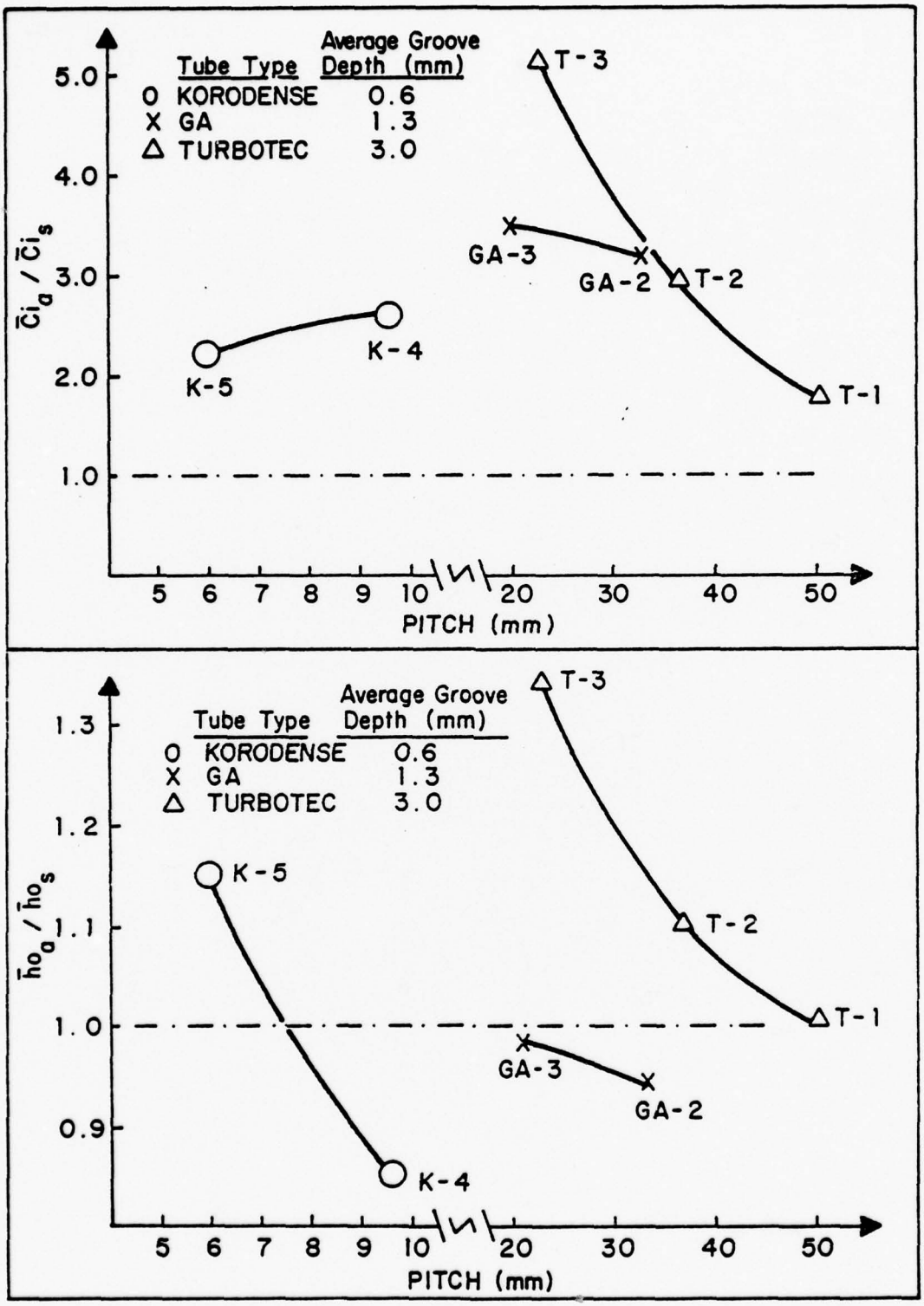


Figure 41. Comparative Effect of Tube Pitch (Helix Angle) on Both Inside and Outside Heat Transfer Coefficients (for Constant Groove Depth)

## APPENDIX A

### OPERATING PROCEDURES

1. Light-off Procedure

   a. Boiler Operation

      (1) Energize main circuit breaker located in power panel P-2.

      (2) Turn key switch on--located on right side of main control board.

      (3) Energize circuit breaker on left side of main control panel by depressing start button.

      (4) Energize individual circuit breakers on left side of main control panel. The following list identifies each circuit breaker:

         (a) #1 - Feed pump

         (b) #2 - Outlets

         (c) #3 - Hot water heater (feedwater tank)

         (d) #4 - Condensate pump

         (e) #5 - Boiler

         (f) #6 - Cooling tower

         (g) #7 - Cooling water pump (only when using closed cooling water system)

      (5) Insure water level is up in the feedwater tank, and turn on switch to energize heater.

      (6) Turn on the switch to the feed pump to recirculate water in the feedwater tank.

(7) Energize instrumentation.

(a) Multichannel pyrometer.

(b) Autodata 9 recorder and amplifier.

(c) Program Autodata using following procedure:

SET TIME:

- all alarms and output switches off
- set date/time on thumbwheels (24 Hour clock)
- depress the STOP/ENTER switch
- set the DISPLAY switch to "time"
- lift the SET TIME switch to enter time.

ASSIGNING MULTIPLE CHANNELS:

- depress the STOP/ENTER switch
- check that all alarms and output switches are still off
- set the SCAN switch to "continuous"
- set the FIRST CHANNEL and LAST CHANNEL thumbwheels to 001
- set the DISPLAY switch to "all" and depress the SLOW switch
- lift the SCAN START switch to start scanning channel 1. To assign channel 1 depress and hold the AUTO and STD RES buttons for at least one scan
- set the LAST CHANNEL thumbwheels to 039 before setting the FIRST CHANNEL thumbwheels to 002

- depress the SKIP button to skip channels 2 through 39 (may have to depress the T/$^{o}$C button first to break unit out of automode)
- set the LAST CHANNEL thumbwheels to 052 before setting the FIRST CHANNEL thumbwheels to 040
- to assign channels 40 through 52 depress and hold the T/$^{o}$C and HI RES buttons for at least one complete scan

INTERVAL SCAN:

- set thumbwheels to interval desired between scans (usually one minute)
- depress the STOP/ENTER switch
- set the DISPLAY switch to "interval"
- depress the SET INTERVAL switch
- set the SCAN switch to "interval"
- set the FIRST CHANNEL thumbwheels to 001
- set the LAST CHANNEL thumbwheels to 052
- lift the SCAN START switch

Use the following as needed/desired:

- printer on/off
- SLOW switch
- single channel display

(8) Energize cold trap refrigeration unit, insure that flammable stowage locker exhaust fan is on, and start vacuum pump.

(9) After feedwater tank has reached a temperature of 60°C, insure water level in boiler is above low level mark and energize boiler.

(10) Open valve DS-1 (set rotameter to 15-20% flow)

b. House Steam Operation

Follow steps (1) through (4), (6) and (8) as outlined above for the boiler.

2. Operation

a. Cooling Water System

(1) Open valve CW-1; then open valve CW-2 one turn to prime the cooling water pump, keeping valves SW-3 and CW-4 closed.

(2) Energize cooling water pump (switch near pump), and close valve CW-2. Open valve CW-3 one turn until flow is established, then open valve CW-4 to purge air.

(3) Open valves CW-3 and CW-4 to obtain desired flow rates.

(4) Vent both sides of the 3.66 meter manometer.

(5) When using the house water supply remove plug from sump and open valve CW-2 with valve CW-1 closed. Follow step 3.

(6) Begin flow to secondary condenser (valve behind column next to boiler).

b. Steam System

(1) Boiler Operation

(a) When boiler has reached the desired pressure (approximately 20.7 kPa) open valve MS-1.

(b) Insure valves MS-6 and MS-5 are open.

(c) Open valve MS-3 to obtain desired steam flow rate to test condenser. Open valve MS-4 as necessary to maintain boiler pressure at desired level (34.5 kPa).

(2) House Steam

(a) Insure valve MS-1 is closed. Open valve MS-2.

(b) Follow steps (b) and (c) for boiler use.

c. Condensate and Feedwater System

(1) Using Boiler

(a) To collect drains in test condenser hotwell operate with valve C-1 closed. After test run has been completed, open valve and condensate will drain into secondary condenser.

(b) The condensate pump is operated intermittently, when level in secondary condenser dictates. When pump is secured, keep valve C-2 closed. When pump is required, start pump and then open valve C-2. In this mode keep valve C-3 closed.

(c) While feed pump is running (continuous operation) valve FW-1 must be fully open and valve FW-2 must be throttled so that a

positive flow is insured. Valve FW-3 is a solenoid valve which is actuated by the boiler controls.

(d) When boiler is energized, valve FW-4 must be fully open.

(e) Make-up is added to the system through the top of the feedwater tank by removing anode.

(2) Using House Steam

(a) Follow step (a) for using boiler.

(b) To pump condensate from secondary condenser hotwell, start pump, and open valve C-3. In this mode keep valve C-2 closed.

(c) Delete steps (c) through (e) for using boiler.

3. Securing System

a. Using Boiler

(1) Close valves MS-3 and MS-4. Secure power to boiler and then close MS-1.

(2) Close valve DS-1 and drain desuperheater hotwell.

(3) Pump condensate from secondary condenser hotwell to feedwater tank. Secure valve C-2.

(4) Secure vacuum pump and refrigeration unit.

(5) Secure power to heater (switches on side and stand).

(6) Secure flow to secondary condenser.

(7) Bottom blow boiler to remove deposits. Repeat twice, blowing from high water mark to low water mark each time.

(8) Secure cooling water pump or close valve CW-2 when using house water supply. Close valves CW-3 and CW-4.

(9) Secure instrumentation.

(10) Secure power to feed pump.

(11) De-energize individual circuit breakers.

(12) De-energize circuit breaker on control panel; depress stop button. Turn key switch off.

b. Using House Steam

(1) Close valve MS-2.

(2) Pump condensate into return line; close valve C-3.

(3) Follow steps (4) through (6), (9) and (10) as outlined for procedure using boiler.

4. Secondary Systems

a. Vacuum System

Vacuum is established by a mechanical vacuum pump and is controlled by a vacuum regulator mounted on instrument board mounted by test condenser. The vacuum pump is separated from the condenser system by a refrigerated cold trap to prevent moisture from entering the pump.

b. Desuperheater

Valve DS-1 controls flow of feedwater (60$^{o}$C) to spray nozzles. Optimum flow level is between 15 and 20 percent flow on rotameter. Condensate is collected in a small tank below desuperheater so the mass flow rate can be determined.

5. Safety Devices

a. Emergency Power Shut-Off

To secure all power to the system in an emergency, depress the red button on the right of the main control panel next to the key switch.

b. Boiler

(1) The mercury switches mounted on the main control panel secure power to the heating elements of the boiler when the steam pressure exceeds 172.4 kPa. Power is restored to the heating elements when the pressure drops to approximately 103.4 kPa.

(2) A low water level limit switch is contained within the boiler, and when the water level inside the boiler drops below a preset level, power is secured to the boiler and will not be restored until the water level is above this preset height.

(3) The relief valve mounted on the boiler is set to lift at 206.8 kPa.

## APPENDIX B

### SAMPLE CALCULATIONS

A sample calculation is performed here to illustrate how the data reduction program [11] progresses to the results. The KORODENSE, copper-nickel-MHT Tube (K-2), run number 12 at 50 percent flow on the high flow rotameter was selected at random to perform this analysis. This tube and run number are the same as that used for the error analysis in Appendix C.

Section 2 of this appendix corresponds to the calculations performed for plain end inside diameter. The water property calculations are shown in section 1.

INPUT PARAMETERS

| | |
|---|---|
| Tube | KORODENSE, CuNi-MHT, Tube K-2 |
| Run Number | 12 |
| Tube Inside Diameter, Plain End ($D_i$) | 0.01339 m |
| Tube Outside Diameter, ($D_o$) | 0.01588 m |
| Overall Tube Length (L) | 1.22 m |
| Enhanced Section Lenght ($L_{TS}$) | 0.9144 m |
| Enhanced Section Cross Sectional Flow Area,* (Ac) | 0.0001316 $m^2$ |
| Outside Nominal Surface Area, ($A_n$) | 0.045604 $m^2$ |
| Tube Thermal Conductivity, ($k_w$) | 44.652 W/m $^oC$ |
| Wall Resistance, ($R_w$) | 30.315 x $10^{-6}$ $m^2$ $^oC$/W |

*This area, Ac, was determined by measuring the liquid volume contained within the enhanced section of each tube and dividing by the enhanced section length.

| | |
|---|---|
| Cooling Water In, ($Tc_i$) | 22.9 $^oC$ |
| Cooling Water Out, ($Tc_o$) | 27.8 $^oC$ |
| Average Cooling Water Temperature ($T_b$,$T_{br}$) | 25.35 $^oC$, 298.5 $^oK$ |
| Steam Vapor Temperature, ($T_v$) | 67.6 $^oC$ |
| Tube Wall Temperature, ($T_w$) | 314.0 $^oK$ |
| Tube Pressure Drop, ($\Delta P_m$) | 36.148 kPa |
| % Flow | 50 |
| Tube Inlet Contraction Factor | Kc } Ke + Kc = 0.030 |
| Tube Outlet Expansion Factor | Ke } |

Section 1, Water Properties

$$\mu = (4.134 \times 10^{-4}) \exp\{[(0.008291758)(298.5)+(2644.2189)/(298.5)] - 10.59252566\}$$

$$\mu = 8.6717 \times 10^{-4} \text{ kg/m·sec} = 3.1218 \text{ kg/m·hr}$$

$$k = 0.5565919 + (0.002174417)(25.35) - (0.70127 \times 10^{-5})(25.35)^2 - (2.0914 \times 10^{-10})(25.35)^3$$

$$k = 0.6072035 \text{ W/m·}^oC$$

$$\rho = 1004.44434 - (0.12673368)(25.35) - (0.0023913147)(25.35)^2$$

$$\rho = 999.695 \text{ kg/m}^3$$

$$c_p = 4.2377955 - (0.0018553514)(25.35) + (1.3948314 \times 10^{-5})(25.35)^2$$

$$c_p = 4.1997259 \text{ kJ/kg·}^oC$$

$$\dot{m} = \ell/m \times \rho = (35.582)(60)(0.001)(999.695)$$

$$\dot{m} = 2134.2688 \text{ kg/hr} = 0.59285 \text{ kg/sec}$$

$$Pr = \frac{\mu c_p}{k} = \frac{(8.6717 \times 10^{-4})(4.1997259 \times 10^{3})}{(0.6072035)}$$

$$Pr = 5.997$$

Section 2, Plain-End-Tube Reduction

1. Determination of cooling water velocity

$$v = \frac{4\dot{m}}{\rho\pi D_i^2} \qquad v_{TS} = \frac{\dot{m}}{\rho Ac} = v_a$$

$$v = \frac{(4)(2134.2688)}{(999.695)(\pi)(0.01339)^2} \qquad v_{TS} = \frac{(2134.2688)}{(999.695)(0.0001316)}$$

$$v = 15161.094 \text{ m/hr} \qquad v_{TS} = 16222.795 \text{ m/hr}$$

$$= 4.211 \text{ m/sec} \qquad = 4.506 \text{ m/sec}$$

2. Determination of Mass Flow Rate per Unit Area

$$G = \frac{4\dot{m}}{\pi D_i^2} = \rho v$$

$$= (999.695)(15161.094)$$

$$= 15,156,469. \text{ kg/m}^2 \text{ hr}$$

$$= 4210.13 \text{ kg/m}^2 \text{ sec}$$

3. Determination of Reynolds Number

$$Re = \frac{D_i G}{\mu_{H_2O}}$$

$$= \frac{(0.01339)(4210.13)}{(8.6717 \times 10^{-4})}$$

$$Re = 65,008.75$$

4. Determination of Overall Heat Transfer Coefficient

$$U_n = \frac{\dot{m} c_p}{A_n} \ln \left(\frac{T_v - Tc_i}{T_v - Tc_o}\right)$$

$$= \frac{(0.59285)(4.1997259 \times 10^3)}{(0.045604)} \ln \left(\frac{67.6 - 22.9}{67.6 - 27.8}\right)$$

$$= 6339.01 \text{ W/m}^2 \text{ }^\circ\text{C}$$

5. Determination of Corrected Overall Heat Transfer Coefficient

$$U_c = \frac{1}{\frac{1}{U_n} - R_w}$$

$$= \frac{1}{\frac{1}{6339.01} - 30.315 \times 10^{-6}}$$

$$= 7846.932 \text{ W/m}^2 \text{ }^\circ\text{C}$$

6. Determination of Friction Factor

$$f_s = \frac{0.046}{Re^{0.2}}$$

$$= \frac{0.046}{65008.75^{0.2}}$$

$$= 0.005014$$

$$\Delta P_s = \frac{4 f_s G^2 \left(\frac{L_s}{D_i}\right)}{\rho \, 2g_c}$$

$$= \frac{(4)(0.005014)(4210.13)^2 \left(\frac{0.3842}{0.01339}\right)}{(999.695)(2)}$$

$$= 5.103 \text{ kPa}$$

$$\Delta P_{exp/con} = \frac{\rho\, v_{TS}^2}{2g_c} \quad (Kc + Ke)$$

$$= \frac{(999.695)(4.506)^2}{(2)} \quad (0.030)$$

$$= 0.3045 \text{ kPa}$$

$$\Delta P_{TS} = \Delta P_m - \Delta P_s - \Delta P_{exp/con}$$

$$= 36.147502 - 5.102 - .3045$$

$$= 30.741 \text{ kPa}$$

$$f_a = \frac{\rho \Delta P_{TS} 2g_c}{4G^2 \left(\frac{L_{TS}}{D_i}\right)}$$

$$= \frac{(999.695)(30.741 \times 10^3)(2)}{(4)(4210.13)^2\left(\frac{0.9144}{0.01339}\right)}$$

$$= 0.0126943$$

7. Determination of Wilson Plot Parameters

(a) Ordinate

$$Y = \frac{1}{U_n}$$

$$= \frac{1}{6339.01} = 1.578 \times 10^{-4} \quad \frac{m^2\, {}^\circ C}{W}$$

(b) Abscissa

$$X = \frac{1}{Re^{0.8} Pr^{1/3}} \left(\frac{\mu}{\mu_w}\right)^{0.14}$$

$$\mu_w = (4.134 \times 10^{-4}) \exp\{[(0.008291758)(314.0) + (2644.2189)/(314.0)] - 10.59252566\}$$

$$= 6.368799 \times 10^{-4} \text{ kg/m·sec}$$

$$X = \frac{1}{(65008.75)^{0.8}(5.997)^{1/3}(\frac{8.6717}{6.368799})^{0.14}}$$

$$= 7.4395 \times 10^{-5}$$

8. Determination of Sieder Tate Coefficient

$C_i = \frac{D_o}{Mk}$ , where M = slope of linear regression subroutine

M = 0.4726852, from linear regression subroutine

$$C_i = \frac{(0.01588)}{(0.4726852)(0.6072035)}$$

$C_i = 0.055328$

9. Determination of Inside Heat Transfer Coefficient

$$h_i = \frac{C_i}{D_i} k \, Re^{0.8} Pr^{1/3} (\frac{\mu}{\mu_w})^{0.14}$$

$$= (\frac{0.055328}{0.01339}) \, (0.6072035)(65008.75)^{0.8}(5.997)^{1/3} \, (\frac{8.6717}{6.368799})^{0.14}$$

$h_i = 33725.222 \ W/m^2 \ ^oC$

10. Determination of Outside Heat Transfer Coefficient

$$h_o = \frac{1}{\frac{1}{U_n} - R_w - \frac{D_o}{D_i h_i}}$$

$$= \frac{1}{1.577533 \times 10^{-4} - 30.315 \times 10^{-6} - \frac{(0.01588)}{(0.01339)(33725.222)}}$$

$h_o = 10837.413 \ W/m^2 \ ^oC$

11. Determination of Nusselt Number

$$Nu = \frac{h_i D_i}{k} = \frac{(33725.22)(.01339)}{(.6072035)}$$

$$= 743.706$$

12. Determination of Stanton Number

$$St = \frac{Nu}{RePr}$$

$$= \frac{(743.706)}{(65008.75)(5.997)}$$

$$= 1.90764 \times 10^{-3}$$

13. Determination of Performance Factor

$$TPF = \frac{2j}{f_a}$$

$$j = St\ Pr^{2/3} = (1.90764 \times 10^{-3})(5.997)^{2/3}$$

$$j = 6.2968 \times 10^{-3}$$

$$TPF = \frac{(2)(6.2969 \times 10^{-3})}{(0.0126943)}$$

$$TPF = 0.9921$$

14. Determination of Area Ratios

a. $R_{ext} = 0$

$$Re_s = \sqrt{\frac{0.027\ f_a\ Re_a^3}{0.046\ \ Nu_a/Pr^{1/3}\ (\mu/\mu_w)^{0.14}}}$$

$$= 74195.57$$

$$f_s = \frac{0.046}{Re_s^{0.2}}$$

$$= 0.00488295$$

$$\frac{A_a}{A_s} = \frac{Re_s^3 f_s}{Re_a^3 f_a}$$

$$= 0.579$$

14. b. $R_{ext} \neq 0$

Correction factors $F_1$, $F_2$ and $F_3$ were obtained from reference [23] and applied as outlined in reference [22].

$F_1$ = 1.0 (fouling correction)

$F_2$ = 0.9 (material correction for 90-10 copper-nickel)

$F_3$ = 1.02 (temperature correction from coolant inlet temperature of 23.2°C to 21.1°C)

$C'$ = 2883 (from III.B.5.(b)(2))

$C = F_1 F_2 F_3 C' = 2595$

$U_a = U_n/F_3 = 6214.72 \text{ W/m}^2 \text{ °C}$

$$v_s = [\frac{f_a v_a^3 C}{0.046 U_a}(\frac{\rho D_i}{\mu})^{1/5}]^{1/2.3}$$

$$= 5.89 \text{ m/s}$$

$$U_s = C (v_s)^{0.5}$$

$$= 6297.9 \text{ W/m}^2 \text{ °C}$$

$$\frac{A_a}{A_s} = \frac{U_s}{U_a} = \frac{6297.9}{6214.72}$$

$$= 1.013$$

## APPENDIX C

## ERROR ANALYSIS

The basic equations used in this section are reproduced from Reilly [11]. The general form of the Kline and McClintock [27] "second order" equation is used to compute the probable error in the results. For some resultant, R, which is a function of primary variables $X_1$, $X_2$, ... $X_n$, the probable error in R, $\delta R$ is given by:

$$\delta R = [(\frac{\delta R}{\delta X_1} \delta X_1)^2 + (\frac{\delta R}{\delta X_2} \delta X_2)^2 + \ldots + (\frac{\delta R}{\delta X_n} \delta X_n)^2]^{1/2} \qquad (C\text{-}1)$$

where $\delta X_1$, $\delta X_2$, ..., $\delta X_n$ is the probable error in each of the measured variables.

### C.1. Uncertainty in Overall Heat Transfer Coefficient, $U_n$

The overall heat transfer coefficient is given by equation (4), in Chapter III as:

$$U_n = \frac{\dot{m} c_p}{A_n} \ln [\frac{T_v - Tc_i}{T_v - Tc_o}] \quad . \qquad (4)$$

By applying equation (C-1) to equation (4), the following equation results:

$$\frac{\delta U_n}{U_n} = \left[\left(\frac{\delta A_n}{A_n}\right)^2 + \left(\frac{\delta c_p}{c_p}\right)^2 + \left(\frac{\delta \dot{m}}{\dot{m}}\right)^2 + \left(\frac{\delta T_v\,(Tc_i - Tc_o)}{(T_v - Tc_i)(T_v - Tc_o)\ln\frac{T_v - Tc_i}{T_v - Tc_o}}\right)^2\right.$$

$$\left. + \left(\frac{\delta Tc_i}{(T_v - Tc_i)\ln\frac{T_v - Tc_i}{T_v - Tc_o}}\right)^2 + \left(\frac{\delta Tc_o}{(T_v - Tc_o)\ln\frac{T_v - Tc_i}{T_v - Tc_o}}\right)^2\right]^{1/2}$$

(C-2)

The following are the values assigned to the variables.

$\delta c_p = 0.0042$ kj/kg $^oC$

$\delta \dot{m} = 0.01\ \dot{m}$ kg/sec

$\delta_{T_v} = 1.0\ ^oC$

$\delta Tc_o = 0.1\ ^oC$

$\delta Tc_i = 0.1\ ^oC$

$\delta A_n = 0.00074\ m^2$

For Run 12 at 50 Percent Flow

$$\frac{\delta U_n}{U_n} = \left[\left(\frac{.00074}{.045604}\right)^2 + \left(\frac{.0042}{4.19973}\right)^2 + \left(\frac{.01\ \dot{m}}{\dot{m}}\right)^2 + \left(\frac{(1.0)(-4.9)}{(44.7)(39.8)\ln(1.123)}\right)^2\right.$$

$$\left. + 2 + \left(\frac{(0.1)}{(39.8)\ln(1.123)}\right)^2\right]^{1/2}$$

$$\frac{\delta U_n}{U_n} = .051$$

$\therefore U_n,\ 50\% = 6339 \pm 326\ W/m^2\ ^oC$

## C.2. Uncertainty in Inside Heat Transfer Coefficient, $h_i$

The probable error in the inside heat transfer coefficient is given by:

$$\frac{\delta h_i}{h_i} = \left[\left(\frac{\delta k}{k}\right)^2 + \left(\frac{\delta D_i}{D_i}\right)^2 + \left(\frac{0.8\delta Re}{Re}\right)^2 + \left(\frac{0.333\delta Pr}{Pr}\right)^2 + \left(\frac{\delta C_i}{C_i}\right)^2 + \left(\frac{0.14\delta(\mu/\mu_w)}{\mu/\mu_w}\right)^2\right]^{1/2}, \quad \text{(C-3)}$$

where:

$\delta k = 0.030$ W/m °C,

$\delta D_i = 0.00051$ m,

$\delta Pr = 0.10$, and

$\delta\left(\frac{\mu}{\mu_w}\right) = 0.050$.

The probable error in the Reynolds number is given by:

$$\frac{\delta Re}{Re} = \left[\left(\frac{\delta G}{G}\right)^2 + \left(\frac{\delta \mu}{\mu}\right)^2 + \left(\frac{\delta D_i}{D_i}\right)^2\right]^{1/2}, \quad \text{(C-4)}$$

where,

$$\frac{\delta G}{G} = \left[\left(\frac{0.01\dot{m}}{\dot{m}}\right)^2 + \left(2\frac{\delta D_i}{D_i}\right)^2\right]^{1/2}, \quad \text{(C-5)}$$

$$\frac{\delta G}{G} = \left[(.01)^2 + \left(\frac{.00013}{.01339}\right)^2\right]^{1/2} = 0.013 .$$

Since $\delta\mu = 0.15$ kg/m·hr, then

$$\frac{\delta Re}{Re} = \left[(.013)^2 + \left(\frac{0.15}{3.1218}\right)^2 + \left(\frac{.00051}{.01339}\right)^2\right]^{1/2} = 0.05$$

$\therefore Re_{50\%} = 65008 \pm 3245$

The probable error in the coefficient $C_i$ is given by:

$$\frac{\delta C_i}{C_i} = \left[\left(\frac{\delta D_o}{D_o}\right)^2 + \left(\frac{\delta slope}{slope}\right)^2 + \left(\frac{\delta k}{k}\right)^2\right]^{1/2} , \qquad (C\text{-}6)$$

where:

$\delta D_o$ = 0.00025 m,

$\delta k$ = 0.03 W/m·°C, and

$\delta slope$ = 0.065 slope.

$$\frac{\delta C_i}{C_i} = \left[\left(\frac{0.00025}{.01588}\right)^2 + (.065)^2 + \left(\frac{0.03}{.6072035}\right)^2\right]^{1/2}$$

$$\frac{\delta C_i}{C_i} = 0.082$$

$$\therefore C_{i,50\%} = 0.053 \pm .004$$

Using the above information, the probable error in the inside heat transfer coefficient can be calculated as:

$$\frac{\delta h_i}{h_i} = \left[\left(\frac{.030}{.6072035}\right)^2 + \left(\frac{0.00051}{.01339}\right)^2 + (.082)^2 + (0.8 \times 0.05)^2 + \left(\frac{.333 \times 0.1}{5.997}\right)^2 + \left(\frac{.14 \times 0.05}{1.361591}\right)^2\right]^{1/2}$$

$$\frac{\delta h_i}{h_i} = 0.096$$

$$\therefore h_{i,50\%} = 33725 \pm 3238 \text{ W/m}^2 \text{ °C}$$

## C.3 The Uncertainty in the Outside Heat Transfer Coefficient, $h_o$

The probable error in the outside heat transfer coefficient is given by:

$$\frac{\delta h_o}{h_o} = \left\{ \left[ \frac{\delta U_n}{U_n^2 \left(\frac{1}{U_n} - R_w - \frac{D_o}{D_i h_i}\right)} \right]^2 + \left[ \frac{\delta R_w}{\left(\frac{1}{U_n} - R_w - \frac{D_o}{D_i h_i}\right)} \right]^2 + \left[ \frac{\left(\frac{D_o}{D_i h_i}\right)\left(\frac{\delta h_i}{h_i}\right)}{\frac{1}{U_n} - R_w - \frac{D_o}{D_i h_i}} \right]^2 \right\}^{1/2}, \qquad \text{(C-7)}$$

where:

$$\frac{\delta U_n}{U_n} = .051,$$

$$\delta R_w = 1.54 \times 10^{-6} \text{ m}^2 \text{ }^\circ\text{C/W, and}$$

$$\frac{\delta h_i}{h_i} = 0.096$$

also, $\frac{1}{U_n} - R_w - \frac{D_o}{D_i h_i} = 9.2273 \times 10^{-5} \text{ m}^2 \text{ }^\circ\text{C/W.}$

With this information:

$$\frac{\delta h_o}{h_o} = \left\{ \left[ \frac{.051}{(6339.01)(9.2273 \times 10^{-5})} \right]^2 + \left[ \frac{1.54 \times 10^{-6}}{9.2273 \times 10^{-5}} \right]^2 + \left[ \frac{(.01588)(.096)}{(.01339)(33725)(9.2273 \times 10^{-5})} \right]^2 \right\}^{1/2}$$

$$\frac{\delta h_o}{h_o} = .096$$

$$\therefore h_o = 10837 \pm 1041 \text{ W/m}^2 \text{ }^\circ\text{C}$$

## C.4 Uncertainty in Tube Performance Factor, 2j/f

Since the Colburn Analogy defines j as St $Pr^{2/3}$, the probable error in the Tube Performance Factor 2j/f is given by:

$$\frac{\delta TPF}{TPF} = \left[\left(\frac{\delta St}{St}\right)^2 + \left(\frac{2}{3}\frac{\delta Pr}{Pr}\right)^2 + \left(\frac{\delta f_a}{f_a}\right)^2\right]^{1/2}, \qquad \text{(C-8)}$$

where

$$\frac{\delta St}{St} = \left[\left(\frac{\delta Nu}{Nu}\right)^2 + \left(\frac{\delta Re}{Re}\right)^2 + \left(\frac{\delta Pr}{Pr}\right)^2\right]^{1/2}, \qquad \text{(C-9)}$$

$$\frac{\delta Nu}{Nu} = \left[\left(\frac{\delta h_i}{h_i}\right)^2 + \left(\frac{\delta D_i}{D_i}\right)^2 + \left(\frac{\delta k}{k}\right)^2\right]^{1/2}, \text{ and} \qquad \text{(C-10)}$$

$$\frac{\delta f_a}{f_a} = \left[\left(\frac{\delta \Delta P_{TS}}{\Delta P_{TS}}\right)^2 + \left(2\,\frac{\delta G}{G}\right)^2 + \left(\frac{\delta L_{TS}}{L_{TS}}\right)^2 + \left(\frac{\delta \rho}{\rho}\right)^2 + \left(\frac{\delta D_i}{D_i}\right)^2\right]^{1/2}. \qquad \text{(C-11)}$$

Assuming $\delta\Delta P_{TS} = .02\ \Delta P_{TS}$, $\delta\rho = 0.1\rho$, and $\delta L_{TS} = .0013$ m, the following numerical values result:

$$\frac{\delta f_a}{f_a} = \left[(.02)^2 + (2 \times .013)^2 + \left(\frac{.0013}{.9144}\right)^2 + (.01)^2 + \left(\frac{.000051}{.01339}\right)^2\right]^{1/2}$$

$$\frac{\delta f_a}{f_a} = 0.03$$

$$\frac{\delta Nu}{Nu} = \left[(.096)^2 + \left(\frac{.000051}{.01339}\right)^2 + \left(\frac{.030}{.6072035}\right)^2\right]^{1/2}$$

$$\frac{\delta Nu}{Nu} = 0.11$$

$$\frac{\delta St}{St} = \left[(0.11)^2 + (.05)^2 + \left(\frac{0.10}{5.997}\right)^2\right]^{1/2}$$

$$\frac{\delta St}{St} = 0.12$$

$$\frac{\delta TPF}{TPF} = \left[(0.12)^2 + \left(\frac{2}{3} \times \frac{0.10}{5.997}\right)^2 + (0.03)^2\right]^{1/2}$$

$$\frac{\delta TPF}{TPF} = 0.124$$

$\therefore TPF_{50\%} = 0.992 \pm 0.123$

---

C. 5 Uncertainty in the Area Ratios

C. 5. 1 $R_{ext} = 0$

Using Equation (24) the probable error in the area ratio ($R_{ext} = 0$) is given by:

$$\frac{\delta(A_a/A_s)}{(A_a/A_s)} = \left[\left(\frac{\delta Nu_s}{Nu_s}\right)^2 + \left(\frac{\delta Nu_a}{Nu_a}\right)^2\right]^{1/2} \qquad \text{(C-12)}$$

where

$$\frac{\delta Nu_a}{Nu_a} = .11$$

In addition, from equation (26),

$$\frac{\delta Re_s}{Re_s} = \left[\left(\frac{1}{2}\frac{\delta f_a}{f_a}\right)^2 + \left(\frac{3}{2}\frac{\delta Re_a}{Re_a}\right)^2 + \left(\frac{1}{6}\frac{\delta Pr}{Pr}\right)^2 + \left(0.07\frac{\delta(\mu/\mu_w)}{(\mu/\mu_w)}\right)^2 + \left(\frac{1}{2}\frac{\delta Nu_a}{Nu_a}\right)^2\right]^{1/2}$$

$$\therefore \frac{\delta Re_s}{Re_s} = \left[\left(\frac{1}{2}\{.03\}\right)^2 + \left(\frac{3}{2} \times 0.05\right)^2 + \left(\frac{1}{6} \times \frac{0.10}{5.997}\right)^2 + \left(0.07 \times \frac{0.050}{1.361591}\right)^2 + \left(\frac{1}{2} \times 0.11\right)^2\right]^{1/2}$$

$$\frac{\delta Re_s}{Re_s} = 0.094$$

and using equation (25)

$$\frac{\delta Nu_s}{Nu_s} = \left[\left(0.8\frac{\delta Re_s}{Re_s}\right)^2 + \left(\frac{1}{3} \times \frac{\delta Pr}{Pr}\right)^2 + \left(.14 \times \frac{\delta(\mu/\mu_w)}{(\mu/\mu_w)}\right)^2\right]^{1/2} \quad \text{(C-13)}$$

$$\frac{\delta Nu_s}{Nu_s} = \left[(.8 \times .094)^2 + \left(\frac{1}{3} \times \frac{.10}{5.997}\right)^2 + \left(.14 \times \frac{.15}{1.36159}\right)^2\right]^{1/2}$$

$$\frac{\delta Nu_s}{Nu_s} = .075$$

$$\frac{\delta(A_a/A_s)}{(A_a/A_s)} = [(.075)^2 + (0.11)^2\ ]^{1/2} = .13$$

$$\therefore A_a/A_{s(R_{ext}=0)50\%} = 0.57 \pm 0.07$$

C. 5. 2 $R_{ext} \neq 0$

From equation (29), the probable error in the Area Ratio ($R_{ext} \neq 0$) is given by:

$$\frac{\delta(A_a/A_s)}{(A_a/A_s)} = [(\frac{\delta U_s}{U_s})^2 + (\frac{\delta U_a}{U_a})^2\ ]^{1/2} \qquad \text{(C-14)}$$

where:

$$\frac{\delta U_a}{U_a} = .051$$

and from equation (30)

$$\frac{\delta U_s}{U_s} = \frac{1}{2}\frac{\delta v_s}{v_s} \ . \qquad \text{(C-15)}$$

Equation (27) can be used as follows:

$$\frac{\delta v_s}{v_s} = [(\frac{\delta Re_s}{Re_s})^2 + (\frac{\delta D_i}{D_i})^2 + (\frac{\delta \rho}{\rho})^2 + (\frac{\delta \mu}{\mu})^2]^{1/2} \qquad \text{(C-16)}$$

$$\frac{\delta v_s}{v_s} = \left[(.094)^2 + \left(\frac{.000051}{.01339}\right)^2 + (.01)^2 + \left(\frac{.15}{3.1218}\right)^2\right]^{1/2}$$

$$\frac{\delta v_s}{v_s} = .11 ,$$

and

$$\frac{\delta(A_a/A_s)}{(A_a/A_s)} = \left[\left(\frac{1}{2} \times .11\right)^2 + (.051)^2\right]^{1/2} = .075$$

$$\therefore A_a/A_{s_{(R_{ext} \neq 0)50\%}} = 1.013 \pm .076$$

---

## BIBLIOGRAPHY


1. Search, H. T., A Feasibility Study of Heat Transfer Improvement in Marine Steam Condensers, MSME, Naval Postgraduate School, Monterey, CA December 1977.

2. Bergles, A. E., Enhancement of Heat Transfer, Keynote paper presented at the Sixth International Heat Transfer Conference, Toronto, Canada, 7-11 August 1978.

3. Palen, J., Cham, B., and Taborek, J., Comparison of Condensation of Steam on Plain and Turbotec Spirally Grooved Tubes in a Baffled Shell-and-Tube Condenser, Heat Transfer Research, Inc., Report 2439-300/6, January 1971.

4. Young, E. H., Withers, J. G., and Lampert, W. B., Heat Transfer Characteristics of Corrugated Tubes in Steam Condensing Applications, AIChE Paper No. 3, August 11, 1975.

5. Catchpole, J. P., Drew, B. C. H., "Evaluation of Some Shaped Tubes for Steam Condensers," Steam Turbine Condenser, NEL Report No. 619, pp 68-82, August, 1976.

6. Newson, I. H., Hodgson, T. K., "The Development of Enhanced Heat Transfer Condenser Tubing," 4th International Symposium on Fresh Water From the Sea, Vol. 1, pp 69-94, 1973.

7. Combs, S. K., An Experimental Study of Heat Transfer Enhancement for Ammonia Condensing on Vertical Fluted Tubes, Oak Ridge National Laboratory, Report ORNL-5356, January, 1978.

8. Combs, S. K., Mailen, G. S., Murphy, R. W., Condensation of Refrigerants on Vertical Fluted Tubes, Oak Ridge National Laboratory, Report ORNL/TM-5848, August, 1978.

9. Beck, A. C., A Test Facility to Measure Heat Transfer Performance of Advanced Condenser Tubes, MSME, Naval Postgraduate School, Monterey, CA, January 1977.

10. Pence, D. T., An Experimental Study of Steam Condensation on a Single Horizontal Tube, MSME, Naval Postgraduate School, Monterey, CA, March 1978.

11. Reilly, D. J., An Experimental Investigation of Enhanced Heat Transfer on Horizontal Condenser Tubes, MSME, Naval Postgraduate School, Monterey, CA, March, 1978.

12. Metals Handbook, 8th ed., v. 2, p 665, American Society for Metals, 1964.

13. Acurex Autodata, Autodata Nine Technical Manual.

14. Brundrett, E., "Modified Hydraulic Diameter for Turbulent Flow," Proceedings of NATO Advanced Studies Institute on Turbulent Forced Convection in Channels, Istanbul, July 1978.

15. Holman, J. P., Heat Transfer, 4th ed., McGraw-Hill, 1976.

16. Wilson, E. E., A Basis for Rational Design of Heat Transfer Apparatus, paper presented at the Spring Meeting of the Society of Mechanical Engineers, Buffalo, NY, June 1935.

17. Briggs, D. E., and Young, E. H., "Modified Wilson Plot Techniques for Obtaining Heat Transfer Correlations for Shell and Tube Heat Exchangers," Heat Transfer-Philadelphia, v. 65, No. 92, pp 35-45, 1969.

18. Subroutine, NPS COMPUTER FACILITY, LEAST SQUARES POLYNOMINAL FITTING, LSQPL2, Programmed By D. E. Harrison, November 1969.

19. Kays, W. M., and London, A. L., Compact Heat Exchangers, pp 92-97, 2nd ed., McGraw-Hill, 1964.

20. Knudsen, J. G., and Katz, D. L., Fluid Dynamics and Heat Transfer, pp 332-335, McGraw-Hill, 1958.

21. Bergles, A. E. and Jensen, M. K., Enhanced Single-Phase Heat Transfer for Ocean Thermal Energy Conversion Systems, Report HTL-13 ISU-ERI-AMES-77314, ERI Project 1278, April 1977.

22. Department of the Navy, Bureau of Ships, Design Data Sheet DDS 4601-1, 15 OCT 1953.

23. Standards for Steam Surface Condensers, 6th ed., Heat Exchange Institute, NY, 1970.

24. Reynolds, O., Transactions of the Royal Society, 174A:935, London, 1883.

25. Colburn, A. P., Trans. AIChE, 29:174, 1933.

26. Cunningham, J., Milne, H. K., The Effect of Helix Angle on the Performance of Roped Tubes, paper presented at Sixth International Heat Transfer Conference, Toronto, Canada, 7-11 August, 1978.

27. Kline, S. J., McClintock, F. A., "Describing Uncertainties In Single Sample Experiments," Mechanical Engineering, v. 74, pp 3-8, January 1953.

INITIAL DISTRIBUTION LIST

| | | No. Copies |
|---|---|---|
| 1. | Defense Documentation Center<br>Cameron Station<br>Alexandria, Virginia 22314 | 2 |
| 2. | Library, Code 0142<br>Naval Postgraduate School<br>Monterey, California 93940 | 2 |
| 3. | Department Chairman, Code 69<br>Department of Mechanical Engineering<br>Naval Postgraduate School<br>Monterey, California 93940 | 2 |
| 4. | Office of Research Administration, Code 012A<br>Naval Postgraduate School<br>Monterey, California 93940 | 1 |
| 5. | Professor Paul J. Marto, Code 69Mx<br>Department of Mechanical Engineering<br>Naval Postgraduate School<br>Monterey, California 93940 | 20 |
| 6. | LT James Fenner<br>1081 Debolt Road<br>Utica, Ohio 43080 | 4 |
| 7. | CDR W. W. Baline, USN<br>Naval Sea Systems Command (033) (acting)<br>2221 Jefferson Davis Highway, CP#6<br>Arlington, Virginia 20360 | 1 |
| 8. | Mr. Charles Miller<br>Naval Sea Systems Command (0331)<br>2221 Jefferson Davis Highway, CP#6<br>Arlington, Virginia 20360 | 2 |
| 9. | Mr. Frank Ventriglio<br>Naval Sea Systems Command (0331)<br>2221 Jefferson Davis Highway, CP#6<br>Arlington, Virginia 20360 | 1 |
| 10. | Dr. Earl Quandt<br>Naval Ship Research & Development Center<br>Annapolis Laboratory<br>Annapolis, Maryland 21402 | 1 |
| 11. | Mr. J. W. Murrin<br>Naval Sea Systems Command (0331)<br>2221 Jefferson Davis Highway, CP#6<br>Arlington, Virginia 20360 | 1 |

12. CAPT R. E. Greer, USN — 1
Naval Sea Systems Command (PMS-301)
2221 Jefferson Davis Highway, CP#6
Arlington, Virginia 20360

13. CDR D. W. Barns, USN — 1
Naval Sea Systems Command (PMS-301.B)
2221 Jefferson Davis Highway, CP#6
Arlington, Virginia 20360

14. Mr. Walter Aerni — 1
Naval Ship Engineering Center (6145)
Washington, D. C. 20360

15. Mr. Wayne L. Adamson — 1
Naval Ship Research & Development Center(2761)
Annapolis, Maryland 21402

16. Mr. Gil Carlton — 1
Naval Ship Engineering Center (6723)
Philadelphia, Pennsylvania 19112

17. Dr. David Eissenberg — 1
Oak Ridge National Laboratory
Post Office Box Y
Oak Ridge, Tennessee 37830

18. Miss Eleanor J. Macnair — 1
Ship Department
Ministry of Defence
Director - General Ships, Block B
Foxhill, Bath, Somerset
ENGLAND

19. Mr. Kurt Bredehorst — 1
NAVSEC 6147D
Department of the Navy
Hyattsville, Maryland 02782

20. Professor Kenneth J. Bell — 1
School of Chemical Engineering
Oklahoma State University
Stillwater, Oklahoma 74074

21. Professor A. E. Bergles — 1
Department of Mechanical Engineering
Iowa State University
Ames, IA 50010

22. Professor James G. Knudsen — 1
Engineering Experimental Station
Oregon State University
Covell Hall-219
Corvallis, Oregon 97331

23. Dr. Ken Read — 1
OTEC Branch
Division of Solar Energy
Department of Energy
Washington, D. C. 20545

24. Dr. A. L. London — 1
4020 Amaranta Avenue
Palo Alto, California 94306

25. Mr. Norman F. Sather — 1
Argonne National Laboratory
9700 S. Cass Avenue
Argonne, Illinois 60439

26. Dr. Jeff Horowitz — 1
Argonne National Laboratory
9700 S. Cass Avenue
Argonne, Illinois 60439

27. Mr. J. B. Henderson — 2
Market Development Manager
Wolverine Tube Division
Universal Oil Products Incorporated
Post Office Box 2202
Decatur, Alabama 35602

28. Mr. M. K. Ellingsworth — 1
Office of Naval Research
800 N. Quincy Street
Arlington, Virginia 22217

29. Mr. R. Muench — 1
David W. Taylor Naval Ship
Research and Development Center
Annapolis Laboratory
Annapolis, Maryland 21402

30. Mr. W. Thielbar — 1
Naval Weapons Center
China Lake, California 93555

31. CAPT Bress (Code 03) — 1
Naval Sea Systems Command
Washington, D. C. 20362

32. Mr. John Michele — 1
Oak Ridge National Laboratory
Oak Ridge, Tennessee 37830

33. Mr. Robert W. Perkins — 2
Spiral Tubing Corporation
533 John Downey Drive
New Britian, Connecticut 06051

34. Mr. Jack S. Yampolsky — 2
Senior Technical Advisor
Advanced Projects Division
General Atomic Company
Post Office Box 81608
San Diego, California 92138

35. Dr. Win Aung — 1
Division of Engineering, National Science Foundation
1800 "G" Street NW
Washington, D. C. 20550

36. Mr. John W. Ward — 1
Marine Division
Westinghouse Electric Corporation
Hendy Avenue
Sunnyvale, California 94088